INSTITUTE OF GENETICS
AND ANIMAL BIOTECHNOLOGY
of the Polish Academy of Sciences

INSTYTUT GENETYKI
I BIOTECHNOLOGII ZWIERZĄT
Polskiej Akademii Nauk

Institute of Genetics and Animal Biotechnology

Polish Academy of Sciences

Department of Experimental Genomics

The effect of opioid receptors blockade on atherosclerosis-related processes in ApoE-deficient mice

Wpływ zablokowania receptorów opioidowych na procesy związane z miażdżycą u myszy z wyłączonym genem ApoE

Kinga Jaskuła M.Sc.

Ph.D. Thesis

Research Supervisors

Prof. Dr hab. Mariusz Sacharczuk

Institute of Genetics and Animal Biotechnology
of the Polish Academy of Sciences

Dr Dominik Skiba

Institute of Genetics and Animal Biotechnology
of the Polish Academy of Sciences

Jastrzębiec, 2025

The research presented in this doctoral dissertation
was supported by funding from the National Science Centre, Poland.
Sonata 15, grant no. 2019/35/D/NZ5/02820

Table of Contents

List of publications to be included, along with impact factors and ministry points

1. **Jaskuła K**, Nawrocka A, Poznański P, Stachowicz A, Łazarczyk M, Sacharczuk M, Skiba DS. Opioid System Antagonism Alters Vascular Proteome and Collagen Deposition in ApoE$^{-/-}$ Mice. *Cells*. 2025; 14(19):1559. https://doi.org/10.3390/cells14191559

   Impact Factor: 5.2

   Ministry Points : 140

2. **Jaskuła K**, Nawrocka A, Poznański P, Stachowicz A, Łazarczyk M, Sacharczuk M, Gaciong Z, Skiba DS. Targeting the Opioid System in Cardiovascular Disease: Liver Proteomic and Lipid Profile Effects of Naloxone in Atherosclerosis. *Biomedicines*. 2025; 13(8):1802. https://doi.org/10.3390/biomedicines13081802

   Impact Factor: 3.9

   Ministry Points : 100

3. **Jaskuła K**, Sacharczuk M, Gaciong Z, Skiba DS. Cardiovascular Effects Mediated by HMMR and CD44. *Mediators Inflamm*. 2021; 2021:4977209. https://doi.org/10.1155/2021/4977209

   Impact Factor: 3.9

   Ministry Points : 100

Authors' contributions

Jaskuła K, Nawrocka A, Poznański P, Stachowicz A, Łazarczyk M, Sacharczuk M, Skiba DS. Opioid System Antagonism Alters Vascular Proteome and Collagen Deposition in ApoE$^{-/-}$ Mice. Cells. 2025; 14(19):1559. https://doi.org/10.3390/cells14191559

No.	***Full Name***	***Description of the author's participation***	***Participation in the publication in %***	***Institution***
1.	Kinga Jaskuła	conceptualization, methodology, validation, data collection, formal analysis, investigation, resources, data curation, writing - original draft preparation, writing-review and editing, visualization, supervision	55%	Institute of Genetics and Animal Biotechnology PAS
2.	Agata Nawrocka	validation, formal analysis, writing - review and editing,	10%	Institute of Genetics and Animal Biotechnology PAS
3.	Piotr Poznański	methodology, validation, writing - review and editing	5%	Institute of Genetics and Animal Biotechnology PAS
4.	Aneta Stachowicz	software, formal analysis, visualization	5%	Jagiellonian University Medical College
5.	Marzena Łazarczyk	writing - review and editing	5%	Institute of Genetics and Animal Biotechnology PAS

6.	Mariusz Sacharczuk	conceptualization, methodology, resources, writing - review and editing, supervision, funding acquisition	10%	Institute of Genetics and Animal Biotechnology PAS Warsaw Medical University
7.	Dominik S. Skiba	conceptualization, methodology, software, validation, formal analysis, investigation, resources, writing - original draft preparation and editing, visualization, supervision, funding acquisition	10%	Institute of Genetics and Animal Biotechnology PAS

Jaskuła K, Nawrocka A, Poznański P, Stachowicz A, Łazarczyk M, Sacharczuk M, Gaciong Z, Skiba DS. Targeting the Opioid System in Cardiovascular Disease: Liver Proteomic and Lipid Profile Effects of Naloxone in Atherosclerosis. *Biomedicines*. 2025; 13(8):1802. https://doi.org/10.3390/biomedicines13081802

No.	***Full Name***	***Description of the author's participation***	***Participation in the publication in %***	***Institution***
1.	Kinga Jaskuła	conceptualization, methodology, validation, data collection, formal analysis, investigation, resources, data curation, writing - original draft preparation, writing- review and editing, visualization, supervision	51%	Institute of Genetics and Animal Biotechnology PAS
2.	Agata Nawrocka	validation, formal analysis, writing - review and editing,	10%	Institute of Genetics and Animal Biotechnology PAS
3.	Piotr Poznański	methodology, validation, writing - review and editing	5%	Institute of Genetics and Animal Biotechnology PAS
4.	Aneta Stachowicz	software, formal analysis, visualization	5%	Jagiellonian University Medical College
5.	Marzena Łazarczyk	writing - review and editing	5%	Institute of Genetics and Animal Biotechnology PAS
6.	Mariusz Sacharczuk	conceptualization, methodology, resources, writing - review and editing, supervision, funding acquisition	7%	Institute of Genetics and Animal Biotechnology PAS Warsaw Medical University

7.	Zbigniew Gaciong	writing - review and editing, supervision	7%	Warsaw Medical University
8.	Dominik S. Skiba	conceptualization, methodology, software, validation, formal analysis, investigation, resources, writing - original draft preparation and editing, visualization, supervision, funding acquisition	10%	Institute of Genetics and Animal Biotechnology PAS

Jaskuła K, Sacharczuk M, Gaciong Z, Skiba DS. Cardiovascular Effects Mediated by HMMR and CD44. *Mediators Inflamm*. 2021;2021:4977209.2021 doi:10.1155/2021/4977209

No.	***Full Name***	***Description of the author's participation***	***Participation in the publication in %***	***Institution***
1.	Kinga Jaskuła	Conceptualization, writing - original draft preparation, Writing - Review end Editing, Supervision	65%	Institute of Genetics and Animal Biotechnology PAS
2.	Mariusz Sacharczuk	Writing - Review end Editing, Supervision	10%	Institute of Genetics and Animal Biotechnology PAS Warsaw Medical University
3.	Zbigniew Gaciong	Supervision	5%	Warsaw Medical University
4.	Dominik S. Skiba	Conceptualization, Writing - Review end Editing, Supervision	20%	Institute of Genetics and Animal Biotechnology PAS

Abstract

The endogenous opioid system is increasingly recognized as an important regulator of vascular function, inflammation, and lipid metabolism - key processes in atherogenesis. Atherosclerosis is a progressive inflammatory disease of the arterial wall, primarily driven by lipid accumulation and dysregulated immune responses. It represents the principal underlying cause of cardiovascular disease (CVD). Formation of atherosclerotic plaque is the hallmark of atherosclerosis development, which gradually leads to arterial wall thickening, loss of elasticity, and lumen narrowing, thereby reducing blood flow to tissues and organs. Plaque rupture may result in myocardial infarction, stroke, or peripheral artery disease, and most importantly, CVD remains a leading cause of death worldwide.

In the present studies, the effects of opioid receptor blockade with naloxone (NLX) on molecular, structural, and immunological parameters associated with the development and progression of atherosclerosis in ApoE$^{-/-}$ mice were investigated. Young (8-week-old) and aged (36-week-old) animals, representing early and advanced stages of the disease, respectively, were treated with NLX. In both age groups, NLX administration significantly reduced *Hmmr* gene expression in the aorta, suggesting a role for this gene in vascular remodeling. NLX also modulated collagen expression in a stage-dependent manner: *Col3a1* expression decreased in young mice but increased in aged animals, which was accompanied by a significant thickening of the aortic collagen layer in 36-week-old mice. These findings indicate that opioid receptor blockade influences extracellular matrix organization and vascular stiffness in an age-dependent manner. Analysis of splenic T-cell subpopulations showed that NLX did not markedly affect the proportions of CD4^{+} and CD8^{+} T-cells but significantly altered Hmmr expression within several T-cell subpopulations, linking opioid system to adaptive immune modulation. In 36-week-old mice, the effects of opioid system blockade on lipid metabolism were also examined. NLX treatment increased plasma HDL levels without affecting total cholesterol, LDL, or triglycerides. Histological analysis revealed no changes in atherosclerotic plaque size or hepatic steatosis. Expression of selected genes involved in lipid metabolism was also examined, resulting in reduced expression of *Fabp4* gene. Moreover, proteomic analysis of the aorta and liver identified NLX-induced alterations in proteins involved in lipid metabolism, inflammation, and oxidative stress. These included reduced expression of Apobr, Saa2, and Nnmt in the liver, and decreased levels of Aldob, Gsta3, and Arg1 in the aorta.

Collectively, these findings suggest that opioid receptor blockade with NLX influences multiple biological processes including vascular remodeling, immune regulation, and lipid metabolism. Although short-term NLX treatment did not significantly impact atherosclerotic plaque progression or hepatic steatosis, the observed molecular and proteomic changes highlight the complex role of the opioid system in atherogenesis and its potential as a therapeutic target for modulating cardiovascular and metabolic pathways.

Streszczenie

Endogenny układ opioidowy jest coraz częściej postrzegany jako istotny regulator funkcji naczyniowych, procesów zapalnych oraz metabolizmu lipidów - kluczowych mechanizmów odgrywających rolę w aterogenezie. Miażdżyca to postępująca choroba zapalna ściany tętnic, u podstaw której leży przede wszystkim odkładanie lipidów oraz zaburzenia regulacji odpowiedzi immunologicznej. Stanowi ona główną przyczynę rozwoju chorób sercowo-naczyniowych. Miażdżyca charakteryzuje się tworzeniem blaszek miażdżycowych, które z czasem prowadzą do pogrubienia ściany tętnicy, utraty jej elastyczności i zwężenia światła naczynia, co ogranicza przepływ krwi do tkanek i narządów. Pęknięcie i oderwanie blaszki może skutkować wystąpieniem zawału mięśnia sercowego, udaru mózgu lub choroby tętnic obwodowych. Należy podkreślić że choroby sercowo-naczyniowe wciąż pozostają jedną z głównych przyczyn zgonów na świecie.

W niniejszej pracy zbadano wpływ blokady receptorów opioidowych za pomocą naloksonu (NLX) na parametry molekularne, strukturalne i immunologiczne związane z rozwojem oraz progresją miażdżycy u myszy ApoE$^{-/-}$. W badaniach wykorzystano młode (8-tygodniowe) i starsze (36-tygodniowe) osobniki, reprezentujące odpowiednio wczesne i zaawansowane stadium miażdżycy, którym podano NLX. W obu grupach wiekowych podawanie NLX prowadziło do istotnego obniżenia ekspresji genu *Hmmr* w aorcie, co wskazuje na jego potencjalną rolę w przebudowie naczyń. NLX modulował również ekspresję kolagenu w sposób zależny od stadium choroby - ekspresja *Col3a1* uległa obniżeniu u młodych myszy, natomiast wzrosła u starszych, czemu towarzyszyło istotne pogrubienie warstwy kolagenowej w aorcie zwierząt 36-tygodniowych. Wyniki te sugerują, że blokada receptorów opioidowych wpływa na organizację macierzy zewnątrzkomórkowej oraz sztywność naczyń w zależności od stadium miażdżycy. Analiza subpopulacji limfocytów T w śledzionie wykazała, że NLX nie wpływał istotnie na proporcje komórek CD4$^+$ i CD8$^+$, jednak znacząco zmieniał ekspresję białka Hmmr w wybranych subpopulacjach limfocytów T, co wskazuje na związek pomiędzy układem opioidowym a modulacją odpowiedzi immunologicznej typu adaptacyjnego. U starszych, 36-tygodniowych myszy oceniono również wpływ blokady układu opioidowego na metabolizm lipidów. Podanie NLX spowodowało wzrost poziomu frakcji HDL w osoczu, bez istotnych zmian stężenia cholesterolu całkowitego, LDL i trójglicerydów. Analiza histologiczna nie wykazała różnic w wielkości blaszki miażdżycowej ani w nasileniu stłuszczenia wątroby. Dodatkowo, w badaniu ekspresji wybranych genów związanych

z metabolizmem lipidów stwierdzono obniżoną ekspresję genu *Fabp4*. Analiza proteomiczna aorty i wątroby wykazała, że zastosowanie NLX indukuje zmiany w poziomie białek zaangażowanych w metabolizm lipidów i procesy zapalne.

Podsumowując, uzyskane wyniki wskazują, że blokada receptorów opioidowych za pomocą NLX oddziałuje na wiele procesów biologicznych, w tym przebudowę naczyń, regulację odpowiedzi immunologicznej i metabolizm lipidów. Choć krótkotrwałe leczenie NLX nie wpływało istotnie na wielkość blaszki miażdżycowej ani na poziom stłuszczenia wątroby, zaobserwowane zmiany molekularne i proteomiczne podkreślają złożoną rolę układu opioidowego w aterogenezie oraz sugerują jego potencjał jako celu terapeutycznego w modulacji szlaków sercowo-naczyniowych i metabolicznych.

1. Introduction

Atherosclerosis is a chronic, progressive inflammatory disease of the arterial wall, driven primarily by lipid accumulation and dysregulated immune responses, constituting the leading cause of cardiovascular disease (CVD). It is characterized by the formation of atherosclerotic plaques composed of cholesterol, lipids, inflammatory cells, and fibrous tissue within the intima of large and medium-sized arteries. Over time, plaque growth leads to arterial wall thickening, loss of elasticity, and lumen narrowing, resulting in reduced blood flow to tissues and organs. Plaque rupture can lead to thrombosis and acute vascular occlusion, resulting in clinical events such as myocardial infarction, stroke, or peripheral arterial disease [1–3], a conditions that collectively represent CVD and are the leading cause of mortality in developed countries [4]. Key cellular players involved in the development of atherosclerosis include endothelial cells (ECs), leukocytes, and smooth muscle cells (SMCs), which contribute to the formation of atherosclerotic plaques in response to inflammatory stimuli [4,5]. The vascular endothelium forms a continuous monolayer of cells lining the entire cardiovascular system and plays a crucial role in maintaining vascular function. The early stages of atherosclerosis are characterized by multiple mechanisms, including endothelial dysfunction, recruitment of inflammatory cells, modification of lipoprotein particles, and impaired blood flow [6]. These and other factors collectively impair ECs function, increasing their permeability and enabling low-density lipoproteins (LDL) and triglyceride-rich lipoproteins to penetrate the vessel wall via trans-endothelial transport or diffusion at cell junctions [7]. These lipoproteins undergo oxidation, activating ECs and upregulating adhesion molecules such as P-selectin, E-selectin, VCAM-1, and ICAM-1, which promote leukocyte adhesion to vascular endothelial cells and the secretion of chemotactic factors [8,9]. Monocytes migrate into the intima and differentiate into macrophages in response to macrophage colony-stimulating factor (M-CSF), subsequently internalizing modified lipoproteins and transforming into foam cells - cholesterol-loaded macrophages that promote plaque growth and instability [10–12]. The next central players in the development of atherosclerosis are T-cells, contributing to both initiation and progression of the disease. Within the arterial wall, they participate in immune surveillance by recognizing modified lipoproteins and triggering inflammatory pathways. $CD4^+$ T-cells are particularly important in shaping the inflammatory milieu, whereas $CD8^+$ T-cells are thought to influence the structural stability of plaques. Through these mechanisms, T-cells activity promotes endothelial dysfunction, stimulates SMC proliferation, and supports foam cell formation, all of which promote plaque development. Moreover, T-cells modulate the balance between pro- and anti-inflammatory signals, thereby affecting disease progression and plaque vulnerability [13,14].

Furthermore, studies have demonstrated that ApoE knockout mice with disrupted TGF-β signaling in T-cells develop larger aortic lesions and exhibit greater lesion areas in the aortic root. Notably, when the lesions of comparable size were examined, mice lacking T-cell - specific TGF-β signaling showed higher T-cell infiltration, enhanced macrophage activation, and reduced collagen content [15]. Another crucial cellular component contributing to atherosclerotic plaque development are SMCs. Under pathological conditions, these cells migrate from the media to the intima, producing extracellular matrix (ECM) proteins, including collagen types I and III, encoded by *Col1a1* and *Col3a1* genes, respectively [16–19]. While the majority of the ECM in a healthy artery consists of type I and type III collagens, atherosclerotic lesions are typically enriched in type I collagen and fibronectin [20]. SMCs and inflammatory cells also release matrix metalloproteinases (MMPs), which degrade ECM components, leading to plaque destabilization through a dynamic imbalance between collagen synthesis and degradation [21,22]. This destabilization can ultimately result in plaque rupture and the onset of clinical complications such as myocardial infarction.

Although the above mechanisms are well characterized, current treatments are still primarily symptomatic, underscoring the need to identify new factors contributing to the development of atherosclerosis. Recent studies indicate the involvement of less conventional molecular pathways in the development of atherosclerosis. A promising new factor contributing to the development of atherosclerosis may be the hyaluronan-mediated motility receptor (HMMR also known as RHAMM), a receptor for hyaluronic acid (HA), widely studied in cancer biology [23–25]. Evidence suggests that HMMR and its ligand HA may also be implicated in CVD [26], for instance, in both zebrafish and rat models of myocardial injury, *Hmmr* expression was upregulated in damaged heart tissues, indicating its involvement in scar tissue formation [27]. Given that atherosclerosis shares many features with wound healing and tissue remodeling processes, it is possible that Hmmr may also contribute to atherosclerotic plaque progression. This is further supported by studies linking another HA receptor, CD44, to atherosclerosis development [28]. CD44 mediates leukocyte adhesion and migration into the intima, supports macrophage retention as well as foam cell formation, and promotes vascular smooth muscle cell (VSMC) proliferation and migration [28]. These actions contribute significantly to early lesion development, even before significant luminal narrowing occurs. CD44-null mice develop significantly fewer aortic lesions than their wild-type counterparts, and migration of CD44-null macrophages to atherosclerotic sites is markedly reduced (Figure 1) [29].

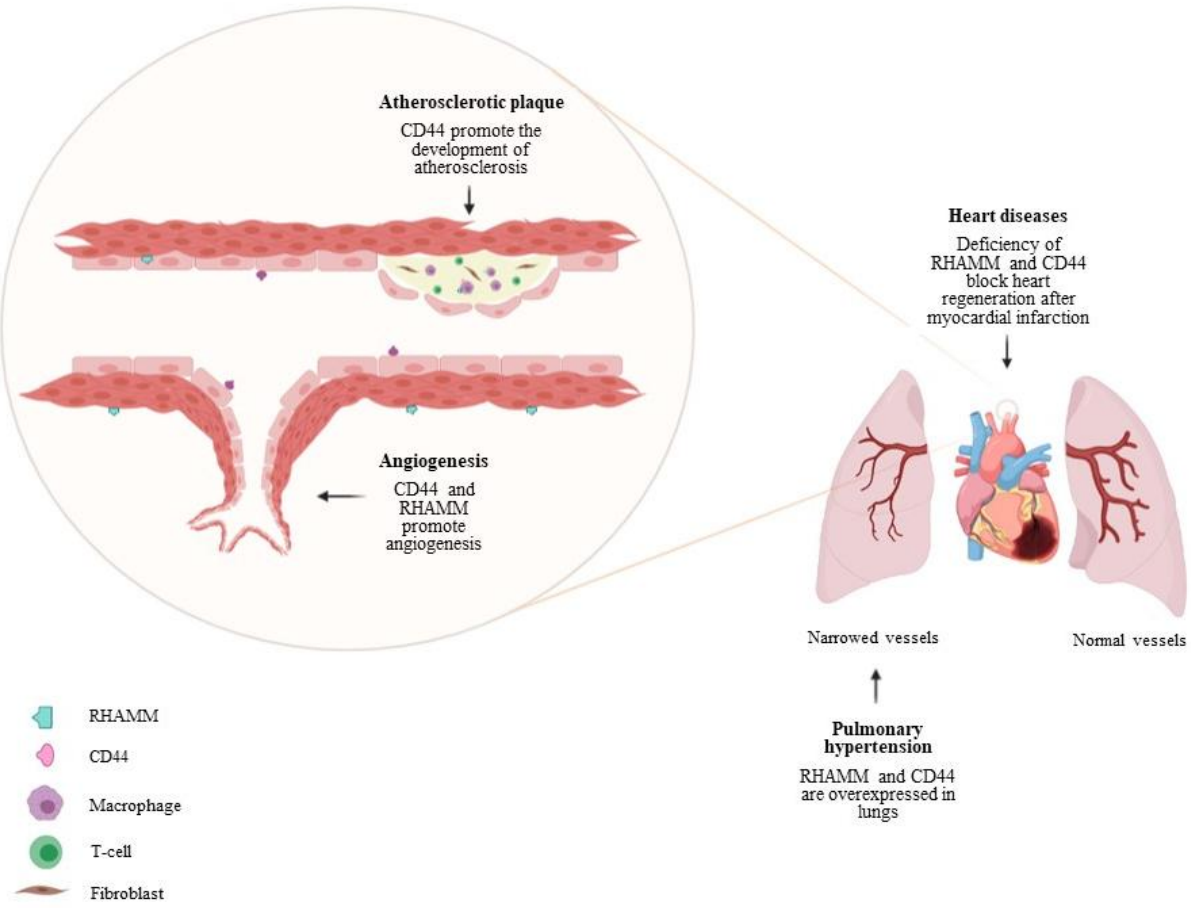

Figure 1. The role of RHAMM (HMMR) and CD44 receptors in the cardiovascular system. (Figure 2, publication 3)

Another new factor that, through its multisystemic action, may also influence the development of atherosclerosis is the endogenous opioid system (EOS). The EOS comprises endogenous opioid peptides such as endorphins, enkephalins, and dynorphins, which interact with three primary receptor types: mu (μ, MOR), delta (δ, DOR), and kappa (κ, KOR) [30]. While traditionally associated with modulation of nociceptive signaling and stress-induced analgesia [31,32], the EOS has also been recognized for its broader role in regulating mood, gastrointestinal function, and cardiovascular physiology [33–36]. Opioid receptors are present on the surface of many cell types within the cardiovascular system, including cardiomyocytes, ECs, and SMC, where they influence cellular function, for instance can induce vasodilation and maintain vascular tone, influencing blood pressure and blood flow. Opioid receptors are also expressed by the cells of the immune system such as T-cells, B-cells and macrophages which are a key players in the development of atherosclerosis [37]. The broad distribution of opioid receptors in tissues and organs outside the central nervous system, such as immune cells, indicates that opioids may exert additional peripheral effects, including immunomodulation. The increased incidence of infections observed in epidemiological studies involving individuals who abuse opioids further

underscores their immunosuppressive effects [38]. Opioid receptors on ECs communicate with VSMC through paracrine signaling and modulate angiogenesis, vascular tone, and vascular integrity [39]. Recent studies have highlighted the EOS involvement in atherosclerotic plaque progression and instability. Chronic infusion of β-endorphin, an endogenous μ opioid receptor ligand, in ApoE$^{-/-}$ mice led to increased atherosclerotic plaque area and macrophage content, suggesting a pro-atherogenic role of EOS activation [14,15]. Conversely, administration of opioid receptor antagonists such as naloxone (NLX) in lipopolysaccharide-treated ApoE$^{-/-}$ mice significantly reduced plasma TNF-α levels, indicating decreased macrophage activation [21]. NLX is an antagonist of all three main opioid receptors. It counteracts both central and peripheral effects of endogenous and exogenous opioids, reversing the reactions they cause: respiratory depression, pupil constriction, hypotension, and sedation. On its own, NLX exhibits minimal pharmacological activity and does not induce tolerance or physical dependence. Through its comprehensive activity on the opioid system, NLX may exert beneficial effects across a range of physiological and pathological conditions. Consistent with its pharmacological profile, pretreatment with another opioid receptor antagonist, NLX, has been shown to prevent stress-induced hypercholesterolemia in rats. Moreover, δ opioid receptor agonist treatment in patients with ischemic heart disease improved their lipid profiles [22,23]. Interestingly, the connection between the EOS and *Hmmr* expression is gaining importance. Our unpublished data show increased *Hmmr* expression in aorta of mice with increased opioid system activity, and a statistically significant reduction in its expression following opioid receptor blockade with NLX [27,28]. These observations suggest a possible regulatory axis between EOS and *Hmmr* in the pathogenesis of atherosclerosis.

Taken together, these findings highlight the multifactorial nature of atherosclerosis development and suggest a potential role of the EOS and *Hmmr* as novel factors influencing its progression. Given the predominantly symptomatic nature of current therapies, understanding these novel mechanisms may provide new targets for therapeutic intervention. Our research therefore focuses on the impact of EOS modulation, specifically opioid receptor blockade, on lipid metabolism and atherosclerotic plaque development. Through the examination of these interconnected pathways, I seek to enhance understanding of the mechanisms underlying atherosclerosis and to assess their potential biological relevance. Our research was conducted using ApoE$^{-/-}$ mice with a knockout gene for apolipoprotein E which plays a key role in lipid metabolism and cholesterol transport. The absence of this protein in ApoE$^{-/-}$ mice leads to hypercholesterolemia and the development of atherosclerotic lesions, making them a popular model for studying cardiovascular diseases, particularly atherosclerosis.

2. Hypotheses

- Blocking the opioid system affects the lipid profile of mice with advanced atherosclerosis.

- Inhibition of the opioid system modulates vascular remodeling in the aorta of $ApoE^{-/-}$ mice.

- Blocking the opioid system in a model of advanced atherosclerosis alters the aortic and hepatic proteome in $ApoE^{-/-}$ mice.

- Opioid system blockade alters *Hmmr* gene expression in both early and advanced stages of atherosclerosis in $ApoE^{-/-}$ mice.

3. Objectives

- To investigate the effect of opioid receptors blockade on the lipid profile in mice with advanced atherosclerosis.

- To investigate whether the opioid system is involved in vascular remodeling that occurs during the development of atherosclerosis.

- To investigate whether blocking the opioid system in a model of advanced atherosclerosis affects proteomic changes in the aorta and liver.

- To investigate *Hmmr* gene expression at different stages of atherosclerosis development, as well as after opioid receptors blockade.

4. Materials and Methods

4.1 Animals

All experiments were performed on 8-week and 36-week-old, male B6.129P2-Apoe^{tm1Unc}/J (strain. no. 002052) mice on the C57BL/6J background (further referred to as ApoE$^{-/-}$). Animals were housed in groups of 4–5 individuals and maintained in animal facility of the Institute of Genetics and Animal Biotechnology of the Polish Academy of Sciences, under standard environmental conditions (ambient temperature of 22 ± 2℃ and 55 ± 5 % relative humidity) under a 12 h light/dark cycle (lights on at 7 a.m.). Access to tap water and food (LABOFEED H, Kcynia, Poland) was provided *ad libitum*. Study procedures were conducted in accordance with the ethical approval (permission no. WAW2/093/2024) received from the II Local Ethics Committee for Experiments on Animals in Warsaw.

4.2 Drug & experiment design

Both 8-week and 36-week-old mice were assigned to either a saline-treated control group or naloxone-treated experimental group. A non-selective opioid system antagonist, naloxone hydrochloride (NLX) (Sigma-Aldrich, St. Louis, MO, USA) was administered. Individuals belonging to NLX-treated group received daily intraperitoneal injections of freshly prepared NLX dissolved in saline (0.9% NaCl) at a dose of 10 mg/kg for 7 consecutive days. Mice of control group were administered an equivalent volume of saline.

4.3. Measurement of mRNA expression

Total RNA was isolated from liver lobes and aortas using TRItidy G reagent (PanReac AppliChem, Darmstadt, Germany) according to the manufacturer's instructions. RNA concentration and purity were assessed using a NanoDrop 2000 spectrophotometer (Thermo Fisher Scientific, Waltham, MA, USA). Reverse transcription of RNA was performed using the High Capacity cDNA Reverse Transcription Kit (Applied Biosystems, Foster City, CA, USA) following manufacturer's protocol. The expression of *Hmmr*, *Col1a1* and *Col3a1* at mRNA level in the aortas of 8-week-old and 36-week-old mice and the expression of *Lpl*, *Srebf1* and *Fabp4* at mRNA level in the livers of 36-week-old mice were analyzed using TaqMan® probes (Thermo Fisher Scientific, Waltham, MA, USA; catalogue numbers: Mm00469183_m1; Mm00802300_m1; Mm00802300_m1; Mm00434764_m1; Mm00550338_m1; Mm00445878_m1, respectively) and the TaqMan® Real-Time PCR Master Mix (Thermo Fisher Scientific, Waltham, MA, USA). Reactions were performed on 96-well plates on the LightCycler 96 System (Roche Diagnostics, Germany) according to standard Real-Time PCR protocol.

Calculations were made using LightCycler 96 Software. Data were normalized to *Tbp* mRNA levels and relative quantification was calculated.

4.4. Trichrome staining

Liver lobes and thoracic aortas were fixed in formalin and dehydrated through a graded ethanol series (70%, 80%, 96%, and 99.8%), with two changes at each concentration for 30 minutes at room temperature. The tissues were then cleared in two changes of xylene (Warchem, Warsaw, Poland) for 15 minutes each. Subsequently, samples were transferred to a toluene - paraffin mixture (1:1) and incubated for 2 hours at 60 °C. In the final step, each specimen was immersed in pure molten paraffin overnight and embedded in paraffin blocks. Paraffin-processed tissues were sectioned at 6 µm thickness using a microtome (Hyrax M25, Zeiss, Germany) and mounted on microscope slides. Prior to staining, the sections were deparaffinized in two changes of xylene and rehydrated through a descending ethanol series. Further, trichrome stain was performed with Trichrome Stain (Masson) Kit (Sigma-Aldrich, St.Louis, MO, USA) according to manufacturer's protocol. The total fibrosis stained lesion area in right lobe of livers were quantified using ImageJ software (version 1.53e) by two independent investigators. Three separate areas of stained lesion were counted and averaged to yield one value per slide. The final data were expressed as a percentage of positive-staining areas relative to the total aortic area. Thickness of the collagen layer was determined by averaging 15 measurements taken from one section per subject at equal intervals around the circumference of aorta using ImageJ 1.54g software.

4.5. Flow cytometry

Spleens of both 8-week and 36-week-old mice were harvested and mashed through 70-µm strainers (VWR International, Avantor, Radnor Township, PA, USA) to isolate single cells. RBC lysis buffer (Biolegend, San Diego, CA, USA) was used to deplete red blood cells. Splenocytes were stained in FACS buffer for 20 min at 4 °C in the dark with the monoclonal antibodies (Table 1). For intracellular staining of CD168, BD Cytofix/Cytoperm™ Fixation/Permeabilization Solution was used (BD Biosciences, NJ, USA. Cells were analyzed by a CytoFLEX flow cytometer (Beckman Coulter, Brea, CA, USA), and data were analyzed using Flow Jo v.10 (Ashland, OR, USA). For each experiment, fluorescence-minus-one controls (FMO) were performed. In selected experiments, FMO gating strategies were confirmed by isotype controls (Figure 2).

Table 1. List of antibodies used for flow cytometry

Specificity	Fluorochrome	Clone Name	Supplier
CD3ε	PerCP	145-2C11	BioLegend
CD8a	AF700	53-6.7	BioLegend
CD4	BV750	GK 4.5	BioLegend
CD69	PEC7	H1.2F3	BioLegend
CD44	AF647	IM7	BioLegend
CD62L	PE594	MEL-14	BioLegend
CD168	CoraLite488	Polyclonal antibody	Proteintech

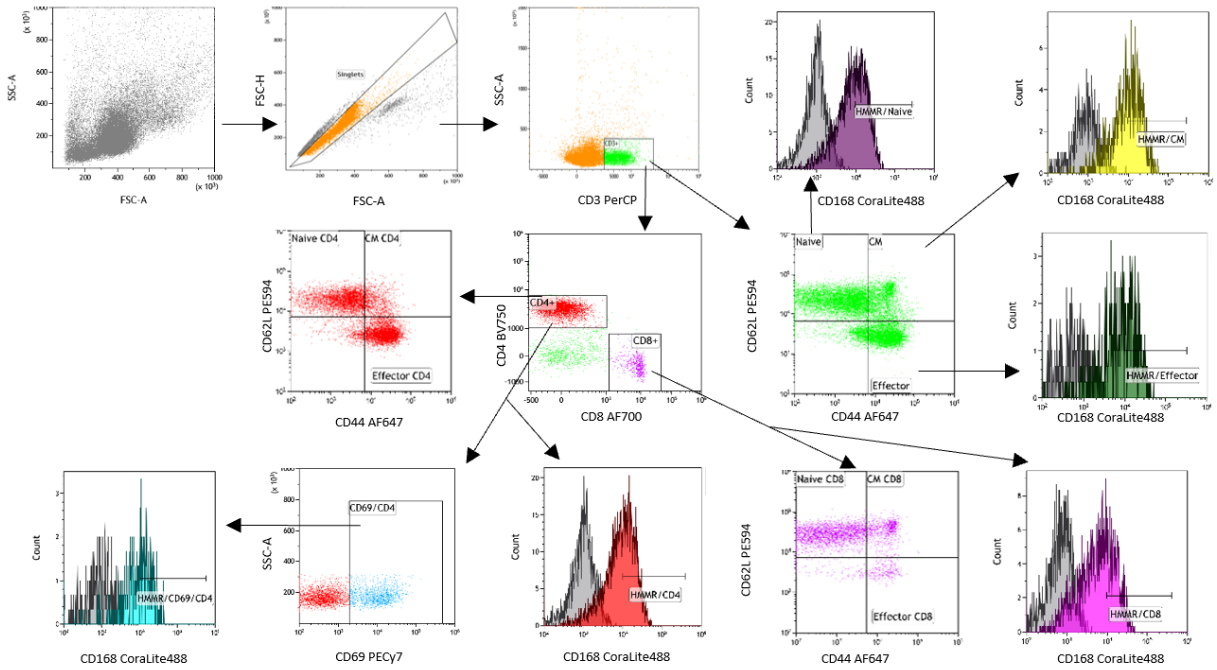

Figure 2. Gating strategy of flow cytometry analysis

4.6. Lipid profile analysis

Lipid profile analysis was performed on 36-week-old mice. Blood samples were collected directly from heart of anesthetized mice to heparin coated syringes. Then samples were centrifuged at 3000×*g* at 4°C for 10 min, then plasma was collected for lipid profile analysis including levels of total cholesterol, low-density cholesterol (LDL), high-density cholesterol (HDL) and triglycerides. Analysis was performed using COBAS 6000 analyzer (Roche Diagnostics, Germany).

4.7. Oil red O (ORO) staining

Oil red O (ORO) staining was done on aortic arches and right lobes of liver of 36-week-old mice to visualize atherosclerotic lesions and fat deposits, respectively. The aortic arches were harvested after prior perfusion with phosphate-buffered saline (PBS), then fixed in 10% formalin for 24 hours at 4°C and stained according to adjusted protocol [17]. Briefly, fixed aortic arches were opened longitudinally and pinned onto black silicone plates. Specimens were rinsed in distilled water and then briefly washed in 60% isopropanol. The tissues were subsequently stained with ORO working solution (0.625% ORO in isopropanol diluted with distilled water at a ratio of 1.5:1) for 30 minutes at room temperature. Excess dye was removed by washing the specimens with 60% isopropanol, followed by three rinses in distilled water. Right lobe of the liver was collected and fresh frozen in -80°C. Prior to sectioning, sample was transferred for 30 minutes to -20°C to avoid tissue crumbling during cutting. Tissue was sectioned in cryostat (Jung CM1800, Leica, Germany) set to -20°C and 6µm thick sections. Before ORO staining sections were fixed in 10% formalin for 10 minutes at room temperature. Liver fragments were stained similarly to aortic arches as described above.

The total area of ORO-stained lipid deposits in the aortic arches and right liver lobe were quantified using ImageJ software (version 1.53e) by two independent investigators. The final data were expressed as a percentage of positive-staining areas relative to the total aortic area.

4.8. Macrophages immunofluorescence staining

The immunohistochemical staining was performed using F4/80 Monoclonal Antibody (BM8) (Thermo Fisher Scientific, Waltham, MA, USA). Liver lobes were fixed in formalin and dehydrated as describe above. After that, tissues were transferred to mixture of toluene:paraffin (1:1) and incubated for 2h in 60°C. In the final step, each liver lobe was placed in pure molten paraffin overnight and embedded in paraffin blocks. Processed tissue was sectioned on microtome (Hyrax M25, Zeiss, Germany) for 6µm thick slices and placed on microscopic slides. Prior to staining, the specimens were deparaffinized in two changes of xylene and rehydrated through a graded series of alcohols. Heat-induced epitope retrieval was then performed at 90 °C in 10 mM sodium citrate buffer (pH 6.0) for 20 minutes. Sections were blocked in 3% bovine serum albumin (BSA). Primary antibody conjugated witch Alexa Fluor 488 (1:50) was incubated overnight at 4°C. Slides were washed in distilled water and mounted with VECTASHIELD® Antifade Mounting Medium with DAPI (Vector Laboratories, Inc. Newark, CA United States). Appropriate positive and negative controls were included with the study sections. The immunostaining was quantified using ImageJ software (version 1.53e) by two independent

investigators. Three separate areas of stained lesion were counted and averaged to yield one value per slide. The final data were expressed as a percentage of positive-staining areas relative to the total aortic area.

4.9. Liquid chromatography-tandem mass spectrometry (LC–MS/MS) analysis

Mouse livers (n=7 biological replicates per group, in total 14 samples) and thoracic aorta (n = 7 in control group, n=8 in NLX group, in total 15 samples) were homogenized using a Tissue Lyser LT (Qiagen, Hilden, Germany) and lysed in a buffer containing 0.1 M Tris-HCl, pH 7.6, 2% sodium dodecyl sulfate, and 50 mM dithiothreitol (Sigma Aldrich, St. Louis, MO, USA) at 96 °C for 10 min. Total protein concentration in lysates and the peptide contents in the digests were assayed using a tryptophan fluorescence-based WF assay [40]. Seventy micrograms of protein were digested overnight using the filter-aided sample preparation (FASP) method [41] with Trypsin/Lys-C mix (Promega, Madison, WI, USA) (enzyme-to-protein ratio 1:35) as the digestion enzymes. Subsequently, the samples were purified with C18 Ultra-Micro Spin Columns (Harvard Apparatus, Holliston, MA, USA). Then, all the samples were dissolved in 0.1% formic acid at a concentration of 0.5 µg/µl and spiked with the iRT peptides (Biognosys, Schlieren, Switzerland). One microgram of peptide was injected into a nanoEaseTM M/Z Peptide BEH C18 75 µm i.d. × 25 cm column (Waters, Milford, MA, USA) via a nanoEaseTM M/Z Symmetry C18 180 µm i.d. × 2 cm trap column (Waters, Milford, MA, USA) and separated using a 1% to 40% B phase linear gradient (A phase - 0.1% FA in water; B phase - 80% ACN and 0.1% FA) with a flow rate of 250 nL/min on an UltiMate 3000 HPLC system (Thermo Scientific, Waltham, MA, USA) coupled to an Orbitrap Exploris™ 480 Mass Spectrometer (Thermo Scientific, Waltham, MA, USA). The nanoelectrospray ion source parameters were: ion spray voltage: 2.2 kV, ion transfer tube 275°C. For data-independent (DIA) acquisition, spectra were collected for 145 min in full scan mode (400–1250 Da), followed by 55 DIA scans using a variable precursor isolation window approach and AGC set to custom 1000%. The DIA MS data were analyzed in Spectronaut (Biognosys, Schlieren, Switzerland) [42] software using directDIATM approach. MS data were filtered by 1% FDR (false discovery rate) at the peptide and protein levels, while quantitation was performed at the MS2 level and global imputation with a missingness rate set to 0.3 was used. Statistical analysis of differential protein abundance was performed at both the MS1 and MS2 levels [43] using unpaired t-tests with multiple testing correction after Storey [44]. A summary of the quality control for the LC-MS/MS runs is shown in Supplemental Figures (Figure 1, publication 2 and figure 2, publication 1 for liver and aorta respectively). The mass spectrometry data have been deposited to the ProteomeXchange Consortium via the PRIDE partner repository [45] with the dataset identifier PXD063243 for liver and PXD064451 for aorta.

4.10. Statistical analysis

Data collected from serum analysis and histopathological evaluation were checked for normality by Shapiro-Wilk test. ANOVA test was utilized to determine any differences between groups with statistical significance set to p-value < 0.05. Data for aortic research underwent normality check by Shapiro-Wilk test followed by two-sided Student's t-test was performed to assess changes between saline-treated and NLX-treated group. Results were considered as statistically significant when p-value was less than 0.05. Results presented on graphs are expressed as means ± SD.

5. Results and discussion

In the present study, the involvement of the opioid system in the development and progression of atherosclerosis was evaluated by analyzing its influence on selected molecular and structural parameters in the vascular wall at different stages of the disease. The following sections discuss the observed effects of opioid receptor blockade with naloxone (NLX) in young and aged ApoE$^{-/-}$ mice, providing insights into potential mechanisms linking opioid system with vascular remodeling processes.

First, the effect of opioid system blockade with NLX on factors related to early atherosclerosis was investigated in young, 8-week-old mice. NLX treatment led to a statistically significant decrease in *Hmmr* gene expression ($p<0.05$) in the aorta of ApoE$^{-/-}$ mice. Subsequently, the expression of two major collagen isoforms, *Col1a1* and *Col3a1*, which are the most abundant structural proteins of the vessel wall [43,44], was analyzed. While no change was observed in *Col1a1* expression, NLX administration resulted in a significant reduction in *Col3a1* expression ($p<0.05$) (Figure 1, publication 1). Moreover, NLX administration did not cause significant changes in the thickness of the collagen layer in the aorta (Figure 2, publication 1). Similarly, the effect of blocking the opioid system on the above factors was examined in 36-week-old mice with advanced atherosclerosis. Following NLX treatment, a statistically significant decrease in *Hmmr* gene expression was observed, as well as no changes in *Col1a1* gene expression. However, in contrast to young mice, administration of NLX to 36-week-old mice resulted in decreased expression in *Col3a1* gene ($p<0.05$) (Figure 5, publication 1). Opioid receptor blockade also resulted in significant thickening of the collagen layer in the aorta compared to the control group ($p<0.05$) (Figure 6, publication 1). After NLX treatment, *Hmmr* expression in aorta significantly decreased in both 8-week-old and 36-week-old mice. This may suggest an important role of the *Hmmr* gene in vascular remodeling during both the early and advanced stages of atherosclerosis development. In the aorta, *Col3a1* expression was significantly decreased in young mice but increased in aged - 36-week-old animals, while *Col1a1* expression showed similar, but non-significant, trends.

It should be noted that prolonged exposure to opioid antagonists has been shown to increase collagen content in skin tissue, as evidenced by studies using naltrexone for wound healing in a rat model as well as for wound treatment after a precise, tissue-sparing surgery for skin cancer removal in humans [46,47]. The ratio of type I to type III collagen was shown to be higher in the tissue surrounding aortic calcium deposits than within the calcified regions, whereas the ratio of type III collagen to elastin was lower in the artery compared to calcium deposits. These abnormalities likely promote the accumulation of calcium salts, an important feature of the

atherosclerotic process [48]. Therefore, it is important to note that for vascular elasticity, the balance between collagen isoforms I and III is crucial factor [49]. However, these proportions change with age, and such changes may vary depending on the tissue type [50]. With advancing age, the content of type III collagen decreases in the heart and aorta, extending to the distal regions [51], therefore, the age-related increase in vascular stiffness represents a natural consequence of the aging process. Vascular stiffening induced by altered collagen expression and production following NLX treatment may facilitate atherosclerotic plaque formation, although increased stiffness is considered a consequence rather than a cause of atherosclerosis. Nonetheless, NLX may exacerbate this pathological process [52]. Opioids, through their receptors, can influence inflammation and vascular remodeling - key mechanisms in atherogenesis. To assess whether opioid receptor blockade affects aortic wall remodeling, the collagen layer thickness in the thoracic aorta was measured in both 8- and 36-week-old mice treated with NLX. Results presented above indicate that NLX may enhance aortic wall resistance, potentially exerting protective effects in conditions such as hypertension and contributing to the prevention of aneurysm formation. Supporting evidence shows that lower collagen content has been reported in aortic dissection and aneurysms, likely contributing to wall weakening while collagenase treatment of pigs aortic rings increased aortic diameter and reduced vessel resistance to rising blood pressure [53,54]. Similarly, topical naltrexone usage in type I diabetic rats promoted collagen production and improved skin integrity compared with vehicle treatment [55].

Next, to investigate whether opioid receptor blockade influences adaptive immunity, splenic T-cell subpopulations in $ApoE^{-/-}$ mice were analyzed, as the spleen - being a major secondary lymphoid organ - provides a robust system for assessing systemic immune modulation. Characterization of the splenic T-cell subpopulation in 8-week-old mice showed that opioid receptors blockade did not affect the percentage of $CD4^+$ T-cells or $CD8^+$ T-cells (Figure 3a, publication 1). A statistically significant increase in the percentage of naive and central memory (CM) but not effector subpopulations was observed (Figure 3b, publication 1). NLX administration caused a statistically significant decrease in the percentage of CM ($p<0.01$) and increase in naive $CD4^+$ T-cells ($p<0.05$) (Figure 3c, publication 1), and a decrease in the CM $CD8^+$ T-cell populations ($p<0.01$) (Figure 3d, publication 1). NLX treatment did not affect Hmmr expression on $CD4^+$ T-cells but decreased its expression on $CD8^+$ T-cells ($p<0.001$) and $CD69^+/CD4^+$ T-cells ($p<0.01$) (Figure 4a, publication 1). A decrease in Hmmr expression was also observed in CM ($p<0.001$) and naive subpopulations ($p<0.01$), but not in effector subpopulation (Figure 4b, publication 1).

The assessment of splenic T-cell subpopulations after NLX administration in 36-week-old mice revealed no changes in the proportions of $CD4^+$ and $CD8^+$ populations, nor in the effector and naive subpopulations. However, statistically significant increase in the percentage of CM T-cells was observed ($p<0.05$) (Figure 7b, publication 1). No changes were observed in the proportion of any $CD4^+$ T-cells, nor in the effector and naive subpopulations within $CD8^+$ T-cells. However, an increase in the percentage of CM $CD8^+$ T-cells was observed ($p<0.01$) (Figure 7d, publication 1). Moreover, NLX administration caused increased Hmmr expression on all $CD4^+$, $CD8^+$, $CD69^+/CD4^+$ as well as CM, effector and naive T-cells ($p<0.001$) (Figure 8, publication 1).

T-cells contribute significantly to vascular inflammation and may influence the development of atherosclerotic plaques [13,56]. It has also been shown that the composition and phenotype of T-cells within atherosclerotic plaques differs from those in circulating blood. The fraction of CD8+ T-cells - key components of the adaptive immune system, was significantly higher in human atherosclerotic plaques than in blood [57]. Modulation of the adaptive immune system by the opioid system was first observed in rodents, in which morphine treatment reduced the function of T-cells and their precursors [58,59]. Opioids are known to modulate immune function, particularly by influencing T-cells activation, differentiation, and cytokine release, processes strongly linked to the initiation and progression of atherosclerosis [13,60]. Therefore, the potential impact of opioid system blockade with NLX on splenic T-cells subpopulations content in $ApoE^{-/-}$ mice was investigated. Furthermore, since Hmmr has been linked to tissue remodeling and immune cell activation, but its role in T-cells during atherosclerosis remains unexplored, its expression in different T-cell subpopulations was assessed. This approach allowed the exploration of a potential link between opioid signaling, immune modulation, and *Hmmr* regulation in adaptive immunity at both early and more advanced stages of the disease. Although the above results do not reveal significant changes in the proportions of T-cell populations, they revealed significant differences in Hmmr expression on T-cells following NLX treatment, suggesting a link between opioid system blockade, *Hmmr* expression, and atherosclerosis progression. Consistent with these findings, administration of cyprodime (a μ-opioid receptor antagonist) in mice selectively bred for strong swim stress-induced analgesia resulted in an increased increase the CM CD8+ T-cells population [61].

To investigate whether blockade of the opioid system would affect factors associated with the development of atherosclerosis, the lipid profile in 36-week-old mice was examined. NLX treatment did not result in significant changes in total cholesterol, LDL, or triglyceride levels; however, an increase in HDL levels was observed (Figure 1b, publication 2).

Multiple studies indicate a relationship between the opioid system and cholesterol levels. Some studies have shown that administration of opioid receptor agonists, such as dynorphin A or DAGO, attenuated the increase in blood total cholesterol, triglycerides, and LDL levels in rats exposed to forced swimming stress [62]. Interestingly, a cross-sectional analysis of 2239 individuals using opioids revealed that opioid consumption correlated with markedly reduced levels of total cholesterol, LDL and HDL [63]. At the same time, among lung cancer patients receiving opioids for pain management, it was observed that a higher proportion of patients with low cholesterol were found to be non-responders to initial doses of opioids compared to those with high cholesterol [64]. Furthermore, several reports indicate that opioid receptor antagonists also affect cholesterol levels. A 5-day pretreatment with naltrexone has been shown to prevent stress-induced cholesterol elevation in female rats fed a diet enriched in cholesterol and cholic acid (CCA) [65]. Furthermore, in the same animal model, 5 days of continuous morphine release resulted in increased plasma total and LDL cholesterol levels, decreased HDL levels, and increased aortic cholesterol deposition. However, daily administration of 1 mg/kg naltrexone completely reversed these effects on both cholesterol levels and aortic cholesterol deposition. The effect of morphine on total and LDL cholesterol levels was also observed in rats fed a normal diet [66].

In the present study, the effect of opioid receptor blockade on atherosclerotic plaque development and hepatic steatosis in mice was also examined. NLX administration did not affect atherosclerotic plaque formation in the aortic arch (Figure 2a,c, publication 2), nor did it influence hepatic steatosis and fibrosis (Figure 2b,d and Figure 4, publication 2). The findings presented above do not demonstrate any significant changes in atherosclerotic plaque development or hepatic lipid deposition following NLX treatment. However, one study reported a marked reduction in atherosclerotic plaque formation after long-term, 10-week administration of NLX in $ApoE^{-/-}$ mice starting at 8 weeks of age [67]. In contrast, a 21-day study using another opioid receptor antagonist - nalmefene (antagonist for μ- and δ-opioid receptors and a partial agonist at κ-opioid receptors) revealed a dose-dependent increase in plaque formation and enhanced development of macrophage-rich lesions in $ApoE^{-/-}$ mice. Furthermore, nalmefene administration significantly increased oxidized LDL uptake by macrophages in RAW264.7 cell line, while simultaneously reducing mRNA expression of μ-, δ-, and κ-opioid receptors [68]. This suggests that extended NLX administration during the early stages of atherosclerotic plaque development - rather than at the advanced stages observed in our study - could markedly limit both the formation and progression of atherosclerotic plaques.

Although a significant increase in plasma HDL levels was observed following NLX treatment, the functional relevance of this change remains to be clarified. Recent evidence suggests that HDL cholesterol levels alone does not adequately represent its atheroprotective functions, such as cholesterol efflux capacity, antioxidant properties, or anti-inflammatory activity [69]. In fact, impaired HDL functionality has been proposed as an independent risk factor for atherosclerosis in patients with non-alcoholic fatty liver disease [70]. Therefore, it is possible that the elevation of HDL levels observed in our model may not necessarily translate into cardiovascular protection. In this context, serum amyloid A (Saa) may be of particular relevance, as its abundance was reduced after NLX treatment in the proteomic analysis of livers presented below (Figure 6b, Publication 2). Elevated serum Saa levels have been shown to interfere with HDL function by displacing apoA-I from HDL particles, thereby reducing cholesterol efflux capacity [71]. This suggests that the observed decrease in Saa levels may contribute to improved HDL functionality, although this hypothesis requires further experimental validation. The liver plays a major role in the regulation of lipid metabolism and may therefore represent a key factor in processes related to the development of atherosclerosis. Conversely, the progression of atherosclerosis contributes to pathological changes in the liver, such as steatosis [72,73]. In the results presented in this dissertation, no changes were observed in hepatic steatosis levels or in atherosclerotic plaque development. These findings are consistent with other reports showing that patients with hepatic steatosis exhibit significantly higher LDL and lower HDL levels compared with individuals without steatosis [74].

Furthermore, studies indicate that hepatic steatosis is more prevalent in patients with carotid atherosclerotic plaques and aortic calcification than in those without vascular damage [75]. Pediatric and adolescent studies have also demonstrated an association between increased carotid intima-media thickness, a high triglyceride-to-HDL ratio, elevated blood pressure, insulin resistance, and non-alcoholic fatty liver disease [76]. Although the presented study did not reveal changes in hepatic steatosis levels following NLX administration, other studies have shown that long-term NLX treatment can reverse morphine-induced histopathological damage [77]. Interestingly, administration of another opioid receptor antagonist, naltrexone, for 28 days in BDL rats (bile duct-ligated rats, used as a model of liver fibrosis [78]) significantly attenuated the development of hepatic fibrosis [79]. Moreover, there were no changes in hepatic fibrosis levels after NLX treatment; however, in rats with hepatotoxin-dimethylnitrosamine-induced liver fibrosis, NLX reduced collagen deposition after five weeks of treatment [80]. It should be noted, though, that in these studies NLX was administered over much longer periods than in our experiments.

Although histological analysis did not reveal any alterations in hepatic steatosis following NLX administration, the expression of genes associated with lipid metabolism was subsequently examined in the livers of 36-week-old mice. Among the analyzed genes, no changes were observed in expression of *Srebf1* or *Lpl*, whereas a significant decrease in *Fabp4* expression was detected (Figure 3, publication 2). The *Srebf1* gene encodes the transcription factor sterol regulatory element binding 1 (Srebf1), which belongs to the family of sterol regulatory element binding proteins (SREBPs) that may regulate lipid homeostasis by controlling target genes essential for cholesterol and fatty acid metabolism [81]. *Srebf1* is a key factor in lipogenesis - the metabolic pathway that through which excess carbohydrates are converted into fatty acids, which are ultimately esterified with glycerol-3-phosphate to triglycerides [82]. The important role of *Srebf1* in lipogenesis is underscored by findings indicating that the expression of this gene is significantly higher in the liver of patients with nonalcoholic steatosis compared with healthy individuals [83]. Moreover, suppression of *Sreb-1c* expression in hepatocytes via activation of 5′AMP-activated protein kinase (Ampk) has been shown to protect against hepatic steatosis and hyperlipidemia in diet-induced, insulin-resistant LDL receptor-deficient mice [84]. Another study revealed that SREBF1/SREBP-1c contributes to hepatic lipid accumulation both through the effect of increased lipid synthesis and in combination with reduced lipid degradation, dependent on autophagic dysregulation [85]. Additionally, polymorphism in the *Srebf-2* gene (which is responsible for the regulation of cholesterol homeostasis [81]), have been shown to predispose to non-alcoholic fatty liver disease and related cardiometabolic abnormalities, as well as to affects liver histology and glucose and lipid metabolism [86]. Collectively, the studies discussed above suggest a negative effect of the *Srebf1* gene in hepatic steatosis. In the studies presented in this dissertation, no changes in *Srebf1* expression were detected in the liver of ApoE$^{-/-}$ mice following NLX administration.

The next gene analyzed was *Lpl*, which encodes a key enzyme responsible for hydrolyzing core triglycerides in chylomicrons and very low-density lipoproteins (VLDL), thereby generating chylomicron remnants and intermediate-density lipoproteins (IDL). The liberated fatty acids and monoacylglycerols are partially taken up by local tissues and further metabolized. For instance, they may be stored as neutral lipids in adipose tissue, oxidized or stored in cardiac and skeletal muscle, or accumulated as cholesterol esters and triglycerides within macrophages [87,88]. Clinical studies have shown that patients with severe hepatic steatosis exhibit markedly higher serum lipoprotein lipase (LPL) activity compared to those with mild or moderate forms of the disease [89]. In addition, morbidly obese individuals display significantly increased hepatic LPL activity relative to healthy individuals, independent of liver fibrosis or steatosis status [90]. It should be noted that the role of LPL in atherosclerosis remains controversial, as both protective

and harmful effects have been reported. Some studies showed that NO-1886, an LPL activator, improves glucose and lipid metabolism and suppresses atherosclerosis [91–93]. LPL derived for example from heart, skeletal muscle, and adipose tissue is generally considered anti-atherogenic by lowering atherogenic lipoproteins and raising HDL [94]. In contrast, LPL in the aorta may have a pro-atherogenic effect [95]. An increase in plasma LPL activity lowers TG levels and raises HDL concentrations, contributing to a protective action against atherosclerosis. However, elevated vessel wall LPL promotes atherogenesis, indicating that the role of LPL in atherosclerosis is location-dependent [96]. In the presented studies, no changes in hepatic *Lpl* mRNA expression were observed following NLX treatment.

The third gene analyzed was *Fabp4*, which encodes a small, highly conserved cytosolic protein that binds long-chain fatty acids and other hydrophobic ligands, thereby regulating intracellular lipid transport [97]. While initially identified in adipose tissue, FABP4 is also expressed in macrophages, ECs, and cardiomyocytes [97,98]. Studies demonstrated that treatment with a *Fabp4* inhibitor (50 mg/kg/day for 8 weeks) in combination with rosiglitazone, a type II diabetes drug that acts as an insulin sensitizer, attenuated rosiglitazone-induced hepatic steatosis in obese diabetic db/db mice [99]. Although, in our study, histological assessment revealed no changes in hepatic steatosis following NLX treatment, molecular analysis showed a significant reduction in *Fabp4* mRNA expression in the liver of $ApoE^{-/-}$ mice (fold change of 0.8). Fabp4 is considered a critical regulator of lipid transport, metabolism, and storage, and elevated protein levels have been linked to hepatic steatosis, particularly in individuals with metabolic disorders such as obesity and diabetes [100]. Thus, the observed decrease in *Fabp4* expression may represent an early molecular indicator of hepatic fat accumulation, not yet detectable at the histological level.

An additional indicator of hepatic steatosis is the accumulation of macrophages within the liver. In the presented study, immunofluorescence staining of liver cross sections showed statistical significance increase in macrophages expression after NLX treatment in $ApoE^{-/-}$ mice (Figure 5, publication 2). This finding is consistent with the previous reports demonstrating elevated macrophage infiltration during liver steatosis. However, macrophages are a heterogeneous cell population with diverse physiological and pathological roles, encompassing both proatherogenic (M1) and protective (M2) subsets [101,102]. A limitation of study presented in this dissertation is the lack of distinction between macrophage subtypes. Notably, Liu et al. demonstrated that NLX pretreatment markedly reduced macrophage secretion of tumor necrosis factor alpha (TNF-α), interleukin-6, monocyte chemoattractant protein-1, and superoxide in response to stimulation [67]. Comparable results were obtained in RAW264.7 murine

macrophage cell line, further supporting the anti-inflammatory effects of NLX on macrophages [103].

To comprehensively investigate changes in protein abundance following NLX administration, a quantitative proteomic analysis, in key organs involved in the development of atherosclerosis, was performed. LC-MS/MS analysis identified and quantified 6574 proteins in the liver and 6869 proteins in the aorta. Using threshold values of $q < 0.05$ and fold change ≥ 2 or ≤ -2, a total of 38 differentially abundant proteins were identified in the livers of NLX-treated mice compared to controls (Figure 6, Publication 2). These proteins were functionally associated with muscle structure and function (e.g., Rb1cc1, Pdlim3), cell migration and proliferation (e.g., Ifit3), inflammatory and immune responses (e.g., Gbp, Steap4, Fgl1), cell death regulation (e.g., Zbp1), and heavy metal binding (e.g., Mt1) (publication 2, Supplementary Materials, Table S1). Furthermore, in the aorta, proteomic profiling identified 587 proteins with significantly altered expression following NLX treatment (Figure 9a, publication 1). Among these, the 29 most markedly abundant proteins with fold change greater than 3 or less than −3 and $q < 0.05$ were selected (Figure 9b, publication 1). These included proteins associated with immune responses (e.g., Ccl9, Saa1), lipid metabolism (e.g., Acsm1, Fabp1), wound healing (e.g., Arg1), as well as those involved in glycolysis and gluconeogenesis (e.g., Pklr, Aldob, Fbp1) (publication 1, Supplementary Materials, Table S2).

Subsequently, proteins implicated in lipid metabolism and the pathogenesis of atherosclerosis were selected for more detailed discussion (Table 2).

Table 2. Key proteins highlighted to detailed discussion

Deregulation	Liver		
	Protein	Name	Gene
↓	Q8VBT6	apolipoprotein B receptor	*Apobr*
↓	P05367	serum amyloid A	*Saa2*
↓	O55239	nicotinamide N-methyltransferase	*Nnmt*
↑	P11588	major urinary protein 1	*Mup1*

Deregulation	Aorta		
	Protein	Name	Gene
↓	Q91Y97	fructose-bisphosphate aldolase B	*Aldob*
↓	P30115	glutathione S-transferase A3	*Gsta3*
↓	Q61176	arginase-1	*Arg1*

The first protein that deserves particular attention is the apolipoprotein B receptor (Q8VBT6), encoded by the *Apobr* gene, whose abundance decreased in liver following NLX treatment. This receptor binds apolipoprotein B (ApoB), a molecule that plays a pivotal role in the development of atherosclerosis [104,105]. ApoB is a large amphipathic glycoprotein essential for lipoprotein metabolism in humans. The *APOB* gene generates two isoforms through post-transcriptional editing: apoB-48, which is essential for the chylomicrons formation in the small intestine, and apoB-100, necessary for the synthesis of VLDL in the liver [104]. Missense mutations in the LDL receptor - binding domain of *APOB* cause familial defective apoB-100 ligand, a condition characterized by hypercholesterolemia and premature coronary artery disease [106]. Studies have also shown that inhibition of ApoB reduces total and LDL cholesterol levels in mice [107] as well as LDL levels in humans [108]. Another protein downregulated in the mice liver after NLX treatment and that warrants mention is serum amyloid A (Saa) (P05367), encoded by the *Saa2* gene. Saa represents a family of small apolipoproteins and binds to HDL particles. It functions as both an acute-phase marker and pro-inflammatory factor, which serum levels are markedly elevated during chronic inflammation in humans [109,110]. Moreover, studies have demonstrated that in patients with endotoxin-induced inflammation, macrophage cholesterol efflux capacity correlates with elevated Saa1 and Saa2 levels. Similarly, in mice, acute inflammation markedly impairs HDL efflux, accompanied by a significant rise in Saa levels [111]. Another protein closely linked to cholesterol regulation which abundance was altered by NLX in the presented study is nicotinamide N-methyltransferase (O55239), encoded by the *Nnmt* gene. The pivotal role of *Nnmt* in lipid metabolism is supported by evidence that its inhibition in

L02 human fetal hepatocyte cell line significantly reversed thiamexotham-induced lipid accumulation [112]. Moreover, transgenic mice overexpressing *Nnmt* and fed a high-fat diet develop hepatic steatosis, characterized by increased expression of genes involved in fatty acid uptake, reduced VLDL secretion, as well as hepatic fibrosis accompanied by the induction of inflammatory and fibrotic genes [113]. Notably, inhibition of Nnmt in obese mice has been shown to reduce total plasma cholesterol levels [114], while deletion of the *Nnmt* gene resulted in lower total and LDL cholesterol levels in mice with non-alcoholic steatohepatitis [115]. Another NLX-responsive hepatic protein involved in lipid metabolism is major urinary protein 1 (Mup1) (P11588), encoded by *Mup1* gene, which abundance increased following NLX administration. Mup1, a member of the lipocalin family, is highly secreted into the circulation by the liver. Beyond its classical role in binding lipophilic pheromones for chemical communication in rodents, Mup1 also regulates glucose and lipid metabolism. Importantly, MUP1 has been shown to suppresses lipogenesis - high hepatic Mup1 levels inhibit the expression of stearoyl-CoA desaturase-1, fatty acid synthase, carbohydrate response element-binding protein (ChREBP), and peroxisome proliferator-activated receptor γ (PPARγ) in db/db mice [116]. Studies also indicated that Mup1 levels in the liver, serum, and urine were significantly decreased in both genetically and high-fat-diet induced non-alcoholic fatty liver disease mice [117]. However, it should be pointed out that there are scientific studies showing that male mice with cluster knockout (deleted region between *Mup4* and *Mup21*) of the major urinary protein gene showed lipid accumulation in plasma and liver, which was accompanied by hepatic transcripts indicating the activation of lipogenesis [118].

Among the most significantly altered proteins in the aorta was fructose-bisphosphate aldolase B (Q91Y97), encoded by *Aldob*, which contributes to VSMC proliferation. This is supported by studies demonstrating that reduced *Aldob* expression prevents fructose-induced overproduction of methylglyoxal and VSMC proliferation [119]. Excessive proliferation of VSMCs is a critical event in the progression of vascular diseases, promoting neointima formation, vessel wall thickening, and arterial stiffness - hallmarks of atherosclerosis [119,120]. Another protein affected by NLX was glutathione S-transferase A3 (Gsta3) (P30115), encoded by *Gsta3*. This enzyme plays a key role in cellular detoxification, particularly in neutralizing reactive oxygen species (ROS) and protecting cells against oxidative stress. Since oxidative stress is a major driver of atherogenesis, elevated Gsta3 expression may represent an adaptive cellular response aimed at mitigating lipid peroxidation and inflammation within atherosclerotic lesions [121]. Additionally, arginase-1 (Q61176), encoded by *Arg1*, exhibited altered expression following NLX administration. Arginase-1 (Arg1) serves as a marker of M2 macrophages, which play an important role in atherosclerotic plaque formation as well as in wound healing and tissue

repair. In the context of atherosclerosis, M2 macrophages contribute to plaque stability by promoting extracellular matrix remodeling; however, they may also participate in excessive fibrotic responses that affect plaque composition. Arg1competes with nitric oxide synthase (NOS) for L-arginine, thereby reducing nitric oxide (NO) production - a key mediator of vasodilation and endothelial function. Decreased NO bioavailability may contribute to vascular dysfunction, increased oxidative stress, and enhanced inflammatory responses, exacerbating atherosclerosis progression [67,122]. It is important to emphasize that despite numerous beneficial effects of the opioid system in cardiovascular diseases, some studies have reported detrimental outcomes. For instance, research has revealed a relationship between the opioid system and atherosclerosis in the context of depression [123]. The comorbidity between these conditions has been attributed to increased atherogenicity, insulin resistance (IR), and immune and oxidative stress. Neural network and logistic regression models demonstrated that severe depression in patients with acute coronary syndrome or unstable angina was best predicted by interleukin-6 (IL-6), MOR, zinc, β-endorphin, calcium, and magnesium, while moderate depression was associated with IL-6, zinc, MOR, β-endorphin, atherogenicity, IR, and calcium [123]. However, it should be noted that administration of U50488H (a selective κ-opioid receptor agonist) attenuated ischemia-induced arrhythmias in rat models [124], while naltrexone, an opioid antagonist, prevented stress-induced hypercholesterolemia in rats, suggesting that endogenous opioid systems may play a role in the regulation of cholesterol homeostasis, a key determinant of atherosclerosis development [65].

6. Conclusions

- Blockade of the opioid system with NLX in ApoE$^{-/-}$ mice induced distinct molecular and structural alterations in the vascular wall, immune system, and liver, depending on the stage of atherosclerosis. In both young and aged animals, NLX treatment significantly downregulated *Hmmr* gene expression in the aorta, suggesting a consistent role of this gene in vascular remodeling. Alterations in collagen gene expression and collagen layer thickness indicate that opioid receptor inhibition modulates extracellular matrix organization in an age-dependent manner, potentially affecting vascular stiffness and resistance.

- Analysis of splenic T-cell subpopulations revealed limited effects of NLX on their overall proportions but demonstrated significant alterations in *Hmmr* expression within specific T-cell subpopulations, particularly CD8^{+} and central memory T-cells. These findings point to a potential link between opioid signaling, adaptive immunity, and vascular inflammation.

- NLX administration in aged mice did not alter atherosclerotic plaque size or hepatic steatosis but increased HDL levels, suggesting subtle modulation of lipid metabolism. At the molecular level, NLX reduced hepatic *Fabp4* expression, which may indicate early protective modulation of lipid metabolism processes. Proteomic profiling further supported NLX-induced alterations in proteins involved in lipid metabolism, inflammation, oxidative stress, and vascular remodeling.

Overall, the findings suggest that opioid receptor blockade influences multiple mechanisms relevant to atherosclerosis - particularly collagen remodeling, lipid metabolism and immune regulation. These effects appear to be stage-dependent and may either mitigate or exacerbate atherosclerotic processes depending on disease progression and tissue environment.

7. Bibliography

[1] Björkegren JLM, Lusis AJ. Atherosclerosis: Recent developments. Cell 2022;185:1630–45. https://doi.org/10.1016/J.CELL.2022.04.004.

[2] Libby P, Ridker PM, Maseri A. Inflammation and Atherosclerosis 2002. https://doi.org/10.1161/hc0902.104353.

[3] Steffensen LB, Mortensen MB, Kjolby M, Hagensen MK, Oxvig C, Bentzon JF. Disturbed laminar blood flow vastly augments lipoprotein retention in the artery wall: A key mechanism distinguishing susceptible from resistant sites. Arterioscler Thromb Vasc Biol 2015;35:1928–35. https://doi.org/10.1161/ATVBAHA.115.305874.

[4] Rafieian-Kopaei M, Setorki M, Doudi M, Baradaran A, Nasri H. Atherosclerosis: Process, Indicators, Risk Factors and New Hopes. Int J Prev Med 2014;5.

[5] Falk E. Pathogenesis of Atherosclerosis. J Am Coll Cardiol 2006;47:C7–12. https://doi.org/10.1016/j.jacc.2005.09.068.

[6] Pepin ME, Gupta RM. The Role of Endothelial Cells in Atherosclerosis: Insights from Genetic Association Studies. American Journal of Pathology 2024;194:499–509. https://doi.org/10.1016/j.ajpath.2023.09.012.

[7] Rahimi N. Defenders and Challengers of Endothelial Barrier Function. Front Immunol 2017;8. https://doi.org/10.3389/FIMMU.2017.01847.

[8] Cybulsky MI, Gimbrone MA. Endothelial expression of a mononuclear leukocyte adhesion molecule during atherogenesis. Science 1991;251:788–91. https://doi.org/10.1126/SCIENCE.1990440.

[9] Gimbrone MA, Nagel T, Topper JN. Biomechanical activation: an emerging paradigm in endothelial adhesion biology. J Clin Invest 1997;99:1809–13. https://doi.org/10.1172/JCI119346.

[10] Robbins CS, Hilgendorf I, Weber GF, Theurl I, Iwamoto Y, Figueiredo JL, et al. Local proliferation dominates lesional macrophage accumulation in atherosclerosis. Nat Med 2013;19:1166–72. https://doi.org/10.1038/NM.3258.

[11] Yu XH, Fu YC, Zhang DW, Yin K, Tang CK. Foam cells in atherosclerosis. Clinica Chimica Acta 2013;424:245–52. https://doi.org/10.1016/J.CCA.2013.06.006.

[12] Zhu SN, Chen M, Jongstra-Bilen J, Cybulsky MI. GM-CSF regulates intimal cell proliferation in nascent atherosclerotic lesions. J Exp Med 2009;206:2141. https://doi.org/10.1084/JEM.20090866.

[13] Tse K, Tse H, Sidney J, Sette A, Ley K. T cells in atherosclerosis. Int Immunol 2013;25:615–22. https://doi.org/10.1093/intimm/dxt043.

[14] Saigusa R, Winkels H, Ley K. T cell subsets and functions in atherosclerosis. Nat Rev Cardiol 2020;17:387–401. https://doi.org/10.1038/S41569-020-0352-5,.

[15] Robertson AKL, Rudling M, Zhou X, Gorelik L, Flavell RA, Hansson GK. Disruption of TGF-beta signaling in T cells accelerates atherosclerosis. J Clin Invest 2003;112:1342–50. https://doi.org/10.1172/JCI18607.

[16] Plenz GAM, Deng MC, Robenek H, Völker W. Vascular collagens: spotlight on the role of type VIII collagen in atherogenesis. Atherosclerosis 2003;166:1–11. https://doi.org/10.1016/S0021-9150(01)00766-3.

[17] Romanic AM, Adachi E, Kadler KE, Hojima Y, Prockop DJ. Copolymerization of pNcollagen III and collagen I: pNcollagen III decreases the rate of incorporation of collagen I into fibrils, the amount of collagen i incorporated, and the diameter of the fibrils formed. Journal of Biological Chemistry 1991;266:12703–9. https://doi.org/10.1016/s0021-9258(18)98956-8.

[18] Fingerle J; Kraft T. The induction of smooth muscle cell proliferation in vitro using an organ culture system. International Angiology 1987;6:65–72.

[19] Souilhol C, Harmsen MC, Evans PC, Krenning G. Endothelial-mesenchymal transition in atherosclerosis. Cardiovasc Res 2018;114:565–77. https://doi.org/10.1093/cvr/cvx253.

[20] Doran AC, Meller N, McNamara CA. Role of smooth muscle cells in the initiation and early progression of atherosclerosis. Arterioscler Thromb Vasc Biol 2008;28:812–9. https://doi.org/10.1161/ATVBAHA.107.159327.

[21] Fingerle J, Au YPT, Clowes AW, Reidy MA, Hoff-Mann- F, Roche L. Intimal Lesion Formation in Rat Carotid Arteries after Endothelial Denudation in Absence of Medial Injury. n.d.

[22] Newby AC, Zaltsman AB. Fibrous cap formation or destruction-the critical importance of vascular smooth muscle cell proliferation, migration and matrix formation. vol. 41. 1999.

[23] Shang J, Zhang X, Hou G, Qi Y. HMMR potential as a diagnostic and prognostic biomarker of cancer—speculation based on a pan-cancer analysis. Front Surg 2023;9. https://doi.org/10.3389/fsurg.2022.998598.

[24] Hinneh JA, Gillis JL, Mah CY, Irani S, Shrestha RK, Ryan NK, et al. Targeting hyaluronan-mediated motility receptor (HMMR) enhances response to androgen receptor signalling inhibitors in prostate cancer. Br J Cancer 2023;129:1350–61. https://doi.org/10.1038/s41416-023-02406-8.

[25] Blanco I, Kuchenbaecker K, Cuadras D, Wang X, Barrowdale D, Ruiz de Garibay G, et al. Assessing Associations between the AURKA-HMMR-TPX2-TUBG1 Functional Module and Breast Cancer Risk in BRCA1/2 Mutation Carriers. Dominique Stoppa-Lyonnet 2015;106. https://doi.org/10.1371/journal.pone.0120020.

[26] Jaskuła K, Sacharczuk M, Gaciong Z, Skiba DS. Cardiovascular Effects Mediated by HMMR and CD44. Mediators Inflamm 2021;2021. https://doi.org/10.1155/2021/4977209.

[27] Missinato MA, Tobita K, Romano N, Carroll JA, Tsang M. Extracellular component hyaluronic acid and its receptor Hmmr are required for epicardial EMT during heart regeneration n.d. https://doi.org/10.1093/cvr/cvv190.

[28] Krolikoski M, Monslow J, Puré E. The CD44-HA axis and inflammation in atherosclerosis: A temporal perspective. Matrix Biology 2019;78–79:201–18. https://doi.org/10.1016/J.MATBIO.2018.05.007.

[29] Cuff CA, Kothapalli D, Azonobi I, Chun S, Zhang Y, Belkin R, et al. The adhesion receptor CD44 promotes atherosclerosis by mediating inflammatory cell recruitment and vascular cell activation. Journal of Clinical Investigation 2001;108:1031–40. https://doi.org/10.1172/JCI12455.

[30] Stein C. Opioid Receptors 2024;29:45. https://doi.org/10.1146/annurev-med-062613-093100.

[31] Cooper K, Carmody J. The characteristics of the opioid-related analgesia induced by the stress of swimming in the mouse. Neurosci Lett 1982;31:165–70. https://doi.org/10.1016/0304-3940(82)90110-0.

[32] Juni A, Klein G, Pintar JE, Kest B. Nociception increases during opioid infusion in opioid receptor triple knock-out mice. Neuroscience 2007;147:439–44. https://doi.org/10.1016/J.NEUROSCIENCE.2007.04.030.

[33] Jelen LA, Stone JM, Young AH, Mehta MA. The opioid system in depression. Neurosci Biobehav Rev 2022;140:104800. https://doi.org/10.1016/j.neubiorev.2022.104800.

[34] Sternini C, Patierno S, Selmer IS, Kirchgessner A. The opioid system in the gastrointestinal tract. Neurogastroenterology and Motility 2004;16:3–16. https://doi.org/10.1111/j.1743-3150.2004.00553.x.

[35] Rabkin SW. Endogenous kappa opioids mediate the action of brain angiotensin II to increase blood pressure. Neuropeptides 2007;41:411–9. https://doi.org/10.1016/J.NPEP.2007.09.003.

[36] Treskatsch S, Shaqura M, Dehe L, Feldheiser A, Roepke TK, Shakibaei M, et al. Upregulation of the kappa opioidergic system in left ventricular rat myocardium in response to volume overload: Adaptive changes of the cardiac kappa opioid system in heart failure. Pharmacol Res 2015;102:33–41. https://doi.org/10.1016/J.PHRS.2015.09.005.

[37] Meng X, Yang J, Dong M, Zhang K, Tu E, Gao Q, et al. Regulatory T cells in cardiovascular diseases. Nat Rev Cardiol 2016;13:167–79. https://doi.org/10.1038/NRCARDIO.2015.169.

[38] Ninković J, Roy S. Role of the mu-opioid receptor in opioid modulation of immune function. Amino Acids 2013;45:9–24. https://doi.org/10.1007/S00726-011-1163-0/TABLES/3.

[39] Ondrovics M, Hoelbl-Kovacic A, Fux DA. Opioids: Modulators of angiogenesis in wound healing and cancer. Oncotarget 2017;8:25783–96. https://doi.org/10.18632/ONCOTARGET.15419,.

[40] Wiśniewski JR, Gaugaz FZ. Fast and sensitive total protein and peptide assays for proteomic analysis. Anal Chem 2015;87:4110–6.

[41] Wiśniewski JR. Quantitative evaluation of filter aided sample preparation (FASP) and multienzyme digestion FASP protocols. Anal Chem 2016;88:5438–43.

[42] Bruderer R, Bernhardt OM, Gandhi T, Miladinović SM, Cheng L-Y, Messner S, et al. Extending the limits of quantitative proteome profiling with data-independent

acquisition and application to acetaminophen-treated three-dimensional liver microtissues*[S]. Molecular & Cellular Proteomics 2015;14:1400–10.

[43] Huang T, Bruderer R, Muntel J, Xuan Y, Vitek O, Reiter L. Combining precursor and fragment information for improved detection of differential abundance in data independent acquisition. Molecular & Cellular Proteomics 2020;19:421–30.

[44] Storey JD. A direct approach to false discovery rates. J R Stat Soc Series B Stat Methodol 2002;64:479–98.

[45] Vizcaíno JA, Deutsch EW, Wang R, Csordas A, Reisinger F, Ríos D, et al. ProteomeXchange provides globally co-ordinated proteomics data submission and dissemination HHS Public Access Author manuscript. Nat Biotechnol 2014;32:223–6. https://doi.org/10.1038/nbt.2839.

[46] Diaz LC, Silva PG de B, Dantas TS, Mota MRL, Alves APNN, Rodrigues MI de Q, et al. Naltrexone accelerated oral traumatic ulcer healing and downregulated TLR-4/NF-kB pathway in Wistar rats. Arch Oral Biol 2024;166. https://doi.org/10.1016/j.archoralbio.2024.106047.

[47] Dunn J, Liu Y, Banov F, Denison S, Banov D. A topical naltrexone formulation for surgical wound healing: A case report. J Cosmet Dermatol 2021;20:838–41. https://doi.org/10.1111/jocd.13604.

[48] Kuzan A, Wisniewski J, Maksymowicz K, Kobielarz M, Gamian A, Chwilkowska A. Relationship between calcification, atherosclerosis and matrix proteins in the human aorta. Folia Histochem Cytobiol 2021;59:8–21. https://doi.org/10.5603/FHC.A2021.0002.

[49] Sansilvestri-Morel P, Rupin A, Badier-Commander C, Kern P, Fabiani JN, Verbeuren TJ, et al. Imbalance in the synthesis of collagen type I and collagen type III in smooth muscle cells derived from human varicose veins. J Vasc Res 2001;38:560–8. https://doi.org/10.1159/000051092.

[50] Mays PK, Bishop JE, Laurent GJ. Age-related changes in the proportion of types I and III collagen. Mech Ageing Dev 1988;45:203–12. https://doi.org/10.1016/0047-6374(88)90002-4.

[51] Maurel E, Shuttleworth CA, Bouissou H. Interstitial collagens and ageing in human aorta. Virchows Arch A Pathol Anat Histopathol 1987;410:383–90. https://doi.org/10.1007/BF00712757.

[52] Hansen L, Taylor WR. Is increased arterial stiffness a cause or consequence of atherosclerosis? Atherosclerosis 2016;249:226–7. https://doi.org/10.1016/J.ATHEROSCLEROSIS.2016.04.014.

[53] de Figueiredo Borges L, Jaldin RG, Dias RR, Stolf NAG, Michel J-B, Gutierrez PS. Collagen is reduced and disrupted in human aneurysms and dissections of ascending aorta. Hum Pathol 2008;39:437–43. https://doi.org/https://doi.org/10.1016/j.humpath.2007.08.003.

[54] Kochová P, Kuncová J, Švíglerová J, Cimrman R, Miklíková M, Liška V, et al. The contribution of vascular smooth muscle, elastin and collagen on the passive mechanics

of porcine carotid arteries. Physiol Meas 2012;33:1335. https://doi.org/10.1088/0967-3334/33/8/1335.

[55] Immonen JA, Zagon IS, Lewis GS, McLaughlin PJ. Topical treatment with the opioid antagonist naltrexone accelerates the remodeling phase of full-thickness wound healing in type 1 diabetic rats. Https://DoiOrg/101177/1535370213502632 2013;238:1127–35. https://doi.org/10.1177/1535370213502632.

[56] Hinkley H, Counts DA, VonCanon E, Lacy M. T Cells in Atherosclerosis: Key Players in the Pathogenesis of Vascular Disease. Cells 2023;12. https://doi.org/10.3390/CELLS12172152,.

[57] Grivel JC, Ivanova O, Pinegina N, Blank PS, Shpektor A, Margolis LB, et al. Activation of T Lymphocytes in Atherosclerotic Plaques. Arterioscler Thromb Vasc Biol 2011;31:2929–37. https://doi.org/10.1161/ATVBAHA.111.237081.

[58] Bryant HU, Yoburn BC, Inturrisi CE, Bernton EW, Holaday JW. Morphine-induced immunomodulation is not related to serum morphine concentrations. Eur J Pharmacol 1988;149:165–9. https://doi.org/10.1016/0014-2999(88)90057-X.

[59] Bryant HU, Bernton EW, Holaday JW. Morphine pellet-induced immunomodulation in mice: temporal relationships. J Pharmacol Exp Ther 1988;245:913–20. https://doi.org/10.1016/s0022-3565(25)24111-8.

[60] Tabas I, Lichtman AH. Monocyte-Macrophages and T Cells in Atherosclerosis. Immunity 2017;47:621–34. https://doi.org/10.1016/j.immuni.2017.09.008.

[61] Skiba D, Jaskuła K, Nawrocka A, Poznański P, Łazarczyk M, Szymański Ł, et al. The Role of Opioid Receptor Antagonists in Regulation of Blood Pressure and T-Cell Activation in Mice Selected for High Analgesia Induced by Swim Stress. Int J Mol Sci 2024;25. https://doi.org/10.3390/ijms25052618.

[62] Solin A V., Lyashev AY, Lyashev YD. Effects of Opioid Peptides on Changes in Lipid Metabolism in Rats Subjected to Swimming Stress. Bull Exp Biol Med 2017;162:313–5. https://doi.org/10.1007/S10517-017-3603-7.

[63] Kazemi M, Bazyar M, Naghizadeh MM, Dehghan A, Rahimabadi MS, Chijan MR, et al. Lipid profile dysregulation in opium users based on Fasa PERSIAN cohort study results. Sci Rep 2021;11. https://doi.org/10.1038/S41598-021-91533-4.

[64] Huang Z, Liang L, Li L, Xu M, Li X, Sun H, et al. Opioid doses required for pain management in lung cancer patients with different cholesterol levels: negative correlation between opioid doses and cholesterol levels. Lipids Health Dis 2016;15. https://doi.org/10.1186/S12944-016-0212-9.

[65] Bryant HU, Story JA, Yim GKW. Assessment of endogenous opioid mediation in stress-induced hypercholesterolemia in the rat. Psychosom Med 1988;50:576–85. https://doi.org/10.1097/00006842-198811000-00003,.

[66] Bryant HU, Story JA, Yim GK. Morphine-induced alterations in plasma and tissue cholesterol levels. Life Sci 1987;41:545–54. https://doi.org/10.1016/0024-3205(87)90406-1.

[67] Liu SL, Li YH, Shi GY, Chen YH, Huang CW, Hong JS, et al. A Novel Inhibitory Effect of Naloxone on Macrophage Activation and Atherosclerosis Formation in Mice. J Am Coll Cardiol 2006;48:1871–9. https://doi.org/10.1016/j.jacc.2006.07.036.

[68] Koga M, Inada K, Yamada A, Maruoka K, Yamauchi A. Nalmefene, an opioid receptor modulator, aggravates atherosclerotic plaque formation in apolipoprotein E knockout mice by enhancing oxidized low-density lipoprotein uptake in macrophages. Biochem Biophys Rep 2024;38:101688. https://doi.org/10.1016/j.bbrep.2024.101688.

[69] Rohatgi A, Khera A, Berry JD, Givens EG, Ayers CR, Wedin KE, et al. HDL Cholesterol Efflux Capacity and Incident Cardiovascular Events. New England Journal of Medicine 2014;371:2383–93. https://doi.org/10.1056/NEJMOA1409065/SUPPL_FILE/NEJMOA1409065_DISCLOSURES.PDF.

[70] Fadaei R, Poustchi H, Meshkani R, Moradi N, Golmohammadi T, Merat S. Impaired HDL cholesterol efflux capacity in patients with non-alcoholic fatty liver disease is associated with subclinical atherosclerosis. Sci Rep 2018;8:11691. https://doi.org/10.1038/S41598-018-29639-5.

[71] Thomas MJ, Sorci-Thomas MG. SAA: a link between cholesterol efflux capacity and inflammation? J Lipid Res 2015;56:1383. https://doi.org/10.1194/JLR.C061366.

[72] Pais R, Giral P, Khan JF, Rosenbaum D, Housset C, Poynard T, et al. Fatty liver is an independent predictor of early carotid atherosclerosis. J Hepatol 2016;65:95–102. https://doi.org/10.1016/j.jhep.2016.02.023.

[73] Libby P. The changing landscape of atherosclerosis. 524 | Nature | 2021;592. https://doi.org/10.1038/s41586-021-03392-8.

[74] Völzke H, Robinson DM, Kleine V, Deutscher R, Hoffmann W, Lüdemann J, et al. Hepatic steatosis is associated with an increased risk of carotid atherosclerosis of Health in Pomerania. World J Gastroenterol 2005;11:1848–53.

[75] Baragetti A, Pisano G, Bertelli C, Garlaschelli K, Grigore L, Fracanzani AL, et al. Subclinical atherosclerosis is associated with Epicardial Fat Thickness and hepatic steatosis in the general population. Nutrition, Metabolism and Cardiovascular Diseases 2016;26:141–53. https://doi.org/10.1016/j.numecd.2015.10.013.

[76] Pacifico L, Bonci E, Andreoli G, Romaggioli S, Di Miscio R, Lombardo C V., et al. Association of serum triglyceride-to-HDL cholesterol ratio with carotid artery intima-media thickness, insulin resistance and nonalcoholic fatty liver disease in children and adolescents. Nutrition, Metabolism and Cardiovascular Diseases 2014;24:737–43. https://doi.org/10.1016/j.numecd.2014.01.010.

[77] Peirouvi T, Mirbaha Y, Fathi-Azarbayjani A, Jalali AS. Co-Administration of Morphine and Naloxone: Histopathological and Biochemical Changes in the Rat Liver. Int J High Risk Behav Addict 2020;9. https://doi.org/10.5812/ijhrba.100594.

[78] Wu S, Wang X, Xing W, Li F, Liang M, Li K, et al. An update on animal models of liver fibrosis. Front Med (Lausanne) 2023;10.

[79] Ebrahimkhani MR, Kiani S, Oakley F, Kendall T, Shariftabrizi A, Tavangar SM, et al. Naltrexone, an opioid receptor antagonist, attenuates liver fibrosis in bile duct ligated rats. Gut 2006;55:1606–16. https://doi.org/10.1136/GUT.2005.076778.

[80] De Minicis S, Candelaresi C, Marzioni M, Saccomano S, Roskams T, Casini A, et al. Role of endogenous opioids in modulating HSC activity in vitro and liver fibrosis in vivo. Gut 2008;57:352–64. https://doi.org/10.1136/GUT.2007.120303.

[81] Liang C, Qiao L, Han Y, Liu J, Zhang J, Liu W. Regulatory Roles of SREBF1 and SREBF2 in Lipid Metabolism and Deposition in Two Chinese Representative Fat-Tailed Sheep Breeds. Animals (Basel) 2020;10:1–14. https://doi.org/10.3390/ANI10081317.

[82] Ferré P, Foufelle F. Hepatic steatosis: A role for de novo lipogenesis and the transcription factor SREBP-1c. Diabetes Obes Metab 2010;12:83–92. https://doi.org/10.1111/j.1463-1326.2010.01275.x.

[83] Kohjima M, Higuchi N, Kato M, Kotoh K, Yoshimoto T, Fujino T, et al. SREBP-1c, regulated by the insulin and AMPK signaling pathways, plays a role in nonalcoholic fatty liver disease. Int J Mol Med 2008;21:507–11. https://doi.org/10.3892/ijmm.21.4.507.

[84] Li Y, Xu S, Mihaylova MM, Zheng B, Hou X, Jiang B, et al. Cell Metabolism Article AMPK Phosphorylates and Inhibits SREBP Activity to Attenuate Hepatic Steatosis and Atherosclerosis in Diet-Induced Insulin-Resistant Mice 2011. https://doi.org/10.1016/j.cmet.2011.03.009.

[85] Nguyen TTP, Kim DY, Lee YG, Lee YS, Truong XT, Lee JH, et al. SREBP-1c impairs ULK1 sulfhydration-mediated autophagic flux to promote hepatic steatosis in high-fat-diet-fed mice. Mol Cell 2021;81:3820-3832.e7. https://doi.org/10.1016/j.molcel.2021.06.003.

[86] Musso G, Cassader M, Bo S, De Michieli F, Gambino R. Sterol regulatory element-binding factor 2 (SREBF-2) predicts 7-year NAFLD incidence and severity of liver disease and lipoprotein and glucose dysmetabolism. Diabetes 2013;62:1109–20. https://doi.org/10.2337/DB12-0858.

[87] Fisher RM, Humphries SE, Talmud PJ. Common variation in the lipoprotein lipase gene: Effects on plasma lipids and risk of atherosclerosis. Atherosclerosis 1997;135:145–59. https://doi.org/10.1016/S0021-9150(97)00199-8.

[88] Spence JD, Ban MR, Hegele RA. Lipoprotein Lipase (LPL) Gene Variation and Progression of Carotid Artery Plaque 2003. https://doi.org/10.1161/01.STR.0000069160.05292.41.

[89] Notarnicola M, Misciagna G, Tutino V, Chiloiro M, Osella AR, Guerra V, et al. Increased serum levels of lipogenic enzymes in patients with severe liver steatosis 2012.

[90] Pardina E, Baena-Fustegueras JA, Llamas R, Catalán R, Galard R, Lecube A, et al. Lipoprotein lipase expression in livers of morbidly obese patients could be responsible for liver steatosis. Obes Surg 2009;19:608–16. https://doi.org/10.1007/s11695-009-9827-5.

[91] Yin W, Liao D, Wang Z, Xi S, Tsutsumi K, Koike T, et al. NO-1886 inhibits size of adipocytes, suppresses plasma levels of tumor necrosis factor-α and free fatty acids,

improves glucose metabolism in high-fat/high-sucrose-fed miniature pigs. Pharmacol Res 2004;49:199–206. https://doi.org/10.1016/j.phrs.2003.09.008.

[92] Yin W, Yuan Z, Tsutsumi K, Xie Y, Zhang Q, Wang Z, et al. A lipoprotein lipase-promoting agent, NO-1886, improves glucose and lipid metabolism in high fat, high sucrose-fed New Zealand white rabbits. Int J Exp Diabesity Res 2003;4:27–34. https://doi.org/10.1080/15438600303732.

[93] Yin W, Tsutsumi K, Yuan Z, Yang B. Effects of the lipoprotein lipase activator NO-1886 as a suppressor agent of atherosclerosis in aorta of mild diabetic rabbits. Arzneimittel-Forschung/Drug Research 2002;52:610–4. https://doi.org/10.1055/S-0031-1299939/BIB.

[94] Yagyu H, Ishibashi S, Chen Z, Osuga JI, Okazaki M, Perrey S, et al. Overexpressed lipoprotein lipase protects against atherosclerosis in apolipoprotein E knockout mice. J Lipid Res 1999;40:1677–85. https://doi.org/10.1016/S0022-2275(20)33414-3.

[95] Pentikäinen MO, Oksjoki R, Öörni K, Kovanen PT. Lipoprotein lipase in the arterial wall: linking LDL to the arterial extracellular matrix and much more. Arterioscler Thromb Vasc Biol 2002;22:211–7. https://doi.org/10.1161/HQ0102.101551.

[96] Clee SM, Bissada N, Miao F, Miao L, Marais AD, Henderson HE, et al. Plasma and vessel wall lipoprotein lipase have different roles in atherosclerosis. J Lipid Res 2000;41:521–31. https://doi.org/10.1016/s0022-2275(20)32399-3.

[97] Furuhashi M, Hotamisligil GS. Fatty acid-binding proteins: role in metabolic diseases and potential as drug targets. Nat Rev Drug Discov 2008;7:489–503. https://doi.org/10.1038/nrd2589.

[98] Furuhashi M, Saitoh S, Shimamoto K, Miura T. Fatty acid-binding protein 4 (FABP4): Pathophysiological insights and potent clinical biomarker of metabolic and cardiovascular diseases. Clin Med Insights Cardiol 2014;2014:23–33. https://doi.org/10.4137/CMC.S17067.

[99] Chen MT, Huang JS, Gao DD, Li YX, Wang HY. Combined treatment with FABP4 inhibitor ameliorates rosiglitazone-induced liver steatosis in obese diabetic db/db mice. Basic Clin Pharmacol Toxicol 2021;129:173–82. https://doi.org/10.1111/BCPT.13621.

[100] Rodríguez-Calvo R, Moreno-Vedia J, Girona J, Ibarretxe D, Martínez-Micaelo N, Merino J, et al. Relationship Between Fatty Acid Binding Protein 4 and Liver Fat in Individuals at Increased Cardiometabolic Risk. Front Physiol 2021;12:781789. https://doi.org/10.3389/FPHYS.2021.781789/FULL.

[101] Stöger JL, Gijbels MJJ, van der Velden S, Manca M, van der Loos CM, Biessen EAL, et al. Distribution of macrophage polarization markers in human atherosclerosis. Atherosclerosis 2012;225:461–8. https://doi.org/10.1016/J.ATHEROSCLEROSIS.2012.09.013.

[102] Waldo SW, Li Y, Buono C, Zhao B, Billings EM, Chang J, et al. Heterogeneity of Human Macrophages in Culture and in Atherosclerotic Plaques. Am J Pathol 2008;172:1112–26. https://doi.org/10.2353/AJPATH.2008.070513.

[103] Wang TY, Su NY, Shih PC, Tsai PS, Huang CJ. Anti-inflammation effects of naloxone involve phosphoinositide 3-kinase delta and gamma. Journal of Surgical Research 2014;192:599–606. https://doi.org/10.1016/J.JSS.2014.06.022.

[104] Olofsson SO, Boren J. Apolipoprotein B: A clinically important apolipoprotein which assembles atherogenic lipoproteins and promotes the development of atherosclerosis. J Intern Med 2005;258:395–410. https://doi.org/10.1111/J.1365-2796.2005.01556.X.

[105] Mehta A, Shapiro MD. Apolipoproteins in vascular biology and atherosclerotic disease. Nat Rev Cardiol 2022;19:168–79. https://doi.org/10.1038/S41569-021-00613-5;SUBJMETA.

[106] Whitfield AJ, Barrett PHR, Van Bockxmeer FM, Burnett JR. Lipid Disorders and Mutations in the APOB Gene. Clin Chem 2004;50:1725–32. https://doi.org/10.1373/CLINCHEM.2004.038026.

[107] Crooke RM, Graham MJ, Lemonidis KM, Whipple CP, Koo S, Perera RJ. An apolipoprotein B antisense oligonucleotide lowers LDL cholesterol in hyperlipidemic mice without causing hepatic steatosis. J Lipid Res 2005;46:872–84. https://doi.org/10.1194/jlr.M400492-JLR200.

[108] Kastelein JJP, Wedel MK, Baker BF, Su J, Bradley JD, Yu RZ, et al. Potent Reduction of Apolipoprotein B and Low-Density Lipoprotein Cholesterol by Short-Term Administration of an Antisense Inhibitor of Apolipoprotein B 2006. https://doi.org/10.1161/CIRCULATIONAHA.105.606442.

[109] van der Westhuyzen DR, de Beer FC, Webb NR. HDL cholesterol transport during inflammation. Curr Opin Lipidol 2007;18.

[110] Clifton PM, Mackinnon AM, Barter PJ. Effects of serum amyloid A protein (SAA) on composition, size, and density of high density lipoproteins in subjects with myocardial infarction. Journal Lipid Research 1985;26:1389–98. https://doi.org/10.1016/S0022-2275(20)34244-9.

[111] Vaisar T, Tang C, Babenko I, Hutchins P, Wimberger J, Suffredini AF, et al. Inflammatory remodeling of the HDL proteome impairs cholesterol efflux capacity. J Lipid Res 2015;56:1519–30. https://doi.org/10.1194/jlr.M059089.

[112] Yang D, Zhang X, Yue L, Hu H, Wei X, Guo Q, et al. Thiamethoxam induces nonalcoholic fatty liver disease in mice via methionine metabolism disturb via nicotinamide N-methyltransferase overexpression. Chemosphere 2021;273:129727. https://doi.org/10.1016/J.CHEMOSPHERE.2021.129727.

[113] Komatsu M, Kanda T, Urai H, Kurokochi A, Kitahama R, Shigaki S, et al. NNMT activation can contribute to the development of fatty liver disease by modulating the NAD+metabolism. Sci Rep 2018;8:8637. https://doi.org/10.1038/s41598-018-26882-8.

[114] Neelakantan H, Vance V, Wetzel MD, Wang H-YL, McHardy SF, Finnerty CC, et al. Selective and membrane-permeable small molecule inhibitors of nicotinamide N-methyltransferase reverse high fat diet-induced obesity in mice. Biochem Pharmacol 2018;147:141–52. https://doi.org/https://doi.org/10.1016/j.bcp.2017.11.007.

[115] Li D, Yi C, Huang H, Li J, Hong S. Hepatocyte-specific depletion of Nnmt protects mice from non-alcoholic steatohepatitis. J Hepatol 2022;77:882–4. https://doi.org/10.1016/j.jhep.2022.03.021.

[116] Zhou Y, Jiang L, Rui L. Identification of MUP1 as a regulator for glucose and lipid metabolism in mice. Journal of Biological Chemistry 2009;284:11152–9. https://doi.org/10.1074/jbc.M900754200.

[117] Gao R, Wang H, Li T, Wang J, Ren Z, Cai N, et al. Secreted MUP1 that reduced under ER stress attenuates ER stress induced insulin resistance through suppressing protein synthesis in hepatocytes. Pharmacol Res 2023;187:106585. https://doi.org/10.1016/J.PHRS.2022.106585.

[118] Greve S, Kuhn GA, Saenz-de-Juano MD, Ghosh A, von Meyenn F, Giller K. The major urinary protein gene cluster knockout mouse as a novel model for translational metabolism research. Sci Rep 2022;12:13161. https://doi.org/10.1038/S41598-022-17195-Y.

[119] Cao W, Chang T, Li X, Wang R, Wu L. Dual effects of fructose on ChREBP and FoxO1/3α are responsible for AldoB up-regulation and vascular remodelling. Clin Sci 2017;131:309–25. https://doi.org/10.1042/CS20160251.

[120] Liu J, Wang R, Desai K, Wu L. Upregulation of aldolase B and overproduction of methylglyoxal in vascular tissues from rats with metabolic syndrome. Cardiovasc Res 2011;92:494–503. https://doi.org/10.1093/cvr/cvr239.

[121] ’t Hoen PAC, Van Der Lans CAC, Eck M Van, Bijsterbosch MK, Van Berkel TJC, Twisk J. Aorta of ApoE-Deficient Mice Responds to Atherogenic Stimuli by a Prelesional Increase and Subsequent Decrease in the Expression of Antioxidant Enzymes 2003. https://doi.org/10.1161/01.RES.0000082978.92494.B1.

[122] Pourcet B, Pineda-Torra I. Transcriptional regulation of macrophage arginase 1 expression and its role in atherosclerosis. Trends Cardiovasc Med 2013;23:143–52. https://doi.org/https://doi.org/10.1016/j.tcm.2012.10.003.

[123] Mousa RF, Smesam HN, Qazmooz HA, Al-Hakeim HK, Maes M. A pathway phenotype linking metabolic, immune, oxidative, and opioid pathways with comorbid depression, atherosclerosis, and unstable angina. CNS Spectr 2022;27:676–90. https://doi.org/10.1017/S1092852921000432,.

[124] Wang GY, Wu S, Pei JM, Yu XC, Wong TM. κ- but not δ-opioid receptors mediate effects of ischemic preconditioning on both infarct and arrhythmia in rats. Am J Physiol Heart Circ Physiol 2001;280:384–91. https://doi.org/10.1152/AJPHEART.2001.280.1.H384,.

8. Appendices

8.1 Information about the authors' participation and contribution to the publications.

Tytuł publikacji: Opioid System Antagonism Alters Vascular Proteome and Collagen Deposition in ApoE$^{-/-}$ Mice

Jastrzębiec, dn. 03.09.2025 r.
date

FORMULARZ ZGŁOSZENIOWY PUBLIKACJI WYNIKÓW BADAŃ[1]
(APPLICATION FORM FOR PUBLISHING RESEARCH RESULTS)

1. Autorzy pracy *(Authors)*:

Lp.	Imię nazwisko *(name and surname)*	Jednostka *(Institution)*
1.	Kinga Jaskuła	Instytut Genetyki i Biotechnologii Zwierząt PAN w Jastrzębcu
2.	Agata Nawrocka	Instytut Genetyki i Biotechnologii Zwierząt PAN w Jastrzębcu
3.	Piotr Poznański	Instytut Genetyki i Biotechnologii Zwierząt PAN w Jastrzębcu
4.	Aneta Stachowicz	Collegium Medicum Uniwersytet Jagielloński w Krakowie
5.	Marzena Łazarczyk	Instytut Genetyki i Biotechnologii Zwierząt PAN w Jastrzębcu
6.	Mariusz Sacharczuk	Instytut Genetyki i Biotechnologii Zwierząt PAN w Jastrzębcu
7.	Dominik S. Skiba	Instytut Genetyki i Biotechnologii Zwierząt PAN w Jastrzębcu

2. Autor wyznaczony do kontaktu w IGiBZ *(Author appointed to contact at IGAB)*:

Imię i nazwisko *(name and surname)*:	Dominik Skiba
Adres mailowy i nr telefonu *(Email address and phone number)*:	d.skiba@igbzpan.pl; +48 227367026

3. Opis udziału autora w opracowaniu publikacji *(Description of the author's participation in preparation of the publication)*:

Lp.	Imię i nazwisko *(name and surname)*	Opis udziału autora *(Description of the author's participation)*	% udział w opracowaniu publikacji *(participation in the publication in %)*	Podpis autora[2] *(author's signature)*
1.	Kinga Jaskuła	Przygotowanie i walidacja metodologii, przeprowadzenie badań, analiza, przygotowanie manuskryptu.	55%	Jaskuła
2.	Agata Nawrocka	Walidacja metodologii, przeprowadzenie badań, edycja manuskryptu	10%	Nawrocka
3.	Piotr Poznański	Walidacja metodologii, edycja manuskryptu	5%	Poznański

4.	Aneta Stachowicz	Przygotowanie metodologii, analiza, edycja manuskryptu	5%	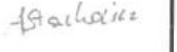
5.	Marzena Łazarczyk	Edycja manuskryptu	5%	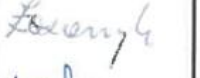
6.	Mariusz Sacharczuk	Przygotowanie metodologii, analiza, edycja manuskryptu	10%	
7.	Dominik S. Skiba	Przygotowanie metodologii, analiza, edycja manuskryptu	10%	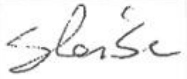

[1] **Formularz musi zostać przygotowany i zaakceptowany przez Dyrekcję Instytutu przed wysłaniem publikacji do czasopisma /** ***The form must be prepared and approved by the Director before sending the publication to the journal.***

[2] **W przypadku autorów spoza IGiBZ dopuszczalne są podpisane przez nich jednostronne oświadczenia o udziale procentowym /** ***authors from other units can send signed individual declaration of their participation in %.***

Tytuł publikacji: Targeting the Opioid System in Cardiovascular Disease: Liver Proteomic and Lipid Profile Effects of Naloxone in Atherosclerosis

Jastrzębiec, dn. 29.04.2025
date

FORMULARZ ZGŁOSZENIOWY PUBLIKACJI WYNIKÓW BADAŃ[1]
(APPLICATION FORM FOR PUBLISHING RESEARCH RESULTS)

1. Autorzy pracy *(Authors)*:

Lp.	Imię nazwisko *(name and surname)*	Jednostka *(Institution)*
1.	Kinga Jaskuła	Instytut Genetyki i Biotechnologii Zwierząt PAN w Jastrzębcu
2.	Agata Nawrocka	Instytut Genetyki i Biotechnologii Zwierząt PAN w Jastrzębcu
3.	Piotr Poznański	Instytut Genetyki i Biotechnologii Zwierząt PAN w Jastrzębcu
4.	Aneta Stachowicz	Collegium Medicum Uniwersytet Jagielloński w Krakowie
5.	Marzena Łazarczyk	Instytut Genetyki i Biotechnologii Zwierząt PAN w Jastrzębcu
6.	Mariusz Sacharczuk	Instytut Genetyki i Biotechnologii Zwierząt PAN w Jastrzębcu
7.	Zbigniew Gaciong	Warszawski Uniwersytet Medyczny
8.	Dominik S. Skiba	Instytut Genetyki i Biotechnologii Zwierząt PAN w Jastrzębcu

2. Autor wyznaczony do kontaktu w IGiBZ *(Author appointed to contact at IGAB)*:

Imię i nazwisko *(name and surname)*:	Mariusz Sacharczuk
Adres mailowy i nr telefonu *(Email address and phone number)*:	m.sacharczuk@igbzpan.pl; +48 227367026

3. Opis udziału autora w opracowaniu publikacji *(Description of the author's participation in preparation of the publication)*:

Lp.	Imię i nazwisko *(name and surname)*	Opis udziału autora *(Description of the author's participation)*	% udział w opracowaniu publikacji *(participation in the publication in %)*	Podpis autora[2] *(author's signature)*
1.	Kinga Jaskuła	Przygotowanie i walidacja metodologii, przeprowadzenie badań, analiza, przygotowanie manuskryptu.	51%	Jaskuła
2.	Agata Nawrocka	Walidacja metodologii, przeprowadzenie badań, edycja manuskryptu	10%	Nawrocka
3.	Piotr Poznański	Walidacja metodologii, edycja manuskryptu	5%	Poznański

4.	Aneta Stachowicz	Przygotowanie metodologii, analiza, edycja manuskryptu	5%	
5.	Marzena Łazarczyk	Edycja manuskryptu	5%	
6.	Mariusz Sacharczuk	Przygotowanie metodologii, analiza, edycja manuskryptu	7%	
7.	Zbigniew Gaciong	Przygotowanie metodologii, edycja manuskryptu	7%	
8.	Dominik S. Skiba	Przygotowanie metodologii, analiza, edycja manuskryptu	10%	

[1] Formularz musi zostać przygotowany i zaakceptowany przez Dyrekcję Instytutu przed wysłaniem publikacji do czasopisma / *The form must be prepared and approved by the Director before sending the publication to the journal.*

[2] W przypadku autorów spoza IGiBZ dopuszczalne są podpisane przez nich jednostronne oświadczenia o udziale procentowym / *authors from other units can send signed individual declaration of their participation in %.*

Tytuł publikacji: Cardiovascular Effects Mediated by HMMR and CD44

Jastrzębiec, dn. 13.05.2021
date

FORMULARZ ZGŁOSZENIOWY PUBLIKACJI WYNIKÓW BADAŃ[1]
(APPLICATION FORM FOR PUBLISHING RESEARCH RESULTS)

1. Autorzy pracy *(Authors)*:

Lp.	Imię nazwisko *(name and surname)*	Jednostka *(Institution)*
1.	Kinga Jaskuła	Instytut Genetyki i Biotechnologii Zwierząt PAN w Jastrzębcu
2.	Mariusz Sacharczuk	Instytut Genetyki i Biotechnologii Zwierząt PAN w Jastrzębcu
3.	Zbigniew Gaciong	Warszawski Uniwersytet Medyczny
4.	Dominik S. Skiba	Instytut Genetyki i Biotechnologii Zwierząt PAN w Jastrzębcu

2. Autor wyznaczony do kontaktu w IGiBZ *(Author appointed to contact at IGAB)*:

Imię i nazwisko *(name and surname)*:	Dominik Skiba
Adres mailowy i nr telefonu *(Email address and phone number)*:	d.skiba@igbzpan.pl; +48 227367026

3. Opis udziału autora w opracowaniu publikacji *(Description of the author's participation in preparation of the publication)*:

Lp.	Imię i nazwisko *(name and surname)*	Opis udziału autora *(Description of the author's participation)*	% udział w opracowaniu publikacji *(participation in the publication in %)*	Podpis autora[2] *(author's signature)*
1.	Kinga Jaskuła	Opracowanie założeń manuskryptu, przygotowanie oryginalnego manuskryptu, edycja manuskryptu	65%	Jaskuła
2.	Mariusz Sacharczuk	Edycja manuskryptu, nadzór merytoryczny	10%	
3.	Zbigniew Gaciong	Nadzór merytoryczny	5%	
4.	Dominik S. Skiba	Opracowanie założeń manuskryptu, przygotowanie oryginalnego manuskryptu, edycja manuskryptu, nadzór merytoryczny	20%	Skiba

[1] **Formularz musi zostać przygotowany i zaakceptowany przez Dyrekcję Instytutu przed wysłaniem publikacji do czasopisma /** ***The form must be prepared and approved by the Director before sending the publication to the journal.***

[2] **W przypadku autorów spoza IGiBZ dopuszczalne są podpisane przez nich jednostronne oświadczenia o udziale procentowym /** ***authors from other units can send signed individual declaration of their participation in %.***

8.2 Publications

cells

MDPI

Article

Opioid System Antagonism Alters Vascular Proteome and Collagen Deposition in ApoE$^{-/-}$ Mice

Kinga Jaskuła [1], Agata Nawrocka [1], Piotr Poznański [2], Aneta Stachowicz [3], Marzena Łazarczyk [1], Mariusz Sacharczuk [1,4] and Dominik S. Skiba [1,*]

1 Department of Experimental Genomics, Institute of Genetics and Animal Biotechnology, Polish Academy of Sciences, Postępu 36A, 05-552 Jastrzębiec, Poland; k.jaskula@igbzpan.pl (K.J.); a.nawrocka@igbzpan.pl (A.N.); m.lazarczyk@igbzpan.pl (M.Ł.); m.sacharczuk@igbzpan.pl (M.S.)
2 Department of Biotechnology and Nutrigenomics, Institute of Genetics and Animal Biotechnology, Polish Academy of Sciences, Postępu 36A, 05-552 Jastrzębiec, Poland; p.poznanski@igbzpan.pl
3 Department of Pharmacology, Faculty of Medicine, Jagiellonian University Medical College, 31-008 Krakow, Poland; aneta.stachowicz@uj.edu.pl
4 Department of Pharmacodynamics, Faculty of Pharmacy, Warsaw Medical University, Banacha 1, 02-697 Warsaw, Poland
* Correspondence: d.skiba@igbzpan.pl; Tel.: +48-227367026

Abstract

Atherosclerosis is common cardiovascular disease, leading to complications such as myocardial infarction and stroke. The main causes of these diseases are lipid accumulation and inflammation in large arteries. In this study, we investigated whether opioid receptor blockade impacts factors involved in atherosclerosis development. We administered naloxone to 8-week-old and 36-week-old ApoE$^{-/-}$ mice, then examined the expression of *Col1a1*, and *Col3a1* in the aorta, as well as the influence of naloxone administration on aortic collagen layer thickness and proteomic changes in the aorta. Additionally, we assessed the impact of naloxone on the splenic T-cell populations. The results showed that *Col3a1* expression decreased in young mice but increased in older mice. In 36-week-old mice, naloxone administration led to an increase in aortic collagen layer thickness, but remained unchanged in young mice. Proteomic analysis identified 587 proteins that were altered following naloxone treatment. Our studies suggest that the opioid system is an important factor in atherosclerosis development.

Keywords: atherosclerosis; opioid system; aorta; naloxone

check for updates

Academic Editor: Kay-Dietrich Wagner

Received: 2 July 2025
Revised: 4 October 2025
Accepted: 6 October 2025
Published: 8 October 2025

Citation: Jaskuła, K.; Nawrocka, A.; Poznański, P.; Stachowicz, A.; Łazarczyk, M.; Sacharczuk, M.; Skiba, D.S. Opioid System Antagonism Alters Vascular Proteome and Collagen Deposition in ApoE$^{-/-}$ Mice. *Cells* **2025**, *14*, 1559. https://doi.org/10.3390/cells14191559

1. Introduction

Atherosclerosis is the most common form of cardiovascular disease (CVD), where the main, but not only, components are lipid accumulation and inflammation in large arteries, which can lead to serious clinical complications such as myocardial infarction or stroke [1,2]. Noteworthy, atherosclerosis remains a leading cause of mortality in developed countries [3]. The major players in the development of this disease are endothelial cells (ECs), leukocytes, and intimal smooth muscle cells (SMCs) that are mobilized in response to inflammation and lead to the formation of atherosclerotic plaque [3,4].

In the early stages of atherosclerosis, disturbed blood flow alters ECs, increasing their permeability and allowing plasma low-density lipoprotein (LDL) and triglyceride-rich lipoproteins to enter the vessel wall through trans-endothelial transport or diffusion at cell junctions [5]. Oxidation of these lipoproteins and other inflammatory mediators then

activate ECs, resulting in the increased expression of P-selectin, E-selectin, vascular cell adhesion molecule-1 (VCAM-1), and intercellular adhesion molecule-1 (ICAM-1), which further promote the adhesion of leukocytes, especially monocytes, and secretion of chemotactic factors [6,7]. Once entering the intima, monocytes differentiate into macrophages in response to macrophage colony-stimulating factor (M-CSF) and other cytokines [8]. These macrophages are crucial to lesion progression, as shown by the fact that M-CSF-null mice on a hypercholesterolemic background are almost entirely resistant to lesion development [9]. Lesional macrophages internalize modified lipoproteins through scavenger receptors or phagocytose-aggregated lipoproteins, becoming cholesterol-loaded foam cells, which contribute to the enlargement and instability of the atherosclerotic plaque [10,11]. T-cells also play a key role in the pathogenesis of atherosclerosis, contributing to both the initiation and progression of the disease. They are involved in the immune response within the arterial walls, where they recognize modified lipoproteins and activate inflammatory pathways. Specifically, $CD4^+$ T-cells can help orchestrate the inflammatory environment, while $CD8^+$ T-cells may influence plaque stability. This immune response promotes endothelial dysfunction, smooth muscle cell proliferation, and foam cell formation, all of which contribute to the development of atherosclerotic plaques. Additionally, T-cells can impact the balance between pro-inflammatory and anti-inflammatory responses, influencing disease outcomes and plaque stability [12,13].

In the initial stages of atherosclerosis, collagen is a key component driving vascular remodelling by shaping the extracellular matrix. The vessel wall contains at least 19 types of collagen, while type I and III collagen encoded by *Col1a1* and *Col3a1* genes, respectively, predominate, providing tensile strength and elasticity [14,15]. In the aortic wall, SMCs synthesize collagen and perform a contractile role. During atherosclerotic plaque formation, SMCs migrate from the media to the intima, increasing collagen content [16]. Mesenchymal SMCs migrating to the vascular intima produce extracellular matrix (ECM) proteins such as collagen, and secrete matrix metalloproteinases (MMPs), contributing to ECM deposits arising and further plaque formation [17]. Inflammatory cells, such as macrophages in inflamed atherosclerotic plaques, also release MMPs, causing degradation of matrix collagen and, along with SMCs apoptosis in the intima, impair collagen synthesis. This dynamic imbalance between collagen synthesis and degradation may potentially make the plaque more prone to rupture [18,19].

Atherosclerosis is a chronic inflammatory disease of the arterial wall characterized by lipid accumulation, immune cell infiltration, ECM remodelling, and progressive structural changes in the vasculature. A key component of this process involves interactions between vascular cells and hyaluronan (HA), a major glycosaminoglycan of the ECM that regulates cellular adhesion, migration, proliferation, and inflammatory responses. These HA-mediated processes are especially critical during the early stages of atherosclerosis, when initial immune cell recruitment and subtle structural remodelling begin to shape the nascent lesion environment.

Among the known HA receptors, CD44 has been extensively studied and is recognized for its central role in coordinating immune responses and vascular remodelling during atherogenesis. CD44 mediates leukocyte adhesion and migration into the intima, supports macrophage retention and foam cell formation, and promotes vascular smooth muscle cell (VSMC) proliferation and migration [20]. These actions contribute significantly to early lesion development, even before significant luminal narrowing occurs. Notably, studies using CD44-deficient mouse models have shown reduced lesion formation, decreased inflammatory cell content, and impaired VSMC accumulation, highlighting CD44 as a key regulator of both the immune and structural remodelling components of early atherosclerosis [21].

Building upon this established role of CD44, we turned our attention to another hyaluronan receptor, HMMR (Hyaluronan-Mediated Motility Receptor, also known as RHAMM). While HMMR is known to regulate cell motility, inflammatory signalling, and cytoskeletal dynamics in various biological contexts, its function in atherosclerosis remains largely unexplored [22–24]. Given that CD44 and HMMR can mediate both overlapping and distinct pathways in HA signalling, we hypothesized that HMMR may also participate in the initiation and progression of atherosclerotic lesions.

Studies indicate that *Hmmr* expression was absent in uninjured hearts but markedly increased throughout the entire heart following ventricular resection in zebrafish [25]. Similarly, in a rat model of myocardial infarction, neither HMMR nor HA was detected in uninjured hearts; however, both were upregulated and localized in the infarct area within the first few days post-injury [25]. These findings confirm that both *Hmmr* and HA play a role in the formation of scar tissue in response to damage. As we know, atherosclerosis development was believed to be initiated by endothelial injury. It was called the "response to injury" hypothesis [26]. However, nowadays, more factors involved in this process have been determined where the endothelial layer remains undamaged; therefore, the term "endothelial dysfunction" is adopted. Despite this, the atherosclerosis development process has a lot in common with the formation of scar tissue in response to damage.

Another new factor playing a role in vascular remodelling during atherosclerosis may be the opioid system. In Human Aortic Vascular Smooth Muscle Cells (HASMC) β-endorphin treatment (an endogenous opioid peptide) significantly increased smooth muscle cells migration and proliferation [27]. Our data show that naloxone may modify lipid profile in ApoE$^{-/-}$ mice after naloxone treatment and affects proteome profile in the liver [28]. Moreover, our unpublished data indicate a statistically significant increase in *Hmmr* expression in mice with high opioid system activity [29,30] after treatment with the opioid receptor antagonist, naloxone.

The above findings allow us to assume there is a connection between the opioid system and vascular remodelling in early atherosclerosis, as well as a role of *Hmmr* in the progression of this disease. Studying the disease under chow diet conditions allows us to better isolate and understand the specific effects of opioid receptor blockade, without the influence of diet-induced processes [31–33].

2. Materials and Methods

2.1. Animals

All experiments were performed on 8-week and 36-week-old, male B6.129P2-Apoe^{tm1Unc}/J (strain. no. 002052) mice on the C57BL/6J background (further referred to as ApoE$^{-/-}$). Animals were housed in groups of 4–5 individuals and maintained in an animal facility of the Institute of Genetics and Animal Biotechnology of the Polish Academy of Sciences, under standard environmental conditions (ambient temperature of 22 ± 2 °C and 55 ± 5% relative humidity) under a 12 h light/dark cycle (lights on at 7 a.m.). Access to tap water and food (LABOFEED H, Kcynia, Poland) was provided *ad libitum*. Study procedures were carried out in accordance with the ethical clearance (permission no. WAW2/093/2024) received from the II Local Ethics Committee for Experiments on Animals in Warsaw.

2.2. Drug and Experiment Design

Both 8-week and 36-week-old mice were assigned to either a saline-treated control group or naloxone-treated experimental group. A non-selective opioid system antagonist, naloxone hydrochloride (NLX) (Sigma-Aldrich, St. Louis, MO, USA) was administered. Individuals belonging to the NLX-treated group received daily intraperitoneal injections of freshly prepared NLX dissolved in saline (0.9% NaCl) at a dose of 10 mg/kg

for 7 consecutive days. Mice of the control group were administered an equivalent volume of saline.

2.3. Measurement of mRNA Expression

RNA from aorta was isolated using TRItidy G (PanReac AppliChem, Darmstadt, Germany) according to manufacturer's protocol. Total RNA concentration was measured by Nanodrop 2000 (Thermo Fisher Scientific, Waltham, MA, USA). Reverse transcription of RNA was carried out using the High Capacity cDNA Reverse Transcription Kit (Applied Biosystems, Foster City, CA, USA). The expression of *Hmmr*, *Col1a1* and *Col3a1* at mRNA level in the aorta was analyzed using TaqMan® probes (Thermo Fisher Scientific, catalogue numbers: Mm00469183_m1; Mm00802300_m1; Mm00802300_m1, respectively) and the TaqMan® Real-Time PCR Master Mix (Thermo Fisher Scientific). Reactions were performed on 96-well plates using the LightCycler 96 System (Roche Diagnostics, Mannheim, Germany) Real-Time PCR according to standard protocol. Data analysis was conducted using LightCycler 96 Software. Data were normalized to *Tbp* (Mm01277042_m1; Thermo Fisher Scientific) mRNA levels and relative quantification was calculated.

2.4. Trichrome Staining

Thoracic aortas were fixed in formalin and dehydrated in increasing series of alcohols (70%, 80%, 96%, 99.8%), two changes each for 30 min at room temperature, followed by clearing in two changes in xylene (Warchem, Warsaw, Poland) for 15 min each. After that, tissues were transferred to mixture of toluene/paraffin (1:1) and incubated for 2 h in 60 °C. In the final step, each aorta was placed in pure molten paraffin overnight and embedded in paraffin blocks. Processed tissue was sectioned on microtome (Hyrax M25, Zeiss, Germany) for 6 µm thick slices and placed on microscopic slides. Before staining, specimens were deparaffinized in two changes in xylene and hydrated in decreasing series of alcohols. Further, trichrome stain was performed with Trichrome Stain (Masson) Kit (Sigma-Aldrich, St. Louis, MO, USA) according to manufacturer's protocol. Thickness of the collagen layer was determined by averaging 15 measurements taken from one section per subject at equal intervals around the circumference of aorta using ImageJ 1.54g software.

2.5. Flow Cytometry

Spleens were harvested and mashed through 70 µm strainers (VWR International, Avantor, Radnor Township, PA, USA) to isolate single cells. RBC lysis buffer (Biolegend, San Diego, CA, USA) was used to deplete red blood cells. Splenocytes were stained in FACS buffer for 20 min at 4 °C in the dark with the monoclonal antibodies (Biolegend, USA). For intracellular staining of CD168 (HMMR) (Proteintech, Rosemont, IL, USA), BD Cytofix/Cytoperm™ Fixation/Permeabilization Solution was used (BD Biosciences, NJ, USA). Cells were analyzed by a CytoFLEX flow cytometer (Beckman Coulter, Brea, CA, USA), and data were analyzed using Flow Jo v.10 (Ashland, OR, USA). For each experiment, fluorescence-minus-one controls (FMO) were performed. In selected experiments, FMO gating strategies were confirmed by isotype controls. To analyze T-cell subpopulations, the gating strategy presented in Figure S1 was applied. Briefly, doublets were excluded by plotting forward scatter height versus area. From the resulting gate, CD3-positive cells were selected to define total T-cells, which were then further subdivided into CD4-positive and CD8-positive subsets. To distinguish naïve, central memory, and effector T-cells in mouse samples, CD44 and CD62L expression was used: naïve T-cells were identified as $CD44^-$ $CD62L^+$, central memory T-cells as $CD44^+$ $CD62L^+$, and effector T-cells as $CD44^+$ $CD62L^-$. CD69-positive cells were gated within the CD4-positive T-cell population. HMMR-positive cells were identified based on histogram plots using FMO (fluorescence-minus-one) controls, and analyzed within $CD4^+$, $CD8^+$, naïve, central

memory, effector, and $CD69^+/CD4^+$ T-cell subsets. A complete list of antibodies used is provided in Supplementary Table S1.

2.6. Liquid Chromatography–Tandem Mass Spectrometry (LC–MS/MS) Analysis

Mouse aortas were homogenized using a Tissue Lyser LT (Qiagen, Hilden, Germany) and lysed in a buffer containing 0.1 M Tris-HCl, pH 7.6, 2% sodium dodecyl sulphate, and 50 mM dithiothreitol (Sigma Aldrich, St. Louis, MO, USA) at 96 °C for 10 min. Total protein concentration in lysates and the peptide contents in the digests were assayed using a tryptophan fluorescence-based WF assay [34]. An amount of 70 µg of protein was digested overnight using the filter-aided sample preparation (FASP) method [35] with Trypsin/Lys-C mix (Promega, Madison, WI, USA) (enzyme-to-protein ratio 1:35) as the digestion enzymes. Next, the samples were purified with C18 Ultra-Micro Spin Columns (Harvard Apparatus, Holliston, MA, USA). All samples were dissolved in 0.1% formic acid (FA) at a concentration of 0.5 µg/µL and spiked with the indexed retention time (iRT) peptides (Biognosys, Schlieren, Switzerland). A total of 1 µg of peptide was injected into a nanoEaseTM M/Z Peptide BEH C18 75 µm i.d. × 25 cm column (Waters, Milford, MA, USA) via a nanoEaseTM M/Z Symmetry C18 180 µm i.d. × 2 cm trap column (Waters, Milford, MA, USA) and separated using a 1% to 40% B phase linear gradient (A phase—0.1% FA in water; B phase—80% acetonitrile (ACN) and 0.1% FA) with a flow rate of 250 nL/min on an UltiMate 3000 HPLC system (Thermo Scientific, Waltham, MA, USA) coupled to an Orbitrap Exploris™ 480 Mass Spectrometer (Thermo Scientific, Waltham, MA, USA). The nanoelectrospray ion source parameters were as follows: ion spray voltage: 2.2 kV, ion transfer tube 275 °C. For data-independent (DIA) acquisition, spectra were collected for 145 min. in full scan mode (400–1250 Da), followed by 55 DIA scans using a variable precursor isolation window approach and automatic gain control (AGC) set to custom 1000%. The DIA MS data were analyzed in Spectronaut 19 (Biognosys, Schlieren, Switzerland) [36] software using directDIATM approach. MS data were filtered by 1% false discovery rate (FDR) at the peptide and protein levels, while quantitation was performed at the MS2 level, and global imputation with a missingness rate set to 0.7 was used. Statistical analysis of differential protein abundance was performed at both the MS1 and MS2 levels [37] using unpaired t tests with multiple testing correction after Storey [38,39]. A summary of the quality control for the LC-MS/MS runs is shown in Supplementary Figure S2 (available in link provided after Conclusions paragraph). The mass spectrometry data have been deposited to the ProteomeXchange Consortium via the PRIDE partner repository [40] with the dataset identifier PXD064451.

2.7. Statistical Analysis

Firstly, data for all analyses underwent normality check by Shapiro–Wilk test, followed by two-sided Student's *t*-test to assess changes between saline-treated and NLX-treated groups. Results were considered as statistically significant when *p*-value was less than 0.05. Results presented on graphs are expressed as means ± SD.

3. Results

3.1. Effect of the NLX Administration on the Expression of Hmmr, Col1a1, Col3a1 in 8-Week-Old Mice

NLX treatment in $ApoE^{-/-}$ mice led to a statistically significant decrease in *Hmmr* gene expression (NaCl 1.07 ± 0.41 vs. NLX 0.61 ± 0.18) ($p = 0.018$). We did not observe changes in the expression of the *Col1a1* (NaCl 1.04 ± 0.31 vs. NLX 0.83 ± 0.16); however, administration of NLX caused decreased expression of *Col3a1* (NaCl 1.03 ± 0.29 vs. NLX 0.66 ± 0.27) ($p = 0.028$) (Figure 1).

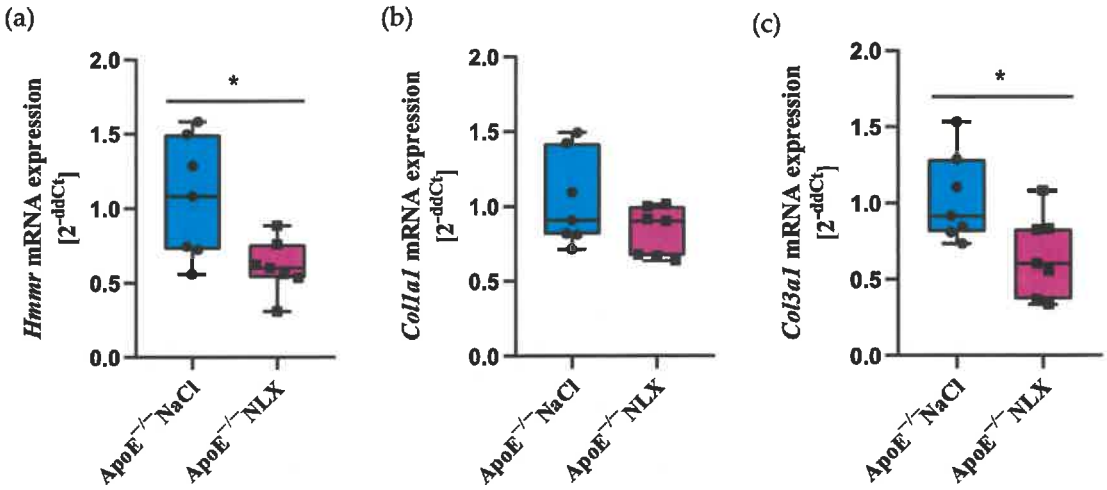

Figure 1. Expression of (**a**) *Hmmr*, (**b**) *Col1a1* and (**c**) *Col3a1* mRNA normalized to *Tpb* in aorta of 8-week-old ApoE$^{-/-}$ mice ($n = 7$ per group) * $p < 0.05$.

3.2. Effect of the NLX Administration on Collagen Layer Thickness in Thoracic Aorta in 8-Week-Old Mice

Blockade of opioid receptors with NLX did not cause significant changes in the thickness of the collagen layer in the aorta of 8-week-old mice (NaCl 8.53 ± 1.4 µm vs. NLX 9.38 ± 1.11 µm) (Figure 2).

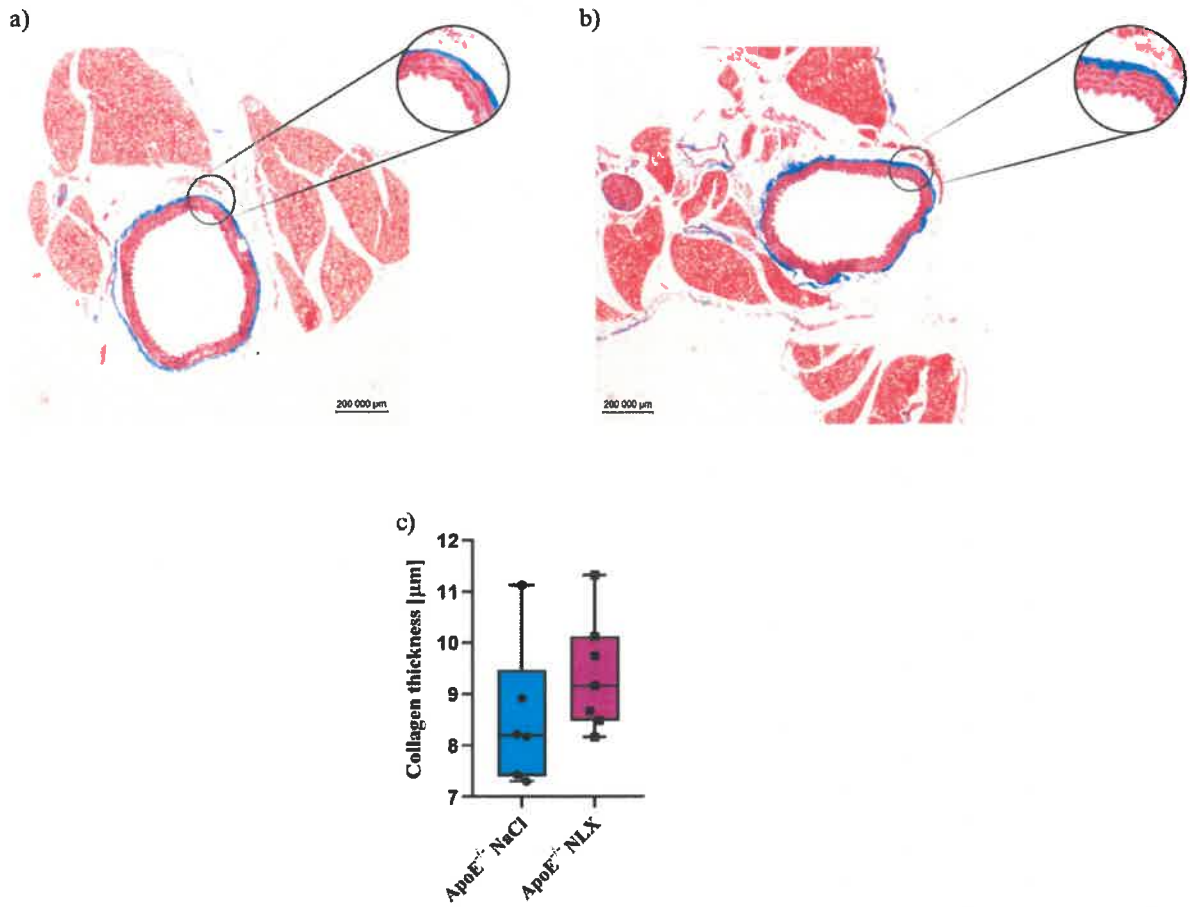

Figure 2. Representative images of Masson's trichrome-stained thoracic aorta evaluated for collagen thickness in 8-week-old mice after NLX administration. (**a**) Control ($n = 6$); (**b**) treatment group ($n = 7$); (**c**) collagen thickness measured in aorta of control and treated group.

3.3. Effect of the Opioid System Blockade on the T-Cell Subpopulations

Subpopulations of splenic T-cells collected from 8-week-old ApoE$^{-/-}$ mice after 7 days of the NLX administration were characterized by flow cytometry. Results revealed that the blockade of the opioid system did not affect a percentage of CD4$^+$ T-cells (NaCl 66.72 ± 3.09% vs. NLX 67.82 ± 2.59%) and CD8$^+$ T-cells (NaCl 28.27 ± 2.55% vs. NLX 27.36 ± 3.05%) (Figure 3a). We observed a statistically significant increase in naive (NaCl 61.25 ± 4.91% vs. NLX 68.06 ± 6.41%) (p = 0.031) and central memory (CM) (NaCl 16.19 ± 1.51% vs. NLX 11.72 ± 1.37%) ($p = 8.22490 \times 10^{-5}$) but not in effector (NaCl 10.03 ± 1.92% vs. NLX 9.21 ± 1.49%) subpopulation (Figure 3b). Administration of NLX did not cause changes in subpopulation of effector (NaCl 11.77 ± 2.23% vs. NLX 10.63 ± 1.96%) and CD69$^+$ (NaCl 11.28 ± 5.09% vs. NLX 8.55 ± 1.35%) CD4$^+$ T-cells, but we observed statistical increase in naive (NaCl 62.03 ± 4.89% vs. NLX 69.78 ± 5.79%) (p = 0.013) and CM (NaCl 16.34 ± 1.96% vs. NLX 11.40 ± 2.45%) (p = 0.001) CD4$^+$ T-cells (Figure 3c). Moreover, we observed decrease in CM (NaCl 9.04 ± 2.05% vs. NLX 5.75 ± 2.04%) (p = 0.007) CD8$^+$ T-cells but not in naive (NaCl 70.75 ± 6.83% vs. NLX 75.25 ± 9.39%) or effector (NaCl 1.78 ± 0.87% vs. NLX 1.28 ± 0.49%) CD8$^+$ T-cells (Figure 3d).

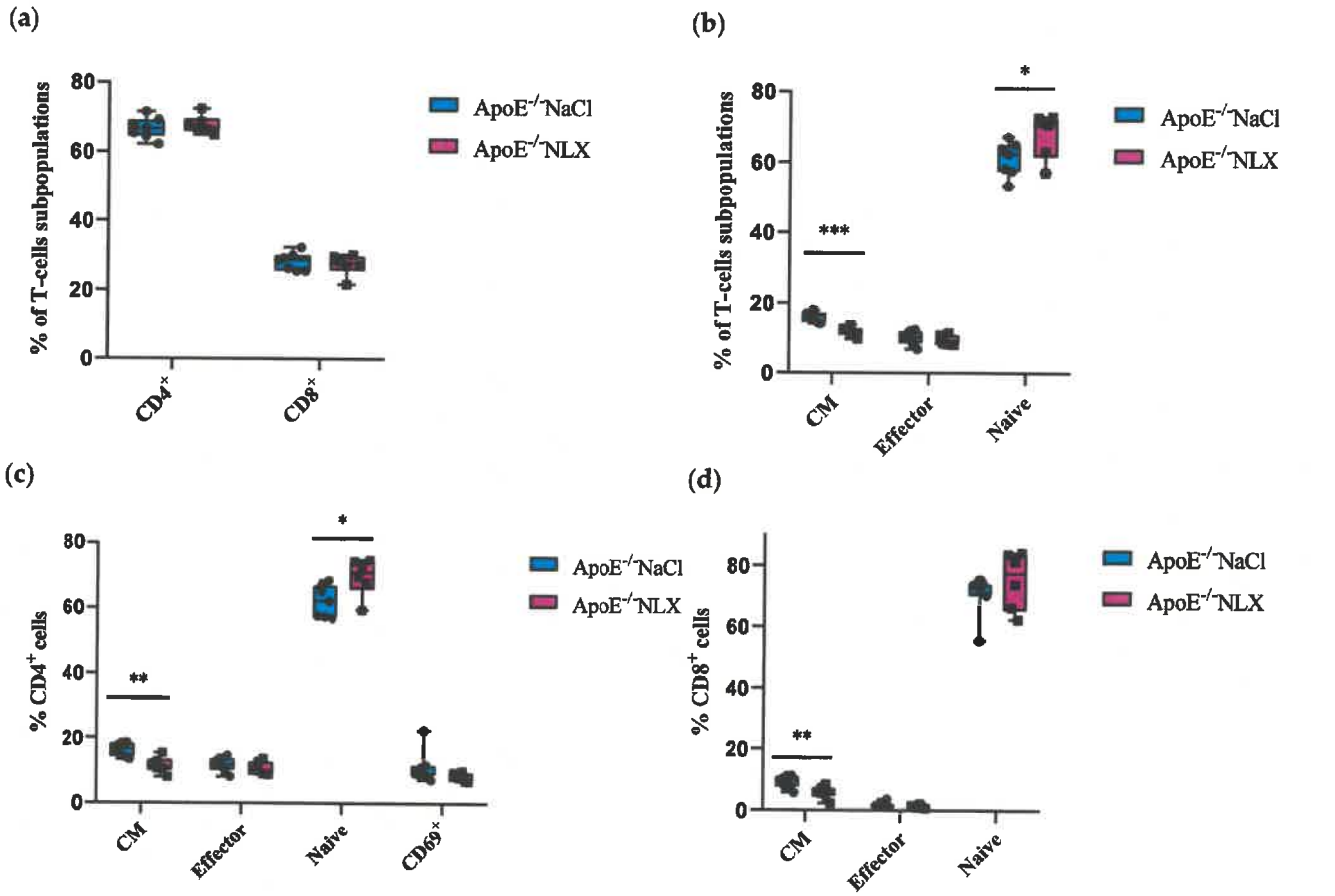

Figure 3. Percentage of T-cell subpopulations (**a**,**b**) isolated from spleen of 8-week-old mice after opioid receptors blockage with NLX. (**c**) Percentage of effector, naive, CM and CD69$^+$ cells among CD4$^+$ cells. (**d**) Percentage of effector, naive, CM cells among CD8$^+$ T-cell subpopulations (n = 7 per group), * $p < 0.05$, ** $p < 0.01$; *** $p < 0.001$.

NLX treatment did not affect *HMMR* expression on CD4$^+$ T-cells (NaCl 42.15 ± 4.29% vs. NLX 36.88 ± 5.57%) but decreased its expression on CD8$^+$ T-cells (NaCl 26.46 ± 4.30% vs. NLX 13.00 ± 6.25%) ($p \approx 0.0008$) and CD69$^+$/CD4$^+$ T-cells (NaCl 40.10 ± 3.31% vs. NLX

29.90 ± 5.64%) ($p = 0.001$) (Figure 4a). We also observed decreased *HMMR* expression in CM (NaCl 42.26 ± 4.03% vs. NLX 29.37 ± 5.09%) ($p = 0.0003$) and naive (NaCl 34.75 ± 2.66% vs. NLX 25.50 ± 6.36%) ($p = 0.007$) but not in effector (NaCl 32.18 ± 4.19% vs. NLX 28.43 ± 3.75%) subpopulations (Figure 4b).

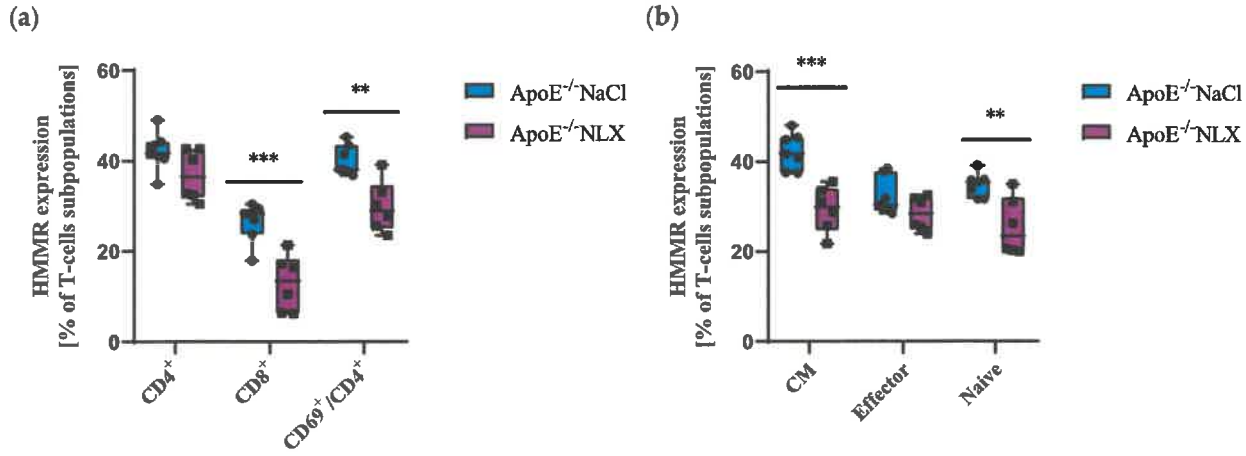

Figure 4. (**a**) *Hmmr* expression on $CD4^+$, $CD8^+$ and activated $CD4^+$ T-cells. (**b**) *Hmmr* expression on effector, naive, and CM subpopulation of T-cells ($n = 7$ per group); ** $p < 0.01$; *** $p < 0.001$.

3.4. Effect of the NLX Treatment on the Expression of HMMR Hmmr, Col1a1, Col3a1 in 36-Week-Old Mice

After NLX administration, we observed a statistically significant decrease in *Hmmr* gene expression in comparison to control group (NaCl 1.29 ± 0.61 vs. NLX 0.78 ± 0.33) ($p = 0.028$). We did not observe changes in the expression of the *Col1a1* gene (NaCl 0.98 ± 0.28 vs. NLX 1.19 ± 0.24); however, NLX treatment led to significant decrease in *Col3a1* gene expression (NaCl 0.97 ± 0.35 vs. NLX 1.31 ± 0.35) ($p = 0.042$) (Figure 5).

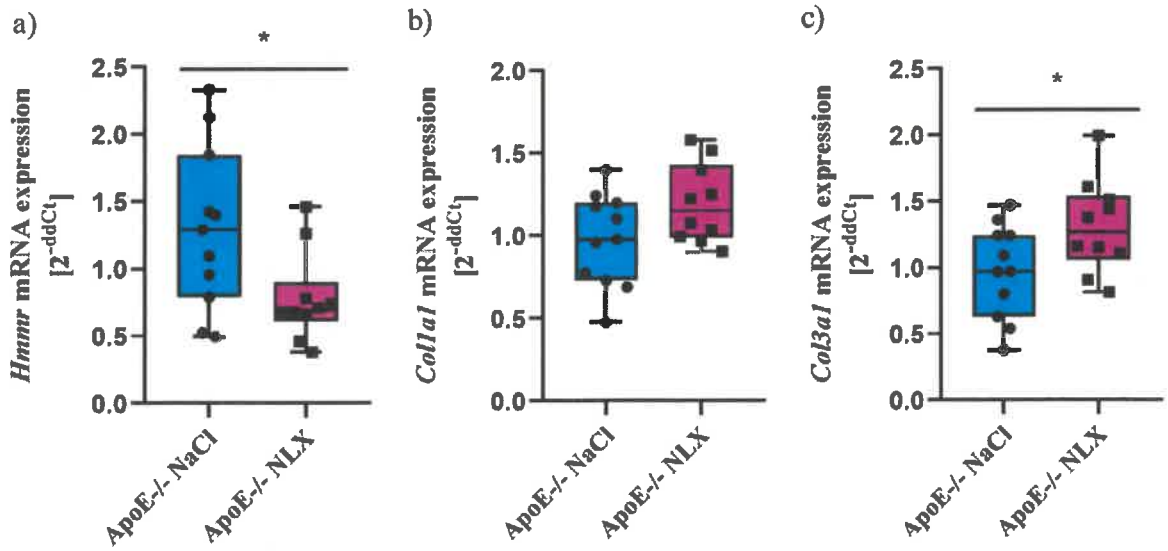

Figure 5. Expression of (**a**) *Hmmr*, (**b**) *Col1a1* and (**c**) *Col3a1* mRNA normalized to *Tbp* in aorta of 36-week-old $ApoE^{-/-}$ mice (NaCl $n = 11$; NLX $n = 10$) * $p < 0.05$.

3.5. Effect of the NLX Administration on Collagen Layer Thickness in Thoracic Aorta in 36-Week-Old Mice

Blockade of opioid receptors with NLX resulted in alterations in the thickness of the collagen layer in the aorta as shown by a significant *t*-test result ($p = 0.022$). Measurement

of the collagen layer revealed that it was significantly thicker in mice treated with NLX (13.43 ± 1.91 µm) compared to the NaCl (control) group (10.89 ± 1.69 µm)(Figure 6).

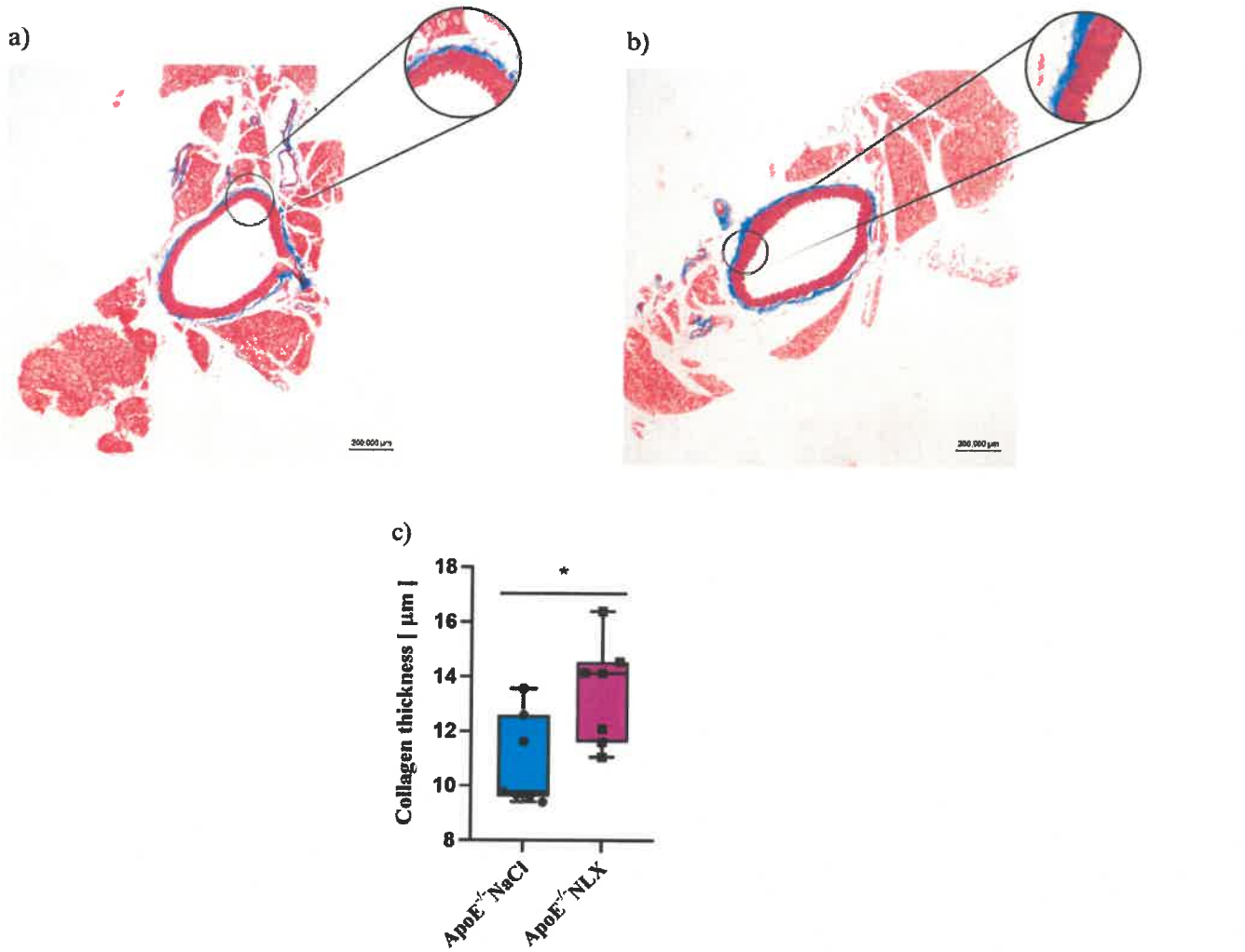

Figure 6. Representative images of Masson's trichrome-stained thoracic aorta evaluated for collagen thickness in 36-week-old mice after NLX administration. (**a**) control (**b**) after NLX treatment (**c**) collagen thickness measured in aorta of control and NLX-treated group ($n = 8$ per group), * $p < 0.05$.

3.6. Effect of the Opioid System Blockade on the T-Cell Subpopulations

Subpopulations of splenic T-cells from 36-week-old ApoE$^{-/-}$ mice after 7 days of the NLX administration were characterized by flow cytometry. Results revealed that the blockade of the opioid system did not affect a percentage of CD4$^+$ T-cells (NaCl 63.73 ± 5.25% vs. NLX 57.82 ± 8.54%) and CD8$^+$ T-cells (NaCl 20.93 ± 3.57% vs. NLX 21.28 ± 3.05%) (Figure 7a). We also did not observe changes in naive (NaCl 37.24 ± 8.72% vs. NLX 32.95 ± 9.52%) or effector (NaCl 37.97 ± 7.56% vs. NLX 37.98 ± 10.85%) subpopulations but we observed statistically significant increase in CM subpopulation (NaCl 12.93 ± 2.00% vs. NLX 17.61 ± 5.04%) ($p = 0.028$) (Figure 7a). Administration of NLX did not cause changes in subpopulation of effector (NaCl 49.06 ± 8.82% vs. NLX 49.86 ± 13.42%), naive (NaCl 32.63 ± 8.52% vs. NLX 30.20 ± 12.43%), CM (NaCl 9.20 ± 1.91% vs. NLX 10.97 ± 3.25%), and CD69$^+$ (NaCl 27.10 ± 7.33% vs. NLX 24.18 ± 7.02%) CD4$^+$ T-cells (Figure 7b). However, we observed increase in CM (NaCl 15.60 ± 2.85% vs. NLX 21.96 ± 3.81%) ($p = 0.002$) CD8$^+$ T-cells but not in naive (NaCl 67.47 ± 6.73% vs. NLX 57.81 ± 12.50%) or effector (NaCl 6.71 ± 2.73% vs. NLX 10.22 ± 6.36%) CD8$^+$ T-cells (Figure 7c).

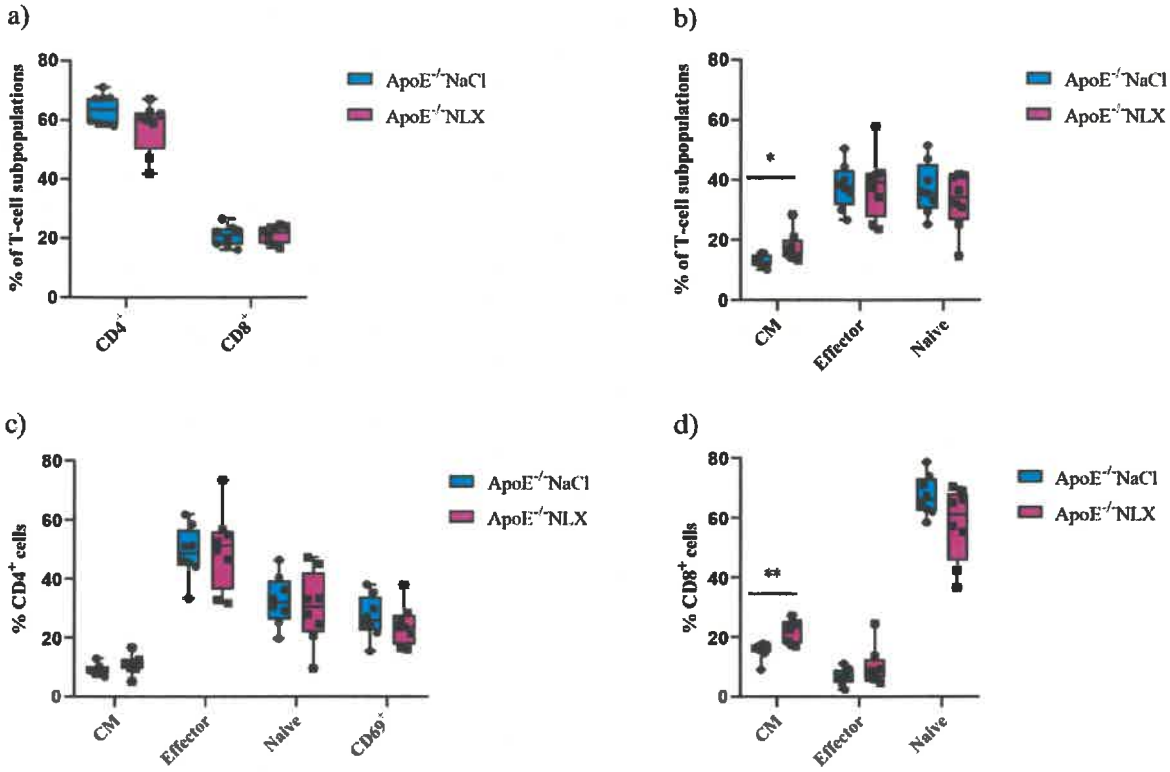

Figure 7. Percentage of T-cell subpopulations (**a**,**b**) isolated from spleen of 36-week-old mice after blockage of the opioid receptors. Percentage of effector, naive, CM, and CD69$^+$ cells among CD4$^+$ cells. (**c**) Percentage of effector, naive, CM cells among CD8$^+$ cells. (**d**) T-cell subpopulations (n = 8 per group) * $p < 0.05$; ** $p < 0.01$.

Furthermore, NLX administration affected HMMR expression on CD4$^+$ T-cells (NaCl 14.63 ± 5.61% vs. NLX 36.30 ± 10.91%) ($p \approx 0.0002$), CD8$^+$ T-cells (NaCl 21.58 ± 6.49% vs. NLX 47.97 ± 13.15%) ($p \approx 0.0002$), and CD69$^+$/CD4$^+$ T-cells (NaCl 21.84 ± 7.09% vs. NLX 47.34 ± 10.10%) ($p = 4.24152 \times 10^{-5}$) (Figure 8b). We also observed statistically significant increase in HMMR expression in CM (NaCl 34.00 ± 8.36% vs. NLX 61.89 ± 8.95%) ($p = 1.54018 \times 10^{-5}$), naive (NaCl 10.36 ± 4.35% vs. NLX 27.24 ± 9.77%) ($p \approx 0.0006$), and effector (NaCl 23.06 ± 5.54% vs. NLX 50.31 ± 10.56%) ($p = 1.49284 \times 10^{-5}$) subpopulations (Figure 8a).

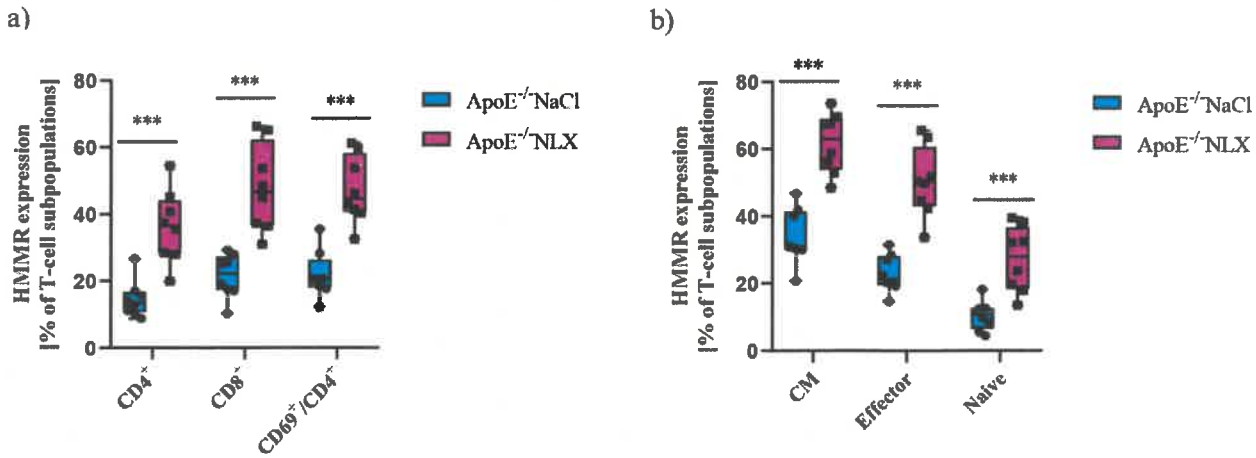

Figure 8. (**a**) HMMR expression on CD4$^+$, CD8$^+$, and activated CD4$^+$ T-cells. (**b**) HMMR expression on effector, naive, and CM subpopulation of T-cells (n = 9 per group) *** $p < 0.001$.

3.7. Impact of NLX Administration on the Proteomic Profile of Aortas in 36-Week-Old Mice

We performed proteomic analysis of aortas collected from ApoE$^{-/-}$ 36-week-old mice following NLX administration. Analysis identified 6869 proteins, with 587 showing significant differential expression (Figure 9a). From this subset, we selected 29 proteins with a fold change greater than 3 or less than −3 (Figure 9b). This subset included proteins involved in muscle function and structure, proteins related to cell migration and proliferation, proteins associated with the inflammatory response and immune system, proteins involved in cell death, and proteins that bind heavy metals (Supplementary Table S2).

a)

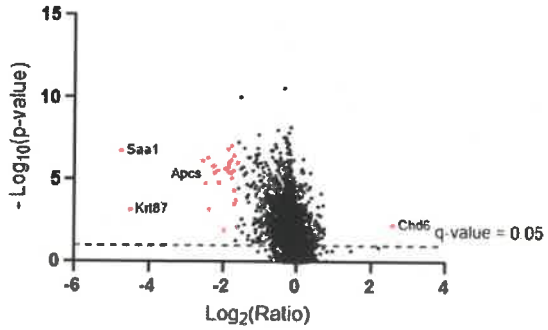

b)

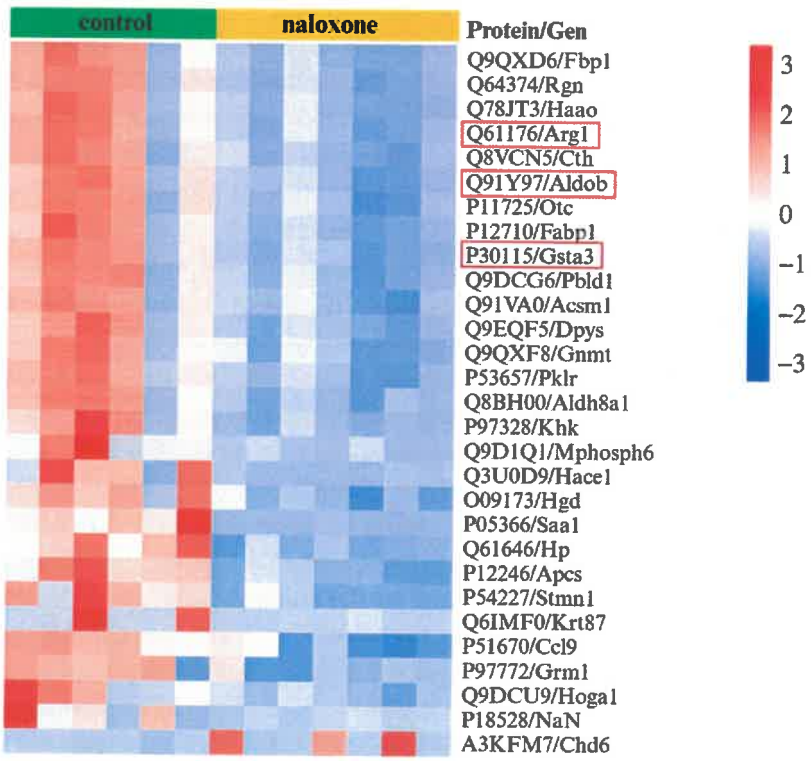

Figure 9. (**a**) Volcano plot for NLX-treated and non-treated mice (cut off; p value < 0.05, fold change ≥ 3.0 and ≤−3.0) with the most up- and downregulated proteins shown (red dots); (**b**) proteomic data obtained from aortas isolated from ApoE$^{-/-}$ mice after NLX administration compared to non-treated. Proteins relevant to vascular dysfunction are highlighted in red (cut off; p value < 0.05, fold change ≥ 3.0 and ≤−3.0) (n = 7 in control group, n = 8 in NLX group).

4. Discussion

Current atherosclerosis treatments have remained unchanged for years, and mainly have focused on lowering cholesterol levels, omitting other important causes of atherosclerosis development [41–43]. Therefore, it is crucial to investigate new potential factors contributing to the development of the disease [44,45]. In this study, we undertook an investigation of the relationship between the opioid system and vascular remodelling involved in the development of atherosclerosis, with particular interest in the *Hmmr* gene role in this process. In order to specifically address the early stages of atherosclerosis development, we employed mice maintained on a chow diet, in which disease progression occurs at a slower rate. Animals were analyzed at two time points, representing an early stage (8-week-old) and a more advanced stage (36-week-old) of atherosclerosis (Supplement, Figure S3). Moreover, to explore whether opioid receptor blockade affects adaptive immunity, we analyzed splenic T-cell subpopulations in ApoE$^{-/-}$ mice following NLX administration. Although macrophages are key mediators of atherosclerotic plaque formation, their numbers in the aortas of chow-fed ApoE$^{-/-}$ mice are very low, making reliable visualization and quantification challenging [46,47]. In contrast, the spleen is a major secondary lymphoid organ that contains abundant naive, effector, and memory T-cells, allowing a robust assessment of systemic immune modulation.

Our previous observations and the literature indicating that the hyaluronan-mediated motility receptor participates in tissue repair, fibrosis, and cardiovascular remodelling, and that its expression can be modulated by opioid system activity, led us to investigate whether NLX administration would affect *Hmmr* expression in ApoE$^{-/-}$ mice. We analyzed both young 8-week-old animals, representing an early stage of atherosclerosis, and 36-week-old mice, which display more advanced vascular changes. In both groups, *Hmmr* expression decreased significantly following NLX treatment. This may suggest an important role of the *Hmmr* gene in vascular remodelling at early and advanced stages of atherosclerosis development. Considering the important role of collagen in the formation of atherosclerotic plaque, we examined the mRNA expression of its two forms *Col1a1* and *Col3a1*, the content of which is highest in the vessel wall [48,49]. In the case of *Col3a1*, we observed a significant decrease in expression after NLX administration in 8-week-old mice compared to saline-treated animals of the same age, and interestingly, a significant increase in expression in 36-week-old mice. A similar trend was noted for *Col1a1*, though these changes were not statistically significant. It is known that prolonged exposure to opioid antagonists can increase tissue collagen content, as evidenced by studies with naltrexone [50,51]. Chronic elevated expression of collagen I isoforms has also been found to increase tissue stiffness and fibrosis, while increased expression of collagen III attenuates stiffness [52], and an imbalance between the synthesis of the two types affects the elasticity of veins [53]. Furthermore, age-related changes in collagen accumulation and the relative proportions of type I and III collagen have been well documented, but these changes may vary across tissue types [54]. With age, collagen type III content decreases in the heart and aorta up to the distal parts [55]; therefore, increased vascular stiffening with age is a natural consequence of ageing. We did not observe significant differences in collagen expression between 8-week-old and 36-week-old saline-treated mice indicating that the observed changes in collagen expression are not due to age differences but to NLX treatment. Changes in vascular stiffness due to affected expression and production of distinct collagen types ration upon naloxone treatment likely support plaque formation, though increased vessel rigidity has been evidenced to be a consequence of atherosclerosis development, rather than a causative factor. However, naloxone may enhance this pathological process [56]. The data suggest a relationship between the opioid system and factors involved in the development of atherosclerosis. Opioids, through their action on opioid receptors, may influence inflammatory processes

and vascular remodelling, which are crucial in the development of atherosclerotic changes. Therefore, to investigate whether the blockade of opioid receptors affects the remodelling of the aortic wall, we measured the thickness of the collagen layer in the thoracic aorta of 8-week-old and 36-week-old mice following NLX treatment. We did not observe changes in the collagen layer in aorta of 8-week-old mice; however, we observed statistically significant thickening of the collagen layer in aorta of mice with advanced atherosclerosis, after NLX administration. This suggests that NLX may enhance the resistance of the aortic wall, which could have a potential protective effect in diseases such as hypertension and could contribute to inhibiting the development of aneurysms. This is supported by studies showing that treatment of aortic rings collected from pigs with collagenase led to an increase in aortic diameter and altered vessel stiffness, making it less resistant to increased blood pressure [57]. Moreover, a lower percentage of collagen in the aortic wall has been observed in aortic dissection and aortic aneurysm. The reduced collagen content in the vessel wall likely contributed to its weakening, which is a fundamental characteristic of both conditions [58]. Additionally, similar studies have been performed using another opioid receptor antagonist—naltrexone. Topical application of naltrexone to wounds in rats with type 1 diabetes resulted in enhanced collagen formation, and thus skin integrity, making the skin more difficult to tear than in vehicle-treated animals [59].

Opioids are known to modulate immune function, particularly by influencing T-cell activation, differentiation, and cytokine release, which are processes strongly implicated in the initiation and progression of atherosclerosis [12,60]. T-cells contribute significantly to vascular inflammation and can influence plaque development [12,61]. We therefore examined whether blockade of the opioid system with NLX would alter splenic T-cell subpopulations in ApoE$^{-/-}$ mice. In addition, since *Hmmr* has been linked to tissue remodelling and immune cell activation, but its role in T-cells during atherosclerosis remains unexplored, we evaluated its expression on different T-cell subsets. This approach allowed us to investigate a novel connection between opioid signalling, immune modulation, and *Hmmr* regulation in adaptive immunity at both early and more advanced stages of the disease. We characterized subpopulations of splenic T-cells from 8-week-old and 36-week-old ApoE$^{-/-}$ mice. Results revealed that in young mice, NLX administration did not affect a percentage of CD4$^+$ T-cells and CD8$^+$ T-cells. We observed significant increase in naïve, decrease in CM, but no changes in effector subpopulation. Subpopulation of effector CD4$^+$ T-cells remained unchanged but we observed statistical increase in naïve and decrease in CM CD4$^+$ T-cells. Moreover, we observed decrease in CM CD8$^+$ T-cells but not in naive or effector CD8$^+$ T-cells. Then, we indicated if NLX treatment affects HMMR expression in T-cell subpopulations. We did not observe any changes in HMMR expression on CD4$^+$ T-cells and effector subpopulation. But decreased HMMR expression was observed on CD8$^+$ T-cells and CD69$^+$/CD4$^+$ T-cells as well as in CM and naive subpopulations. Additionally, we investigated the effects of opioid receptor blockade on the T-cell population in 36-week-old mice. We did not observe changes in CD4$^+$ T-cells and CD8$^+$ T-cells. We also did not observe changes in naive or effector subpopulations but there was statistically significant increase in CM subpopulation. Administration of NLX did not cause changes in effector, naïve, and CM CD4$^+$ T-cells. However, we observed increase in CM CD8$^+$ T-cells, but not in naive or effector CD8$^+$ T-cells. In line with our data, administration of cyprodime (μ-opioid receptor antagonist) to mice selected for high analgesia induced by swim stress caused increase in CM CD8$^+$ T-cells population [62]. NLX administration affected HMMR expression on CD4$^+$ T-cells, CD8$^+$ T-cells, and CD69$^+$/CD4$^+$ T-cells. We also observed statistically significant increase in HMMR expression in CM, naïve, and effector subpopulations. While the results do not reveal a lot of significant changes in the

T-cells population following NLX treatment, they suggest a link between opioid system blockade, HMMR expression, and the progression of atherosclerosis.

In addition to structural changes, NLX administration significantly altered the proteomic landscape of the aorta. We identified 6869 proteins, 587 of which had significantly altered expression after NLX treatment in aorta of 36-week-old ApoE$^{-/-}$ mice compared to control. Among the proteins with most changed expressions were proteins such as fructose-bisphosphate aldolase B (Q91Y97) encoded by the *Aldob* gene, which plays a role in the proliferation of vascular smooth muscle cells. The excessive proliferation of VSMCs is a key event in the progression of vascular diseases, as it contributes to neointima formation, vascular wall thickening, and arterial stiffness, all of which are characteristic of atherosclerosis [63,64]. Another altered protein encoded by the *Gsta3* gene is glutathione S-transferase A3 (P30115). This enzyme plays a critical role in cellular detoxification processes, particularly in neutralizing reactive oxygen species (ROS) and protecting cells from oxidative stress. Since oxidative stress is a major contributor to atherogenesis, increased expression of GSTA3 may indicate an adaptive cellular response aimed at counteracting the damaging effects of lipid peroxidation and inflammation within atherosclerotic lesions [65]. Additionally, another protein with altered expression is arginase-1 (Q61176), encoded by the Arg1. This protein is a marker of M2 macrophages, which play an important role in the formation of atherosclerotic plaque and also play a key role in wound healing and tissue repair. In the context of atherosclerosis, M2 macrophages contribute to plaque stability by promoting extracellular matrix remodelling; however, they may also be involved in excessive fibrotic responses that can affect plaque composition. Arginase-1 competes with nitric oxide synthase (NOS) for L-arginine, leading to a reduction in nitric oxide (NO) production, a crucial molecule responsible for vasodilation and endothelial function. Decreased NO bioavailability can contribute to vascular dysfunction, increased oxidative stress, and heightened inflammatory responses, all of which exacerbate atherosclerotic disease progression [66,67]. However, we need to underline that despite the many beneficial effects of the opioid system in cardiovascular diseases, some studies have reported harmful effects. An example of this is research showing a connection between the opioid system and atherosclerosis in the context of depression. The comorbidity of these conditions is attributed to increased atherogenicity, insulin resistance (IR), and immune as well as oxidative stress. Neural network and logistic regression models demonstrated that severe depression in the presence of ATS/unstable angina was best predicted by interleukin-6 (IL-6), mu opioid receptor (MOR), zinc, β-endorphin, calcium, and magnesium, whereas moderate depression was associated with IL-6, zinc, MOR, β-endorphin, atherogenicity, IR, and calcium [68]. However, it should be noted that there are studies indicating that nalmefene (an antagonist of mu- and delta-opioid receptors and a partial agonist of kappa-opioid receptors) administration enhances the formation of macrophage-rich plaques in ApoE$^{-/-}$ mice. Nalmefene also significantly increased oxLDL uptake by peritoneal macrophages in vitro, and decreased the mRNA expression of mu, delta, and kappa opioid receptors in macrophages [69].

Studies have also shown that administration of U50488H (a selective κ-opioid agonist) attenuated ischemia-induced arrhythmia in a rat model [70]. However, administration of naltrexone, an opioid antagonist, to rats with stress-induced hypercholesterolemia prevented these changes, suggesting that endogenous opioid systems play a role in the treatment of hypercholesterolemia, which is one of the causes of atherosclerosis [71].

5. Limitations

The research results presented above suggest that the opioid system may play a role in processes involved in the development of atherosclerosis and a potential role for the

Hmmr gene in this disease. Further research involving usage of pharmacological agents or transgenic models will be necessary to confirm the presented findings and define potential molecular mechanism-describing changes which occur in the aorta during the development and course of atherosclerosis.

6. Conclusions

Our study demonstrated that blocking opioid receptors through NLX administration caused changes in the percentage of splenic T-cell subpopulations in both 8-week-old and 36-week-old mice, and also affected collagen expression and the thickness of the collagen layer in the aorta. Furthermore, NLX affected the vascular proteome in 36-week-old mice. These findings therefore suggest the involvement of the opioid system in vascular remodelling associated with the development of atherosclerosis. Moreover, the observed decrease in *Hmmr* expression following NLX administration in both young and older mice may indicate this gene's involvement in early as well as in advanced stages of atherosclerosis.

Supplementary Materials: The following supporting information can be downloaded at: https://www.mdpi.com/article/10.3390/cells14191559/s1, Table S1: List of antibodies used for flow cytometry; Figure S1: Gating strategy of flow cytometry analysis; Figure S2: Quality control of MS runs of the aortas of control and naloxone-treated mice; Table S2: An overview of deregulated proteins, their encoding genes, and functions; Figure S3: Single control image of the aortic arch to confirm the presence of atherosclerotic plaque.

Author Contributions: Conceptualization, K.J., D.S.S. and M.S.; methodology, D.S.S., M.S., K.J., P.P. and M.Ł.; software, D.S.S. and A.S.; validation, K.J., D.S.S. and P.P.; formal analysis, D.S.S., A.S., K.J., A.N. and P.P.; investigation, K.J. and D.S.S.; resources, M.S., K.J. and D.S.S.; data curation, K.J.; writing—original draft preparation, K.J. and D.S.S.; writing—review and editing, K.J., D.S.S., M.S., A.N., P.P. and M.Ł.; visualization, K.J., D.S.S. and A.S.; supervision, D.S.S. and M.S.; funding acquisition, D.S.S. and M.S. All authors have read and agreed to the published version of the manuscript.

Funding: This work was supported by National Science Centre, Poland, project number 2019/35/D/NZ5/02820. This research was carried out with the use of research infrastructure co-financed by the Smart Growth Operational Programme POIR 4.2 project no. POIR.04.02.00-00-D023/20.

Institutional Review Board Statement: The animal study protocol was approved by the II Local Ethics Committee for Experiments on Animals in Warsaw (permission no. WAW2/093/2024).

Data Availability Statement: The original data presented in the study are openly available in the ProteomeXchange Consortium via the PRIDE partner repository with the dataset identifier PXD064451.

Conflicts of Interest: The authors declare no conflicts of interest.

References

1. Björkegren, J.L.; Lusis, A.J. Atherosclerosis: Recent developments. *Cell* **2022**, *185*, 1630–1645. [CrossRef] [PubMed]
2. Libby, P.; Ridker, P.M.; Maseri, A. Inflammation and Atherosclerosis. *Circulation* **2002**, *105*, 1135–1143. [CrossRef] [PubMed]
3. Rafieian-Kopaei, M.; Setorki, M.; Doudi, M.; Baradaran, A.; Nasri, H. Atherosclerosis: Process, Indicators, Risk Factors and New Hopes. *Int. J. Prev. Med.* **2014**, *5*, 927–946. [PubMed]
4. Falk, E. Pathogenesis of Atherosclerosis. *J. Am. Coll. Cardiol.* **2006**, *47* (Suppl. 8), C7–C12. [CrossRef]
5. Rahimi, N. Defenders and Challengers of Endothelial Barrier Function. *Front. Immunol.* **2017**, *8*, 1847. [CrossRef]
6. Cybulsky, M.I.; Gimbrone, M.A. Endothelial expression of a mononuclear leukocyte adhesion molecule during atherogenesis. *Science* **1991**, *251*, 788–791. [CrossRef]
7. Gimbrone, M.A.; Nagel, T.; Topper, J.N. Biomechanical activation: An emerging paradigm in endothelial adhesion biology. *J. Clin. Investig.* **1997**, *99*, 1809–1813. [CrossRef]

8. Zhu, S.-N.; Chen, M.; Jongstra-Bilen, J.; Cybulsky, M.I. GM-CSF regulates intimal cell proliferation in nascent atherosclerotic lesions. *J. Exp. Med.* **2009**, *206*, 2141–2149. [CrossRef]
9. Smith, J.D.; Trogan, E.; Ginsberg, M.; Grigaux, C.; Tian, J.; Miyata, M. Decreased atherosclerosis in mice deficient in both macrophage colony-stimulating factor (op) and apolipoprotein E. *Proc. Natl. Acad. Sci. USA* **1995**, *92*, 8264–8268. [CrossRef]
10. Robbins, C.S.; Hilgendorf, I.; Weber, G.F.; Theurl, I.; Iwamoto, Y.; Figueiredo, J.-L.; Gorbatov, R.; Sukhova, G.K.; Gerhardt, L.M.S.; Smyth, D.; et al. Local proliferation dominates lesional macrophage accumulation in atherosclerosis. *Nat. Med.* **2013**, *19*, 1166–1172. [CrossRef]
11. Yu, X.-H.; Fu, Y.-C.; Zhang, D.-W.; Yin, K.; Tang, C.-K. Foam cells in atherosclerosis. *Clin. Chim. Acta* **2013**, *424*, 245–252. [CrossRef]
12. Tse, K.; Tse, H.; Sidney, J.; Sette, A.; Ley, K. T cells in atherosclerosis. *Int. Immunol.* **2013**, *25*, 615–622. [CrossRef]
13. Saigusa, R.; Winkels, H.; Ley, K. T cell subsets and functions in atherosclerosis. *Nat. Rev. Cardiol.* **2020**, *17*, 387–401. [CrossRef]
14. Plenz, G.A.; Deng, M.C.; Robenek, H.; Völker, W. Vascular collagens: Spotlight on the role of type VIII collagen in atherogenesis. *Atherosclerosis* **2003**, *166*, 1–11. [CrossRef] [PubMed]
15. Romanic, A.; Adachi, E.; Kadler, K.; Hojima, Y.; Prockop, D. Copolymerization of pNcollagen III and collagen I. pNcollagen III decreases the rate of incorporation of collagen I into fibrils, the amount of collagen I incorporated, and the diameter of the fibrils formed. *J. Biol. Chem.* **1991**, *266*, 12703–12709. [CrossRef]
16. Fingerle, J.; Kraft, T. The induction of smooth muscle cell proliferation in vitro using an organ culture system. *Int. Angiol.* **1987**, *6*, 65–72. [PubMed]
17. Souilhol, C.; Harmsen, M.C.; Evans, P.C.; Krenning, G. Endothelial–mesenchymal transition in atherosclerosis. *Cardiovasc. Res.* **2018**, *114*, 565–577. [CrossRef]
18. Fingerle, J.; Au, Y.P.; Clowes, A.W.; Reidy, M.A. Intimal Lesion Formation in Rat Carotid Arteries After Endothelial Denudation in Absence of Medial Injury. *Arter. Off. J. Am. Heart Assoc. Inc.* **1990**, *10*, 1082–1087. [CrossRef]
19. Newby, A.C.; Zaltsman, A.B. Fibrous cap formation or destruction-the critical importance of vascular smooth muscle cell prolif-eration, migration and matrix formation. *Cardiovasc. Res.* **1999**, *41*, 345–360. [CrossRef] [PubMed]
20. Krolikoski, M.; Monslow, J.; Puré, E. The CD44-HA axis and inflammation in atherosclerosis: A temporal perspective. *Matrix Biol.* **2019**, *78–79*, 201–218. [CrossRef]
21. Cuff, C.A.; Kothapalli, D.; Azonobi, I.; Chun, S.; Zhang, Y.; Belkin, R.; Yeh, C.; Secreto, A.; Assoian, R.K.; Rader, D.J.; et al. The adhesion receptor CD44 promotes atherosclerosis by mediating inflammatory cell recruitment and vascular cell activation. *J. Clin. Investig.* **2001**, *108*, 1031–1040. [CrossRef]
22. Shang, J.; Zhang, X.; Hou, G.; Qi, Y. HMMR potential as a diagnostic and prognostic biomarker of cancer—Speculation based on a pan-cancer analysis. *Front. Surg.* **2023**, *9*, 998598. [CrossRef] [PubMed]
23. Hinneh, J.A.; Gillis, J.L.; Mah, C.Y.; Irani, S.; Shrestha, R.K.; Ryan, N.K.; Atsushi, E.; Nassar, Z.D.; Lynn, D.J.; Selth, L.A.; et al. Targeting hyaluronan-mediated motility receptor (HMMR) enhances response to androgen receptor signalling inhibitors in prostate cancer. *Br. J. Cancer* **2023**, *129*, 1350–1361. [CrossRef]
24. Blanco, I.; Kuchenbaecker, K.; Cuadras, D.; Wang, X.; Barrowdale, D.; de Garibay, G.R.; Librado, P.; Sánchez-Gracia, A.; Rozas, J.; Bonifaci, N.; et al. Assessing Associations between the AURKA-HMMR-TPX2-TUBG1 Functional Module and Breast Cancer Risk in BRCA1/2 Mutation Carriers. *PLoS ONE* **2015**, *10*, e0120020. [CrossRef]
25. Missinato, M.A.; Tobita, K.; Romano, N.; Carroll, J.A.; Tsang, M. Extracellular component hyaluronic acid and its receptor Hmmr are required for epicardial EMT during heart regeneration. *Cardiovasc. Res.* **2015**, *107*, 487–498. [CrossRef]
26. Ross, R.; Glomset, J.; Harker, L. Response to injury and atherogenesis. *Am. J. Pathol.* **1977**, *86*, 675. [PubMed]
27. Okano, T.; Sato, K.; Shirai, R.; Seki, T.; Shibata, K.; Yamashita, T.; Koide, A.; Tezuka, H.; Mori, Y.; Hirano, T.; et al. β-Endorphin Mediates the Development and Instability of Atherosclerotic Plaques. *Int. J. Endocrinol.* **2020**, *2020*, 4139093. [CrossRef] [PubMed]
28. Jaskuła, K.; Nawrocka, A.; Poznański, P.; Stachowicz, A.; Łazarczyk, M.; Sacharczuk, M.; Gaciong, Z.; Skiba, D.S. Targeting the Opioid System in Cardiovascular Disease: Liver Proteomic and Lipid Profile Effects of Naloxone in Atherosclerosis. *Biomedicines* **2025**, *13*, 1802. [CrossRef]
29. Panocka, I.; Marek, P.; Sadowski, B. Inheritance of stress-induced analgesia in mice. Selective breeding study. *Brain Res.* **1986**, *397*, 152–155. [CrossRef]
30. Mogil, J.S.; Sternberg, W.F.; Balian, H.; Liebeskind, J.C.; Sadowski, B. Opioid and Nonopioid Swim Stress-Induced Analgesia: A Parametric Analysis in Mice. *Physiol. Behav.* **1996**, *59*, 123–132. [CrossRef]
31. Veseli, B.E.; Perrotta, P.; De Meyer, G.R.; Roth, L.; Van der Donckt, C.; Martinet, W.; De Meyer, G.R. Animal models of atherosclerosis. *Eur. J. Pharmacol.* **2017**, *816*, 3–13. [CrossRef] [PubMed]
32. Breslow, J.L. Mouse models of atherosclerosis. *Science* **1996**, *272*, 685–688. [CrossRef]
33. Reddick, R.L.; Zhang, S.H.; Maeda, N. Atherosclerosis in mice lacking apo E. Evaluation of lesional development and progression. *Arter. Thromb. A J. Vasc. Biol.* **1994**, *14*, 141–147. [CrossRef]
34. Wiśniewski, J.R.; Gaugaz, F.Z. Fast and sensitive total protein and peptide assays for proteomic analysis. *Anal. Chem.* **2015**, *87*, 4110–4116. [CrossRef]

35. Wiśniewski, J.R. Quantitative evaluation of filter aided sample preparation (FASP) and multienzyme digestion FASP protocols. *Anal. Chem.* **2016**, *88*, 5438–5443. [CrossRef]
36. Bruderer, R.; Bernhardt, O.M.; Gandhi, T.; Miladinović, S.M.; Cheng, L.-Y.; Messner, S.; Ehrenberger, T.; Zanotelli, V.; Butscheid, Y.; Escher, C.; et al. Extending the limits of quantitative proteome profiling with data-independent acquisition and application to acetaminophen-treated three-dimensional liver microtissues. *Mol. Cell. Proteom.* **2015**, *14*, 1400–1410. [CrossRef]
37. Huang, T.; Bruderer, R.; Muntel, J.; Xuan, Y.; Vitek, O.; Reiter, L. Combining precursor and fragment information for improved detection of differential abundance in data independent acquisition. *Mol. Cell. Proteom.* **2020**, *19*, 421–430. [CrossRef]
38. Storey, J.D. A direct approach to false discovery rates. *J. R. Statist. Soc. Ser. B Stat. Methodol.* **2002**, *64*, 479–498. [CrossRef]
39. Stachowicz, A.; Czepiel, K.; Wiśniewska, A.; Stachyra, K.; Ulatowska-Białas, M.; Kuśnierz-Cabala, B.; Surmiak, M.; Majka, G.; Kuś, K.; Wood, M.E.; et al. Mitochondria-targeted hydrogen sulfide donor reduces fatty liver and obesity in mice fed a high fat diet by inhibiting de novo lipogenesis and inflammation via mTOR/SREBP-1 and NF-κB signaling pathways. *Pharmacol. Res.* **2024**, *209*, 107428. [CrossRef] [PubMed]
40. Vizcaíno, J.A.; Deutsch, E.W.; Wang, R.; Csordas, A.; Reisinger, F.; Ríos, D.; Dianes, J.A.; Sun, Z.; Farrah, T.; Bandeira, N.; et al. ProteomeXchange provides globally coordinated proteomics data submission and dissemination. *Nat. Biotechnol.* **2014**, *32*, 223–226. [CrossRef] [PubMed]
41. Khan, R.; Spagnoli, V.; Tardif, J.-C.; L'ALlier, P.L. Novel anti-inflammatory therapies for the treatment of atherosclerosis. *Atherosclerosis* **2015**, *240*, 497–509. [CrossRef]
42. Fatkhullina, A.R.; Peshkova, I.O.; Koltsova, E.K. The role of cytokines in the development of atherosclerosis. *Biochemistry* **2016**, *81*, 1358–1370. [CrossRef] [PubMed]
43. Khosravi, M.; Poursaleh, A.; Ghasempour, G.; Farhad, S.; Najafi, M. The effects of oxidative stress on the development of atherosclerosis. *Biol. Chem.* **2019**, *400*, 711–732. [CrossRef]
44. Graziano, R.; Valeriana, S. Atherosclerosis: From biology to pharmacological treatment. *J. Geriatr. Cardiol.* **2012**, *9*, 305–317. [CrossRef] [PubMed]
45. Insull, W., Jr. The Pathology of Atherosclerosis: Plaque Development and Plaque Responses to Medical Treatment. *Am. J. Med.* **2009**, *122* (Suppl. S1), S3–S14. [CrossRef]
46. Skiba, D.S.; Nosalski, R.; Mikolajczyk, T.P.; Siedlinski, M.; Rios, F.J.; Montezano, A.C.; Jawien, J.; Olszanecki, R.; Korbut, R.; Czesnikiewicz-Guzik, M.; et al. Anti-atherosclerotic effect of the angiotensin 1–7 mimetic AVE0991 is mediated by inhibition of perivascular and plaque inflammation in early atherosclerosis. *Br. J. Pharmacol.* **2016**, *174*, 4055–4069. [CrossRef]
47. Galkina, E.; Kadl, A.; Sanders, J.; Varughese, D.; Sarembock, I.J.; Ley, K. Lymphocyte recruitment into the aortic wall before and during development of atherosclerosis is partially L-selectin dependent. *J. Exp. Med.* **2006**, *203*, 1273–1282. [CrossRef]
48. Burleigh, M.C.; Brigfs, A.D.; Lendon, C.L.; Davies, M.J.; Born, G.V.; Richardson, P.D. Collagen types I and III, collagen content, GAGs and mechanical strength of human atherosclerotic plaque caps: Span-wise variations. *Atherosclerosis* **1992**, *96*, 71–81. [CrossRef]
49. Wang, Y.; Johnson, J.A.; Fulp, A.; Sutton, M.A.; Lessner, S.M. Adhesive strength of atherosclerotic plaque in a mouse model depends on local collagen content and elastin fragmentation. *J. Biomech.* **2013**, *46*, 716–722. [CrossRef] [PubMed]
50. Diaz, L.C.; Silva, P.G.d.B.; Dantas, T.S.; Mota, M.R.L.; Alves, A.P.N.N.; Rodrigues, M.I.d.Q.; Mesquita, K.C.; Filho, O.V.d.O.; Sousa, F.B. Naltrexone accelerated oral traumatic ulcer healing and downregulated TLR-4/NF-kB pathway in Wistar rats. *Arch. Oral Biol.* **2024**, *166*, 106047. [CrossRef]
51. Dunn, J.; Liu, Y.; Banov, F.; Denison, S.; Banov, D. A topical naltrexone formulation for surgical wound healing: A case report. *J. Cosmet. Dermatol.* **2020**, *20*, 838–841. [CrossRef]
52. Truong, J.L.; Liu, M.; Tolg, C.; Barr, M.; Dai, C.; Raissi, T.C.; Wong, E.; DeLyzer, T.; Yazdani, A.; Turley, E.A. Creating a Favorable Microenvironment for Fat Grafting in a Novel Model of Radiation-Induced Mammary Fat Pad Fibrosis. *Plast. Reconstr. Surg.* **2020**, *145*, 116–126. [CrossRef]
53. Sansilvestri-Morel, P.; Rupin, A.; Badier-Commander, C.; Kern, P.; Fabiani, J.-N.; Verbeuren, T.J.; Vanhoutte, P.M. Imbalance in the synthesis of collagen type I and collagen type III in smooth muscle cells derived from human varicose veins. *J. Vasc. Res.* **2001**, *38*, 560–568. [CrossRef]
54. Mays, P.; Bishop, J.; Laurent, G. Age-related changes in the proportion of types I and III collagen. *Mech. Ageing Dev.* **1988**, *45*, 203–212. [CrossRef]
55. Maurel, E.; Shuttleworth, C.A.; Bouissou, H. Interstitial collagens and ageing in human aorta. *Virchows Arch. A* **1987**, *410*, 383–390. [CrossRef]
56. Hansen, L.; Taylor, W.R. Is increased arterial stiffness a cause or consequence of atherosclerosis? *Atherosclerosis* **2016**, *249*, 226–227. [CrossRef]
57. Kochová, P.; Kuncová, J.; Švíglerová, J.; Cimrman, R.; Miklíková, M.; Liška, V.; Tonar, Z. The contribution of vascular smooth muscle, elastin and collagen on the passive mechanics of porcine carotid arteries. *Physiol. Meas.* **2012**, *33*, 1335–1351. [CrossRef]

58. Borges, L.d.F.; Jaldin, R.G.; Dias, R.R.; Stolf, N.A.G.; Michel, J.-B.; Gutierrez, P.S. Collagen is reduced and disrupted in human aneurysms and dissections of ascending aorta. *Hum. Pathol.* **2008**, *39*, 437–443. [CrossRef] [PubMed]
59. Immonen, J.A.; Zagon, I.S.; Lewis, G.S.; McLaughlin, P.J. Topical treatment with the opioid antagonist naltrexone accelerates the remodeling phase of full-thickness wound healing in type 1 diabetic rats. *Exp. Biol. Med.* **2013**, *238*, 1127–1135. [CrossRef] [PubMed]
60. Tabas, I.; Lichtman, A.H. Monocyte-Macrophages and T Cells in Atherosclerosis. *Immunity* **2017**, *47*, 621–634. [CrossRef] [PubMed]
61. Hinkley, H.; Counts, D.A.; VonCanon, E.; Lacy, M. T Cells in Atherosclerosis: Key Players in the Pathogenesis of Vascular Disease. *Cells* **2023**, *12*, 2152. [CrossRef] [PubMed]
62. Skiba, D.; Jaskuła, K.; Nawrocka, A.; Poznański, P.; Łazarczyk, M.; Szymański, Ł.; Żera, T.; Sacharczuk, M.; Cudnoch-Jędrzejewska, A.; Gaciong, Z. The Role of Opioid Receptor Antagonists in Regulation of Blood Pressure and T-Cell Activation in Mice Selected for High Analgesia Induced by Swim Stress. *Int. J. Mol. Sci.* **2024**, *25*, 2618. [CrossRef]
63. Cao, W.; Chang, T.; Li, X.-Q.; Wang, R.; Wu, L. Dual effects of fructose on ChREBP and FoxO1/3α are responsible for AldoB up-regulation and vascular remodelling. *Clin. Sci.* **2017**, *131*, 309–325. [CrossRef] [PubMed]
64. Liu, J.; Wang, R.; Desai, K.; Wu, L. Upregulation of aldolase B and overproduction of methylglyoxal in vascular tissues from rats with metabolic syndrome. *Cardiovasc. Res.* **2011**, *92*, 494–503. [CrossRef]
65. Hoen, P.A.C.; Van der Lans, C.A.; Van Eck, M.; Bijsterbosch, M.K.; Van Berkel, T.J.; Twisk, J. Aorta of ApoE-Deficient Mice Responds to Atherogenic Stimuli by a Prelesional Increase and Subsequent Decrease in the Expression of Antioxidant Enzymes. *Circ. Res.* **2003**, *93*, 262–269. [CrossRef]
66. Liu, S.-L.; Li, Y.-H.; Shi, G.-Y.; Chen, Y.-H.; Huang, C.-W.; Hong, J.-S.; Wu, H.-L. A Novel Inhibitory Effect of Naloxone on Macrophage Activation and Atherosclerosis Formation in Mice. *J. Am. Coll. Cardiol.* **2006**, *48*, 1871–1879. [CrossRef]
67. Pourcet, B.; Pineda-Torra, I. Transcriptional regulation of macrophage arginase 1 expression and its role in atherosclerosis. *Trends Cardiovasc. Med.* **2013**, *23*, 143–152. [CrossRef] [PubMed]
68. Mousa, R.F.; Smesam, H.N.; Qazmooz, H.A.; Al-Hakeim, H.K.; Maes, M. A pathway phenotype linking metabolic, immune, oxidative, and opioid pathways with comorbid depression, atherosclerosis, and unstable angina. *CNS Spectrums* **2022**, *27*, 676–690. [CrossRef]
69. Koga, M.; Inada, K.; Yamada, A.; Maruoka, K.; Yamauchi, A. Nalmefene, an opioid receptor modulator, aggravates atherosclerotic plaque formation in apolipoprotein E knockout mice by enhancing oxidized low-density lipoprotein uptake in macrophages. *Biochem. Biophys. Rep.* **2024**, *38*, 101688. [CrossRef]
70. Wang, G.-Y.; Wu, S.; Pei, J.-M.; Yu, X.-C.; Wong, T.-M. κ- but not δ-opioid receptors mediate effects of ischemic preconditioning on both infarct and arrhythmia in rats. *Am. J. Physiol. Circ. Physiol.* **2001**, *280*, H384–H391. [CrossRef]
71. Bryant, H.U.; Story, J.A.; Yim, G.K. Assessment of endogenous opioid mediation in stress-induced hypercho-lesterolemia in the rat. *Biopsychosoc. Sci. Med.* **1988**, *50*, 576–585.

Supplementary materials

Table S1. List of antibodies used for flow cytometry

Specificity	Fluorochrome	Clone Name	Supplier
CD3ε	PerCP	145-2C11	BioLegend
CD8a	AF700	53-6.7	BioLegend
CD4	BV750	GK 4.5	BioLegend
CD69	PEC7	H1.2F3	BioLegend
CD44	AF647	IM7	BioLegend
CD62L	PE594	MEL-14	BioLegend
CD168	CoraLite488	Polyclonal antibody	Proteintech

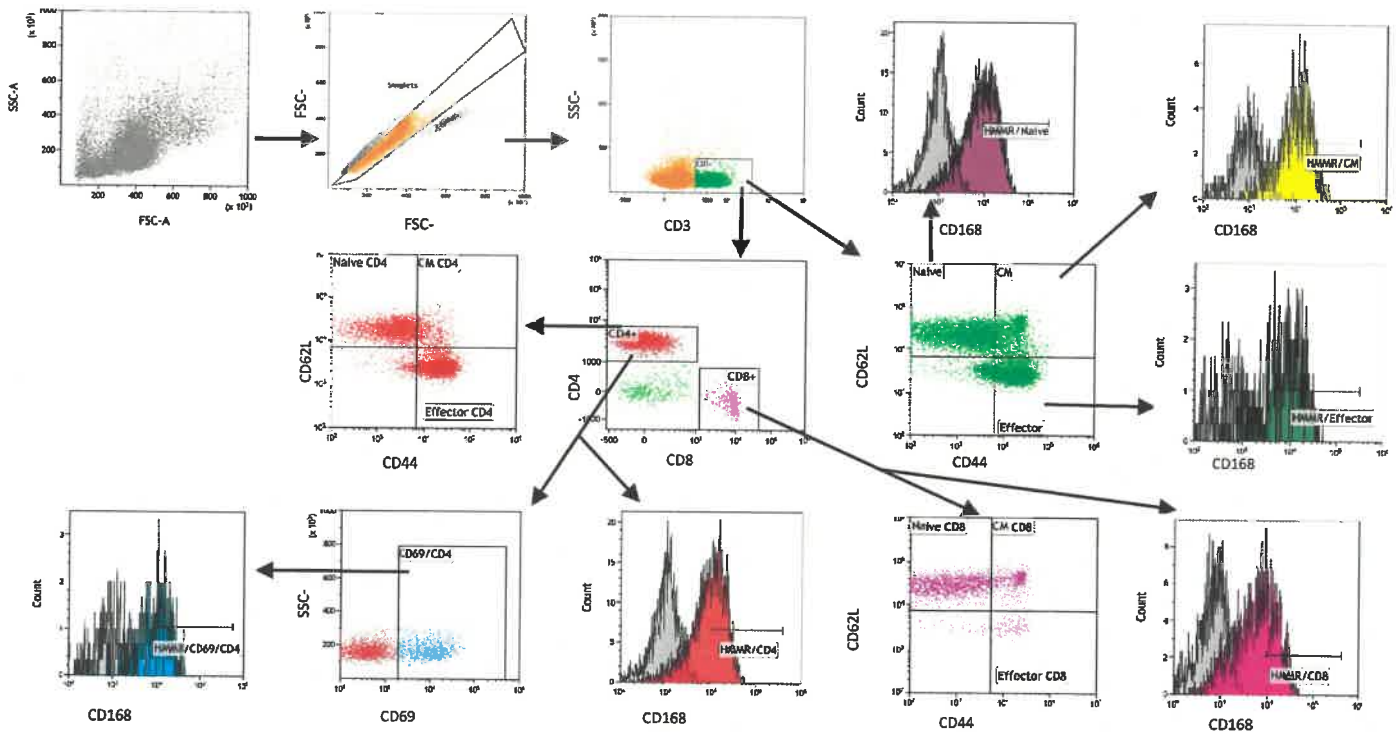

Figure S1. Gating strategy of flow cytometry analysis

A)

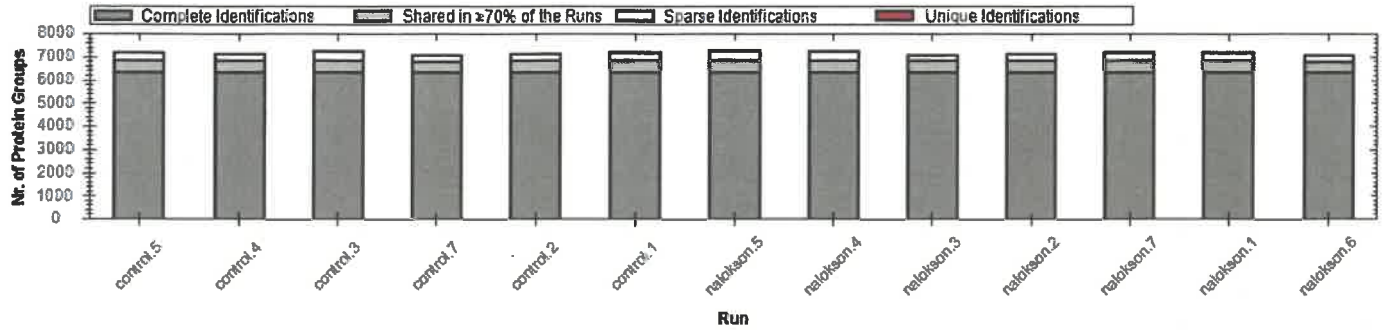

B)

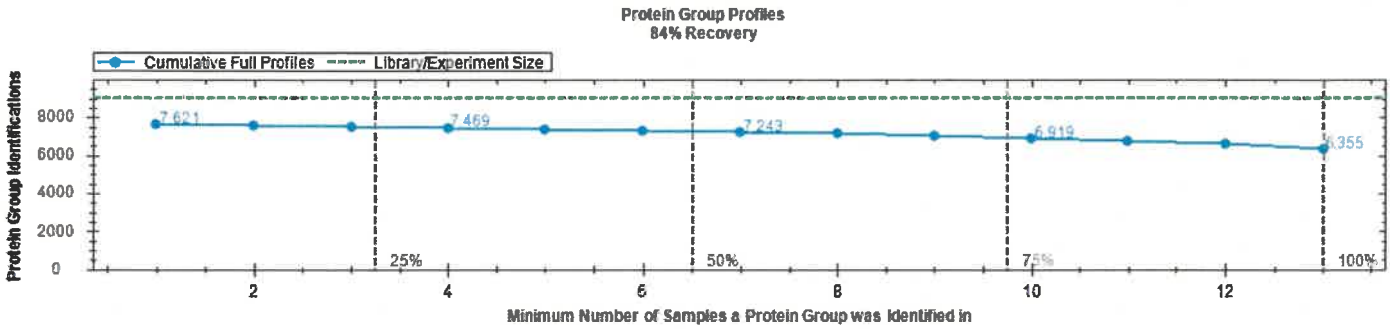

C)

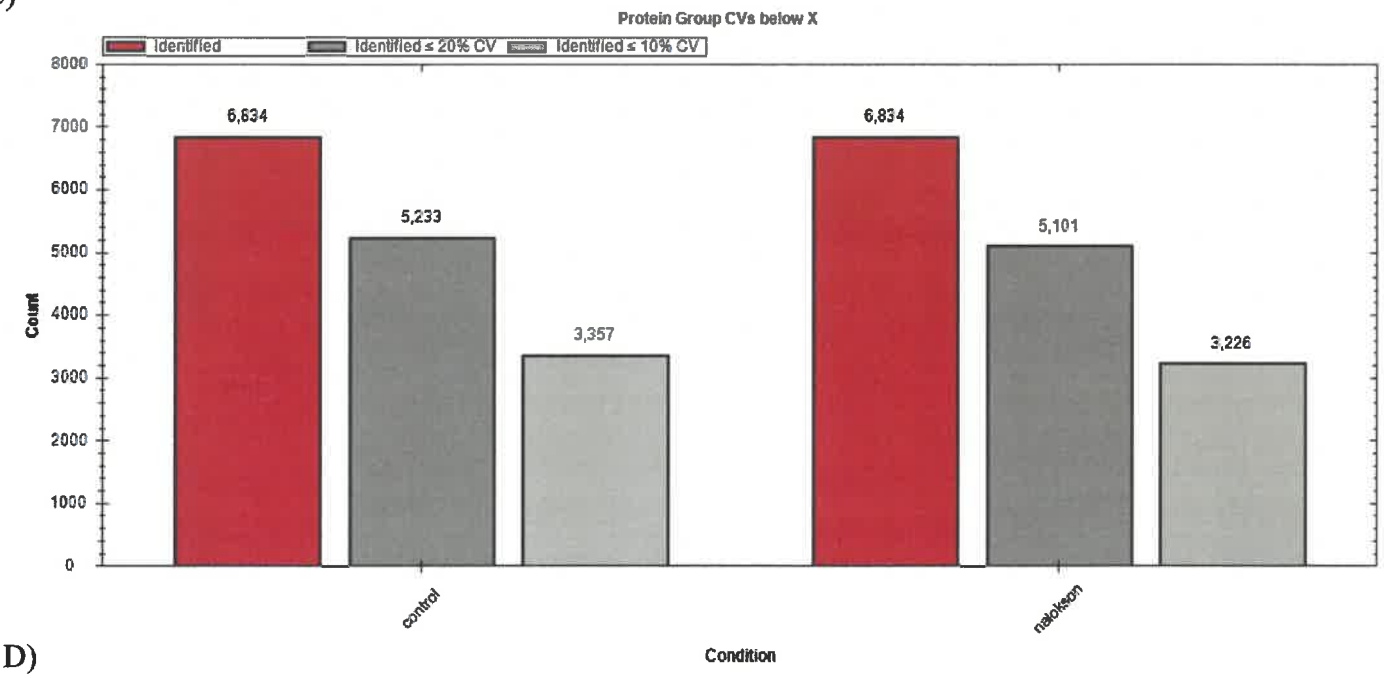

D)

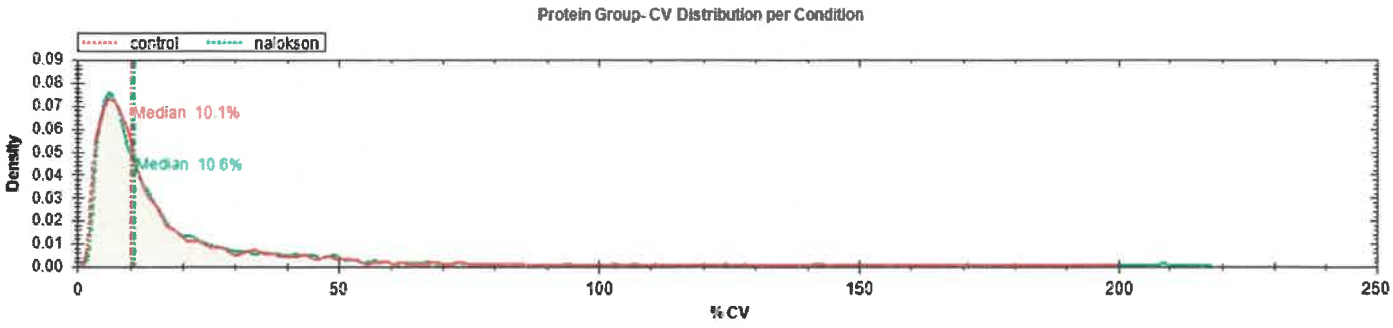

Figure S2. Quality control of MS runs of the aorta of control and naloxone-treated mice. Protein group identification details across all LC-MS runs (A). Spectral library recovery (B). Coefficient of variations (CVs) for protein groups across all biological conditions (C). Distribution of protein group CV in biological conditions (D)

Table S2. An overview of deregulated proteins, their encoding genes, and functions (functions obtained from UniProt database [1]).

Protein	Gene	Fold change	Main function	Function connected to atherosclerosis development
A3KFM7	*Chd6* (Chromodomain-helicase-DNA-binding protein 6)	6.1	DNA-dependent ATPase that plays a role in chromatin remodeling. Regulates transcription by disrupting nucleosomes in a largely non-sliding manner which strongly increases the accessibility of chromatin.	-
P30115	*Gsta3* (Glutathione S-transferase A3)	-3.01	Conjugation of reduced glutathione to a wide number of exogenous and endogenous hydrophobic electrophiles. Catalyzes isomerization reactions that contribute to the biosynthesis of steroid hormones.	The expression of *Gsta3* mRNA in the aortic arch of $ApoE^{-/-}$ mice increased in the period preceding the development of atherosclerotic lesions (age from 6 to 12 weeks), whereas it decreased inversely proportional to the development of lesions (between 12 and 34 weeks) [14].
P18528	Ig heavy chain V region 6.96	-3.01		-
P97772	*Grm1* (Metabotropic glutamate receptor 1)	-3.11	G-protein coupled receptor for glutamate. Ligand binding causes a conformation change that triggers signaling via guanine nucleotide-binding proteins (G proteins) and modulates the activity of down-stream effectors. Signaling activates a phosphatidylinositol-calcium second messenger system.	-
Q9DCU9	*Hoga1* (4-hydroxy-2-oxoglutarate aldolase, mitochondrial)	-3.21	Catalyzes the final step in the metabolic pathway of hydroxyproline.	-
P51670	*Ccl9* (C-C motif chemokine 9)	-3.22	Monokine with inflammatory, pyrogenic and chemokinetic properties. Circulates at high concentrations in the blood of healthy animals. Binding to a high-affinity receptor activates calcium release in neutrophils.	-
O09173	*Hgd* (Homogentisate 1,2-dioxygenase)	-3.22	Catalyzes the conversion of homogentisate to maleylacetoacetate.	-
Q8BH00	*Aldh8a1* (2-aminomuconic semialdehyde dehydrogenase)	-3.23	Catalyzes the NAD-dependent oxidation of 2-aminomuconic semialdehyde of the kynurenine metabolic pathway in L-tryptophan degradation.	-

Q9DCG6	*Pbld1* (Phenazine biosynthesis-like domain-containing protein 1)	-3.34	Involved in maintenance of gastrointestinal epithelium.	-
P53657	*Pklr* (Pyruvate kinase PKLR)	-3.37	Pyruvate kinase that catalyzes the conversion of phosphoenolpyruvate to pyruvate with the synthesis of ATP, and which plays a key role in glycolysis.	-
Q91VA0	*Acsm1* (Acyl-coenzyme A synthetase ACSM1, mitochondrial)	-3.38	Catalyzes the activation of fatty acids by CoA to produce an acyl-CoA, the first step in fatty acid metabolism.	-
Q9QXF8	*Gnmt* (Glycine N-methyltransferase)	-3.40	Catalyzes the methylation of glycine by using S-adenosylmethionine (AdoMet) to form N-methylglycine (sarcosine) with the concomitant production of S-adenosylhomocysteine (AdoHcy).	$ApoE^{-/-}/Gnmt^{-/-}$ mice had significantly increased development of atherosclerotic lesions in the aortic roots compared with $ApoE^{-/-}$ mice. Furthermore, $ApoE^{-/-}$ $GNMT^{-/-}$ mice showed increased levels of *IL-6*, *TNF-α*, *MCP-1*, and *MIP-2* in serum and aorta and higher expression of *VCAM-1* and *iNOS* in aortas than $ApoE^{-/-}$ mice [20].
Q91Y97	*Aldob* (Fructose-bisphosphate aldolase B)	-3.51	Catalyzes the aldol cleavage of fructose 1,6-biphosphate to form two triosephosphates dihydroxyacetone phosphate and D-glyceraldehyde 3-phosphate in glycolysis as well as the reverse stereospecific aldol addition reaction in gluconeogenesis.	The knockdown of *AldoB* expression prevented fructose-induced methylglyoxal overproduction and vascular smooth muscle cells proliferation [19].
Q61176	*Arg1* (Arginase-1)	-3.56	Key element of the urea cycle converting L-arginine to urea and L-ornithine. Plays a role in the immune response of alternatively activated or M2 macrophages in processes such as wound healing and tissue regeneration	*Agr1* gene expression was significantly higher in peritoneal macrophages from 28-week-old Fcγ receptor-deficient mice ($\gamma^{-/-}ApoE^{-/-}$) than in $ApoE^{-/-}$ mice [17].
P11725	*Otc* (Ornithine transcarbamylase, mitochondrial)	-3.58	Catalyzes the second step of the urea cycle, the condensation of carbamoyl phosphate with L-ornithine to form L-citrulline.	Data from databases obtained during two studies conducted in France (MONICA and EVA) indicated that in men, the frequency of the OTC single nucleotide polymorphism rs5963409 was higher in hypertensive than in normotensive subjects [16].
Q61646	*Hp* (Haptoglobin)	-3.58	Haptoglobin captures, and combines with free plasma hemoglobin to allow hepatic recycling of heme iron and to prevent kidney damage. Haptoglobin also acts as an antioxidant, has antibacterial activity and plays a role in modulating many aspects of the acute phase response	Creation a murine type 2 Hp allele and targeted its insertion to the Hp locus by homologous recombination coused increased iron, lipid peroxidation and macrophage accumulation in plaques of $ApoE^{-/-}$ Hp 2-2 mice what suggest that the Hp genotype plays a critical

				role in the oxidative and inflammatory response to intraplaque hemorrhage [6].
Q8VCN5	*Cth* (Cystathionine gamma-lyase)	-3.77	Catalyzes the last step in the trans-sulfuration pathway from L-methionine to L-cysteine in a pyridoxal-5'-phosphate (PLP)-dependent manner.	Studies have shown that in the aortas of $cth^{SMC-/-}$ mice (VSMC-specific *cth* knockout mice), En-face Oil Red O staining showed that the number of aortic plaques increased by about 76% in comparison to the control [18].
Q9D1Q1	*Mphosph6* (M-phase phosphoprotein 6)	-3.89	RNA-binding protein that associates with the RNA exosome complex. Plays a role in recruiting the RNA exosome complex to pre-rRNA	Genetic polymorphisms of MPHOSPH6 (rs1056654) were associated with a decreased risk of coronary artery disease in Chinese Han population [8].
Q9EQF5	*Dpys* (Dihydropyrimidinase)	-4.27	Catalyzes the second step of the reductive pyrimidine degradation, the reversible hydrolytic ring opening of dihydropyrimidines.	-
P97328	*Khk* (Ketohexokinase)	-4.31	Catalyzes the phosphorylation of the ketose sugar fructose to fructose-1-phosphate.	Mice deficient in ketohexokinase (KHK) showed reduce features of non-alcoholic steatohepatitis (NASH) on a high-fat/high-fructose diet. KHK inhibition reduced lipogenic gene expression in the presence of high fructose/glucose. Moreover, activated myofibroblasts exhibit reduced expression of fibrogenic genes when treated with a KHK inhibitor. The KHK inhibitor also decreases hepatic accumulation of lipogenic fructose derivatives and reduces glycolysis in human liver tissue [25].
P12710	*Fabp1* (Fatty acid-binding protein)	-4.59	Plays a role in lipoprotein-mediated cholesterol uptake in hepatocytes. Binds cholesterol. Binds free fatty acids and their coenzyme A derivatives, bilirubin, and some other small molecules in the cytoplasm.	The study cohort included 479 Chinese subjects who underwent carotid intima-media thickness (IMT) measurement. Serum A-FABP levels were positively associated with carotid IMT in both men and women [27].
Q9QXD6	*Fbp1* (Fructose-1,6-bisphosphatase 1)	-4.62	Catalyzes the hydrolysis of fructose 1,6-bisphosphate to fructose 6-phosphate in the presence of divalent cations, acting as a rate-limiting enzyme in gluconeogenesis. Plays a role in regulating glucose sensing and insulin secretion of pancreatic beta-cells.	Studies have shown Selective knockdown of FBP1 significantly enhanced the migration, and proliferation of hESC-ECs (human embryonic stem cell-derived endothelial cells), implying activation of angiogenesis. Moreover, FBP1 inhibition partially reversed the inhibitory effect of retinoic acid on angiogenesis [24].
Q78JT3	*Haao* (3-hydroxyanthranilate 3,4-dioxygenase)	-4.74	Catalyzes the oxidative ring opening of 3-hydroxyanthranilate to 2-amino-3-carboxymuconate semialdehyde, which spontaneously cyclizes to quinolinate.	Research demonstrated that treatment of Ldlr-/- mice with the HAAO inhibitor (NCR-631) significantly reduced atherosclerotic lesion area in the aortic arch compared to PBS controls. NCR-631 treatment also

				resulted in lower plasma levels of total cholesterol and triglycerides compared to controls [23].
Q3U0D9	*Hace1* (E3 ubiquitin-protein ligase HACE1)	-5.10	Acts as a regulator of Golgi membrane dynamics during the cell cycle: recruited to Golgi membrane by Rab proteins and regulates postmitotic Golgi membrane fusion.	-
Q64374	*Rgn* (Regucalcin)	-5.20	Gluconolactonase with low activity towards other sugar lactones, including gulonolactone and galactonolactone. Catalyzes a key step in ascorbic acid (vitamin C) biosynthesis.	Liver regucalcin gene expression is stimulated through action of insulin in liver cells and decreased in type I diabetic model animals. Overexpreesion of regucalcin reveals hepatic insulin resistance, decreased liver triglyceride, total cholesterol and glycogen contents in the liver of rats, inducing a hyperlipidemia. Liver leptin and adiponectin mRNA expressions are decreased by overexpression of regucalcin. Deficiency of regucalcin induces an impairment of glucose tolerance and liver lipid accumulation in mice, and it is associated with the development and progression of nonalcoholic fatty liver disease and fibrosis in human patients [26].
P54227	*Stmn1* (Stathmin)	-5.42	Involved in the regulation of the microtubule (MT) filament system by destabilizing microtubules. Prevents assembly and promotes disassembly of microtubules.	-
P12246	*Apcs* (Serum amyloid P-component)	-5.70	Belonging to the pentraxin family of proteins, which has a characteristic pentameric organization.	-
Q6IMF0	*Krt87* (Keratin, type II cuticular 87)	-22.55	Predicted to be a structural constituent of skin epidermis.	-
P05366	*Saa1* (serum amyloid A1)	-26.78	Major acute phase reactant	$ApoE^{-/-}$ mice overexpressed murine SAA1 exhibited modest but persistent increase in SAA that contributed to increased atherosclerosis via increased inflammatory cell infiltration [29]. $Rag1^{-/-}ApoE^{-/-}$ and $ApoE^{-/-}$ mice injected with adenoviral vector encoding human SAA1 had increased atherosclerosis compared with controls [30].

A) B)

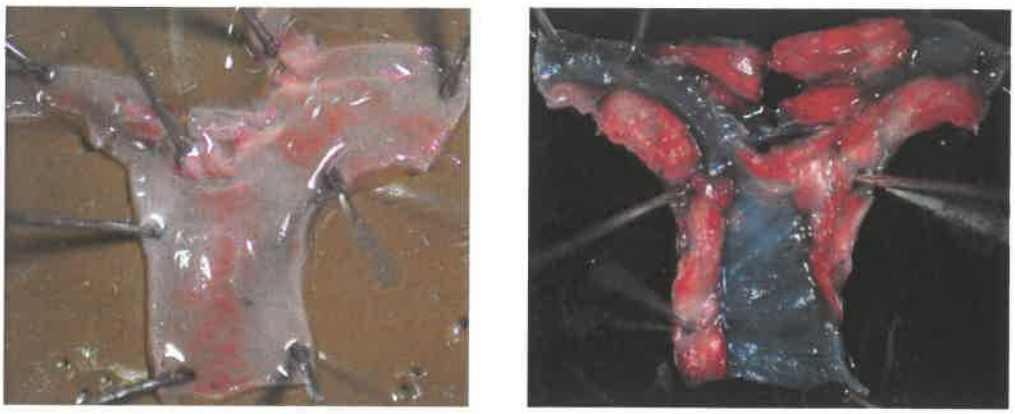

Figure S3. Single control image of the aortic arch to confirm the presence of atherosclerotic plaque. A) 8-week-old NaCl; B) 36- week-old NaCl.

[1] UniProt: the Universal Protein Knowledgebase in 2023. Nucleic Acids Res 2023;51:D523–31. https://doi.org/10.1093/nar/gkac1052.

[2] Oner T, Arslan C, Yenmis G, Arapi B, Tel C, Aydemir B, et al. Association of NFKB1A and microRNAs variations and the susceptibility to atherosclerosis. J Genet 2017;96:251–9. https://doi.org/10.1007/S12041-017-0768-9.

[3] Carlson CS, Heagerty PJ, Nord AS, Pritchard DK, Ranchalis J, Boguch JM, et al. TagSNP evaluation for the association of 42 inflammation loci and vascular disease: evidence of IL6, FGB, ALOX5, NFKBIA, and IL4R loci effects. Hum Genet 2007;121:65–75. https://doi.org/10.1007/S00439-006-0289-8.

[4] Rezq AA, Mahmoud MY. Preventive effect of wheat germ on hypercholesteremic and atherosclerosis in rats fed cholesterol-containing diet. Pakistan Journal of Nutrition 2011;10:424–32. https://doi.org/10.3923/pjn.2011.424.432.

[5] Stachowicz A, Olszanecki R, Suski M, Wiśniewska A, Kuś K, Białas M, et al. Quantitative proteomics reveals decreased expression of major urinary proteins in the liver of apoE/eNOS-DKO mice. Clin Exp Pharmacol Physiol 2018;45:711–9. https://doi.org/10.1111/1440-1681.12927.

[6] Levy AP, Levy JE, Kalet-Litman S, Miller-Lotan R, Levy NS, Asaf R, et al. Haptoglobin Genotype Is a Determinant of Iron, Lipid Peroxidation, and Macrophage Accumulation in the Atherosclerotic Plaque 2006. https://doi.org/10.1161/01.ATV.0000251020.24399.a2.

[7] Chen Y, Yang M, Zhang M, Wang H, Zheng Y, Sun R, et al. Single-Cell Transcriptome Reveals Potential Mechanisms for Coronary Artery Lesions in Kawasaki Disease. Arterioscler Thromb Vasc Biol 2024;44:866–82. https://doi.org/10.1161/ATVBAHA.123.320188.

[8] Song Y, Yan M, Li J, Li J, Jin T, Chen C. Association between TNIP1, MPHOSPH6 and ZNF208 genetic polymorphisms and the coronary artery disease risk in Chinese Han population n.d.

[9] Liu Y, Zhao Y, Hayek T, Chen YE, Rom O, Shukha Y, et al. Dysregulated oxalate metabolism is a driver and therapeutic target in atherosclerosis. CellReports 2021;36:109420. https://doi.org/10.1016/j.celrep.2021.109420.

[10] Boehme B, Schelski N, Makridakis M, Henze L, Vlahou A, Lang F, et al. Role of Cytosolic Serine Hydroxymethyl Transferase 1 (SHMT1) in Phosphate-Induced Vascular Smooth Muscle Cell Calcification. Kidney Blood Press Res 2018;43:1212–21. https://doi.org/10.1159/000492248.

[11] Gu X, Yu Z, Qian T, Jin Y, Xu G, Li J, et al. Transcriptomic analysis identifies the shared diagnostic biomarkers and immune relationship between Atherosclerosis and abdominal aortic aneurysm based on fatty acid metabolism gene set. Front Mol Biosci 2024;11. https://doi.org/10.3389/fmolb.2024.1365447.

[12] Kisucka J, Chauhan AK, Patten IS, Yesilaltay A, Neumann C, Van Etten RA, et al. Peroxiredoxin1 prevents excessive endothelial activation and early atherosclerosis. Circ Res 2008;103:598–605. https://doi.org/10.1161/CIRCRESAHA.108.174870.

[13] Madrigal-Matute J, Fernandez-Garcia CE, Blanco-Colio LM, Burillo E, Fortuño A, Martinez-Pinna R, et al. Thioredoxin-1/peroxiredoxin-1 as sensors of oxidative stress mediated by NADPH oxidase activity in atherosclerosis. Free Radic Biol Med 2015;86:352–61. https://doi.org/10.1016/J.FREERADBIOMED.2015.06.001.

[14] 't Hoen PAC, Van Der Lans CAC, Eck M Van, Bijsterbosch MK, Van Berkel TJC, Twisk J. Aorta of ApoE-Deficient Mice Responds to Atherogenic Stimuli by a Prelesional Increase and Subsequent Decrease in the Expression of Antioxidant Enzymes 2003. https://doi.org/10.1161/01.RES.0000082978.92494.B1.

[15] AGXT2 Polymorphism and CHD Risk n.d.

[16] Dumont J, Meroufel D, Bauters C, Hansmannel F, Bensemain F, Cottel D, et al. Association of Ornithine Transcarbamylase Gene Polymorphisms With Hypertension and Coronary Artery Vasomotion. Am J Hypertens 2009;22:993–1000. https://doi.org/10.1038/AJH.2009.110.

[17] Mallavia B, Oguiza A, Lopez-Franco O, Recio C, Ortiz-Muñ Oz G. Gene Deficiency in Activating Fcc Receptors Influences the Macrophage Phenotypic Balance and Reduces Atherosclerosis in Mice. PLoS One 2013;8:66754. https://doi.org/10.1371/journal.pone.0066754.

[18] Chen Z, Ouyang C, Zhang H, Gu Y, Deng Y, Du C, et al. Vascular smooth muscle cell-derived hydrogen sulfide promotes atherosclerotic plaque stability via TFEB (transcription factor EB)-mediated autophagy 2022. https://doi.org/10.1080/15548627.2022.2026097.

[19] Cao W, Chang T, Li X qiang, Wang R, Wu L. Dual effects of fructose on ChREBP and FoxO1/3α are responsible for AldoB up-regulation and vascular remodelling. Clin Sci 2017;131:309–25. https://doi.org/10.1042/CS20160251.

[20] Chen CY, Ching LC, Liao YJ, Yu Y Bin, Tsou CY, Shyue SK, et al. Deficiency of Glycine N-methyltransferase aggravates atherosclerosis in apolipoprotein E-null mice. Molecular Medicine 2012;18:744–52. https://doi.org/10.2119/molmed.2011.00396.

[21] Van Dongen K, Leleu D, Pilot T, Jalil A, Mangin L, Ménégaut L, et al. Atheroma plaque microenvironment stimulates kynurenine production by macrophages to induce endothelial adhesion molecules in the context of atherogenesis 2023. https://doi.org/10.1101/2023.07.19.549799.

[22] Dong J, Song C, Zhang L, Feng X, Feng R, Lu Q, et al. Identified key genes related to carotid atheroma plaque from gene expression chip. Artif Cells Nanomed Biotechnol 2017;45:1132–7. https://doi.org/10.1080/21691401.2016.1216858.

[23] Berg M, Polyzos KA, Agardh H, Baumgartner R, Forteza MJ, Kareinen I, et al. 3-Hydroxyanthralinic acid metabolism controls the hepatic SREBP/lipoprotein axis, inhibits inflammasome activation in macrophages, and decreases atherosclerosis in Ldlr-/- mice. Cardiovasc Res 2020;116:1948–57. https://doi.org/10.1093/CVR/CVZ258.

[24] Yang Z, Yu M, Li X, Tu Y, Wang C, Lei W, et al. Retinoic acid inhibits the angiogenesis of human embryonic stem cell-derived endothelial cells by activating FBP1-mediated gluconeogenesis. Stem Cell Res Ther 2022;13. https://doi.org/10.1186/S13287-022-02908-X.

[25] Shepherd EL, Saborano R, Northall E, Matsuda K, Ogino H, Yashiro H, et al. Ketohexokinase inhibition improves NASH by reducing fructose-induced steatosis and fibrogenesis. JHEP Rep 2020;3. https://doi.org/10.1016/J.JHEPR.2020.100217.

[26] Yamaguchi M, Murata T. Involvement of regucalcin in lipid metabolism and diabetes. Metabolism 2013;62:1045–51. https://doi.org/10.1016/J.METABOL.2013.01.023.

[27] Yeung D, Xu A, Cheung C, Wat N, Yau M, Fong C, et al. Serum Adipocyte Fatty Acid-Binding Protein Levels Were Independently Associated With Carotid Atherosclerosis 2007. https://doi.org/10.1161/ATVBAHA.107.146274.

[28] Webb NR, De Beer MC, Wroblewski JM, Ji A, Bailey W, Shridas P, et al. Deficiency of Endogenous Acute-Phase Serum Amyloid A Protects apoE-/- Mice From Angiotensin II-Induced Abdominal Aortic Aneurysm Formation. Arterioscler Thromb Vasc Biol 2015;35:1156–65. https://doi.org/10.1161/ATVBAHA.114.304776.

[29] Dong Z, Wu T, Qin W, An C, Wang Z, Zhang M, et al. Serum amyloid A directly accelerates the progression of atherosclerosis in apolipoprotein E-deficient mice. Mol Med 2011;17:1357–64. https://doi.org/10.2119/MOLMED.2011.00186.

[30] Thompson JC, Jayne C, Thompson J, Wilson PG, Yoder MH, Webb N, et al. A brief elevation of serum amyloid A is sufficient to increase atherosclerosis. J Lipid Res 2015;56:286–93. https://doi.org/10.1194/JLR.M054015.

biomedicines

MDPI

Article

Targeting the Opioid System in Cardiovascular Disease: Liver Proteomic and Lipid Profile Effects of Naloxone in Atherosclerosis

Kinga Jaskuła [1], Agata Nawrocka [1], Piotr Poznański [2], Aneta Stachowicz [3], Marzena Łazarczyk [1], Mariusz Sacharczuk [1,4,*], Zbigniew Gaciong [5] and Dominik S. Skiba [1]

1 Department of Experimental Genomics, Institute of Genetics and Animal Biotechnology, Polish Academy of Sciences, Postępu 36A, 05-552 Jastrzębiec, Poland; k.jaskula@igbzpan.pl (K.J.); a.nawrocka@igbzpan.pl (A.N.); m.lazarczyk@igbzpan.pl (M.Ł.); d.skiba@igbzpan.pl (D.S.S.)
2 Department of Biotechnology and Nutrigenomics, Institute of Genetics and Animal Biotechnology, Polish Academy of Sciences, Postępu 36A, 05-552 Jastrzębiec, Poland; p.poznanski@igbzpan.pl
3 Department of Pharmacology, Faculty of Medicine, Jagiellonian University Medical College, 31-008 Krakow, Poland; aneta.stachowicz@uj.edu.pl
4 Department of Pharmacodynamics, Faculty of Pharmacy, Warsaw Medical University, Banacha 1, 02-697 Warsaw, Poland
5 Department and Clinic of Internal Diseases, Hypertension and Angiology, Medical University of Warsaw, Banacha 1A Street, 02-097 Warsaw, Poland; zbigniew.gaciong@wum.edu.pl
* Correspondence: m.sacharczuk@igbzpan.pl; Tel.: +48-227367026

Abstract

Background: The endogenous opioid system plays a pivotal role in numerous physiological processes and is implicated in a range of diseases, including atherosclerosis, a condition contributing to nearly 50% of deaths in Western societies. **Objectives:** This study investigates the effects of opioid receptor blockade, using naloxone, on the plasma lipid profile and atherosclerosis progression. **Methods:** ApoE$^{-/-}$ mice with advanced atherosclerosis were treated with naloxone for seven days, and the effects on atherosclerotic plaque development and liver steatosis were evaluated. **Results:** A proteomic analysis of liver samples post-treatment identified 38 proteins with altered abundance. The results revealed that naloxone treatment led to an increase in HDL cholesterol, a lipid fraction associated with protective cardiovascular effects. Furthermore, naloxone did not influence the progression of atherosclerotic plaques or the development of liver steatosis. **Conclusions:** In conclusion, while short-term naloxone treatment in mice with advanced atherosclerosis does not alter overall atherosclerotic plaque progression or liver steatosis, the observed elevation in HDL cholesterol and the extensive changes in liver protein abundance underscore the complex and multifaceted role of the opioid system in lipid metabolism and cardiovascular health. These findings provide a foundation for further exploration of opioid receptor antagonists as modulators of lipid profiles and potential contributors to cardiovascular therapy.

Keywords: opioid receptors; cholesterol; atherosclerotic plaque; liver steatosis

Academic Editor: Alfredo Caturano

Received: 25 June 2025
Revised: 14 July 2025
Accepted: 17 July 2025
Published: 23 July 2025

Citation: Jaskuła, K.; Nawrocka, A.; Poznański, P.; Stachowicz, A.; Łazarczyk, M.; Sacharczuk, M.; Gaciong, Z.; Skiba, D.S. Targeting the Opioid System in Cardiovascular Disease: Liver Proteomic and Lipid Profile Effects of Naloxone in Atherosclerosis. *Biomedicines* **2025**, *13*, 1802. https://doi.org/10.3390/biomedicines13081802

1. Introduction

The endogenous opioid system (EOS) consists of endogenous opioid peptides (such as endorphins, enkephalins, and dynorphins) that demonstrate high affinity to three main types of target receptors: mu (μ, MOR), delta (δ, DOR), and kappa (κ, KOR), respectively [1]. The main function of EOS is modulation of nociceptive signaling, including involvement

in stress-induced analgesia [2,3]. However, for the past few decades, it has been known that this system plays a role in the proper functioning of many bodily systems, as well as in pathological processes [4–6]. Dysfunction in the opioid system may contribute to mood disorders such as depression and anxiety [7]; for instance, reduced levels of endogenous opioids have been observed in individuals with major depressive disorder [8]. Additionally, opioid receptors are also present in the gastrointestinal tract, where endogenous opioids regulate motility and secretion [9]. Therefore, dysregulation of this system can lead to conditions such as irritable bowel syndrome [10]. Endogenous opioids are also involved in the regulation of cardiovascular function, including heart rate and blood pressure [11]. An EOS malfunction in the cardiovascular system can contribute to the development of hypertension and may lead to heart failure [12,13].

Studies also indicate that EOS influences the progression and instability of atherosclerotic plaque [14,15]. It is worth mentioning that atherosclerosis is a disease that causes about 50% of all deaths in Western society [16]. Atherosclerosis is a complex disease influenced by many factors and systems [17–19]. The primary causes of its development are considered chronic inflammation and lipid metabolism disturbances [20]. Moreover, opioid receptors are expressed on and influence the function of many cell types in the cardiovascular system, including cardiomyocytes, endothelial cells, and smooth muscle cells, including excitation–contraction coupling and the regulation of vascular tone. In addition to regulating cardiac function through modulation of calcium metabolism, opioids also play an important role in vascular function [21]. Opioid receptors can induce vasodilation and maintain vascular tone, influencing blood pressure and blood flow. Opioid receptors on endothelial cells (ECs) communicate with vascular smooth muscle cells (VSMCs) through paracrine signaling and modulate angiogenesis, vascular tone, and vascular integrity [22].

The connection between the opioid system and atherosclerosis is also supported by studies, which describe that the chronic infusion of β-endorphin, a ligand for the μ opioid receptor, into $ApoE^{-/-}$ mice significantly enhances the development of atherosclerotic lesions in the aorta, along with an increase in vascular inflammation [14]. Moreover, long-term pretreatment with the opioid receptor antagonist, naloxone (NLX), followed by lipopolysaccharide (LPS) treatment in young $ApoE^{-/-}$ mice, can inhibit LPS-induced macrophage activation by significantly reducing the tumor necrosis factor α (TNFα) level in plasma, compared to mice treated with LPS and not receiving NLX [23]. Another crucial aspect in the development of atherosclerosis is cholesterol. Previous studies indicated that pretreatment with another opioid receptor antagonist, naltrexone, prevented stress-induced increases in cholesterol levels in cholesterol–cholic acid (CCA)-fed female rats [24], which suggested that EOS may play a role in the treatment of stress-induced hypercholesterolemia. Moreover, in patients with ischemic heart disease treated with δ opioid receptor agonist, levels of total cholesterol, triglycerides, and low-density lipoproteins (LDL) were reduced, which suggested that the role of the opioid system may be strongly receptor-specific [25]. The opioid receptor axis significantly impacts liver function, as well, and is involved in various cellular processes that affect liver cell survival, inflammation, and fibrosis [26]. One of the studies showed that blockade of opioid receptors with naltrexone reduced liver fibrosis and hepatic stellate cell (HSC) activation, along with reduced plasma ALP (Alkaline Phosphatase) and ALT (Alanine Transaminase) activity, but without significantly affecting liver inflammation in BDL rats (rats with ligated bile ducts) [27]. However, another study demonstrated significantly lower μ opioid receptor gene expression in the livers of patients with hepatitis C compared to control subjects. Administration of the μ opioid receptor agonist DAMGO resulted in a significant reduction in the necrotic area, along with a marked decrease in serum ALT. NLX inhibition of the μ opioid receptor in mice with healthy livers and mice with CCl4-induced hepatitis did not alter plasma liver enzyme

levels or liver histological assessments, but it increased liver cytolysis and histological necrosis compared to control animals [28].

The examples presented above illustrate the extensive involvement of the EOS in various physiological and pathological processes, including cardiovascular physiology and pathology. In our research, we aimed to explore the therapeutic potential of modifying the activity of the EOS in mice with developed atherosclerosis, especially focused on investigating its influence on lipid metabolism and the development of atherosclerotic plaque. Secondly, considering the significant potential role of the EOS in regulating lipid levels, our research focused on examining the lipid profile and liver proteome, the site of cholesterol synthesis and metabolism, to gain a better understanding of the mechanisms influencing lipid regulation.

2. Materials and Methods

2.1. Animals

All the experiments were performed on 36-week-old, male B6.129P2-Apoe^{tm1Unc}/J (strain no. 002052) mice on the C57BL/6J background (further referred to as ApoE$^{-/-}$). The animals were housed in groups of 4–5 individuals and maintained in the animal facility of the Institute of Genetics and Animal Biotechnology of the Polish Academy of Sciences under standard environmental conditions (ambient temperature of 22 ± 2 °C and 55 ± 5% relative humidity) under a 12 h light/dark cycle (lights on at 7 a.m.). Access to tap water and food (LABOFEED H, Kcynia, Poland) was provided *ad libitum*. Study procedures were carried out in accordance with the ethical clearance (permission no. WAW2/093/2024) received from the II Local Ethics Committee for Experiments on Animals in Warsaw.

2.2. Drug and Experiment Design

The mice were assigned to a saline-treated (control, NaCl) or NLX-treated (experimental) group. Naloxone hydrochloride (NLX) was purchased from Sigma-Aldrich (St. Louis, MO, USA) and served as a non-selective opioid system antagonist. Individuals belonging to the NLX-treated group were administered daily with freshly prepared NLX dissolved in saline (0.9% NaCl) by intraperitoneal injections in a dose of 10 mg/kg for 7 days. The control group received the saline solution.

2.3. Lipid Profile Analysis

Blood was collected directly from the hearts of anesthetized mice into heparin-coated syringes. The blood samples were centrifuged at 3000× *g* at 4 °C for 10 min, then the plasma was collected for lipid profile analysis, including levels of total cholesterol, LDL, HDL, and triglycerides. The analyses were performed using a COBAS 6000 analyzer (Roche Diagnostics, Mannheim, Germany).

2.4. Oil Red O (ORO) Staining

Oil red O (ORO) staining was performed on aortic arches and right lobes of liver to visualize atherosclerotic lesions and fat deposits, respectively. The aortic arches were harvested after prior perfusion with phosphate-buffered saline (PBS), then fixed in 10% formalin for 24 h at 4 °C and stained according to an adjusted protocol [17]. Briefly, fixated aortic arches were opened and pinned onto black silicone cubes. After that, each specimen was rinsed in distilled water, followed by a quick wash in 60% isopropanol solution. Then, the aortic arches were stained in ORO working solution (0.625% ORO solution in isopropanol mixed with distilled water in a ratio of 1.5:1) for 30 min at room temperature. To remove excess stain, the specimens were washed with 60% isopropanol followed by three dips in distilled water.

The right lobe of the liver was collected and freshly frozen in −80 °C. Prior to sectioning, the sample was transferred for 30 min to −20 °C to avoid tissue crumbling during cutting. The tissue was sectioned into 6 µm thick sections on a cryostat (Jung CM1800, Leica, Düsseldorf, Germany) set to −20 °C. Before ORO staining, the sections were fixed in 10% formalin for 10 min at room temperature. The liver fragments were stained similarly to the aortic arches, as described above.

The total ORO-stained lesion areas in the aortic arches and fat deposits in the right lobe of the liver were quantified using ImageJ software (version 1.53e) by two independent investigators. The final data were expressed as a percentage of positive-staining areas relative to the total aortic area.

2.5. Trichrome Staining

The liver samples were fixed in formalin and dehydrated in an increasing series of alcohols (70%, 80%, 96%, 99.8%), with two changes each for 30 min at room temperature, followed by clearing in two changes of xylene (Warchem, Warsaw, Poland) for 15 min each. After that, the tissues were transferred to a mixture of toluene/paraffin (1:1) and incubated for 2 h at 60 °C. In the final step, each liver lobe was placed in pure molten paraffin overnight and embedded in paraffin blocks. The processed tissue was sectioned into 6 µm thick slices on a microtome (Hyrax M25, Zeiss, Oberkochen, Germany) and placed on microscopic slides. Before staining, the specimens were deparaffinized in two changes of xylene and hydrated in a decreasing series of alcohols. Further, trichrome staining was performed with Trichrome Stain (Masson) Kit (Sigma-Aldrich, St. Louis, MO, USA) according to the manufacturer's protocol. The total stained areas of fibrosis lesions in the right lobes of the livers were quantified using ImageJ software (version 1.53e) by two independent investigators. Three separate areas of stained lesion were counted and averaged to yield one value per slide. The final data were expressed as a percentage of the positive-staining areas relative to the total aortic area.

2.6. Macrophage Immunofluorescence Staining

We performed immunohistochemical staining using F4/80 Monoclonal Antibody (BM8) (Thermo Fisher Scientific, Waltham, MA, USA). The liver lobes were fixed in formalin and dehydrated as described above. After that, the tissues were transferred to a mixture of toluene/paraffin (1:1) and incubated for 2 h at 60 °C. In the final step, each liver lobe was placed in pure molten paraffin overnight and embedded in paraffin blocks. The processed tissue was sectioned into 6 µm thick slices on a microtome (Hyrax M25, Zeiss) and placed on microscopic slides. Before staining, the specimens were deparaffinized in two changes of xylene and hydrated in a decreasing series of alcohols. Heat-induced epitope retrieval was performed at 90 °C using 10 mM Sodium Citrate buffer, pH 6.0, for 20 min. The sections were blocked in 3% BSA. Primary antibodies 1:50 were incubated overnight at 4 °C. The slides were washed in distilled water and mounted with VECTASHIELD Antifade Mounting Medium with DAPI (Vector Laboratories, Inc., Newark, CA, USA). Appropriate positive and negative controls were included with the study sections. The immunostaining was quantified using ImageJ software (version 1.53e) by two independent investigators. Three separate areas of stained lesion were counted and averaged to yield one value per slide. The final data were expressed as a percentage of positive-stained areas relative to the total liver area.

2.7. Measurement of mRNA Expression

RNA from the liver lobe was obtained using TRItidy G (PanReac AppliChem, Darmstadt, Germany) according to the manufacturer's protocol. Total RNA was measured by Nanodrop 2000 (Thermo Fisher Scientific, Waltham, MA, USA). Reverse transcription of

RNA was performed using the High-Capacity cDNA Reverse Transcription Kit (Applied Biosystems, Foster City, CA, USA). The expression of *Lpl*, *Srebf1*, and *Fabp4* at the mRNA level in the liver was analyzed using TaqMan probes (Thermo Fisher Scientific) and the TaqMan Real-Time PCR Master Mix (Thermo Fisher Scientific). Reactions were performed on 96-well plates on the LightCycler 96 System (Roche Diagnostics, Germany) Real-Time PCR according to standard protocol. Calculations were made using the LightCycler 96 Software (v.1.1.0.1320). Data were normalized to *Tbp* mRNA levels, and relative quantification was calculated.

2.8. Liquid Chromatography–Tandem Mass Spectrometry (LC–MS/MS) Analysis

Mouse livers (n = 7 biological replicates per group, in total 14 samples) were homogenized using a Tissue Lyser LT (Qiagen, Hilden, Germany) and lysed in a buffer containing 0.1 M Tris-HCl, pH 7.6, 2% sodium dodecyl sulfate, and 50 mM dithiothreitol (Sigma Aldrich, St. Louis, MO, USA) at 96 °C for 10 min. The total protein concentration in the lysates and the peptide contents in the digests were assayed using a tryptophan fluorescence-based WF assay [29]. Seventy micrograms of protein were digested overnight using the filter-aided sample preparation (FASP) method [30] with Trypsin/Lys-C mix (Promega, Madison, WI, USA) (enzyme-to-protein ratio 1:35) as the digestion enzymes. Next, the samples were purified with C18 Ultra-Micro Spin Columns (Harvard Apparatus, Holliston, MA, USA). All the samples were dissolved in 0.1% formic acid at a concentration of 0.5 µg/µL and spiked with the iRT peptides (Biognosys, Schlieren, Switzerland). One microgram of peptide was injected into a nanoEaseTM M/Z Peptide BEH C18 75 µm i.d. × 25 cm column (Waters, Milford, MA, USA) via a nanoEaseTM M/Z Symmetry C18 180 µm i.d. × 2 cm trap column (Waters, Milford, MA, USA) and separated using a 1% to 40% B phase linear gradient (A phase—0.1% FA in water; B phase—80% ACN and 0.1% FA) with a flow rate of 250 nL/min on an UltiMate 3000 HPLC system (Thermo Scientific, Waltham, MA, USA) coupled to an Orbitrap Exploris 480 Mass Spectrometer (Thermo Scientific, Waltham, MA, USA). The nanoelectrospray ion source parameters were as follows: ion spray voltage: 2.2 kV, ion transfer tube 275 °C. For data-independent (DIA) acquisition, spectra were collected for 145 min in full scan mode (400–1250 Da), followed by 55 DIA scans using a variable precursor isolation window approach and AGC set to a custom 1000%. The DIA MS data were analyzed in Spectronaut 19 (Biognosys, Schlieren, Switzerland) [31] software using the directDIATM approach. MS data were filtered by 1% FDR at the peptide and protein levels, while quantitation was performed at the MS2 level, and global imputation with a missingness rate set to 0.3 was used. Statistical analysis of differential protein abundance was performed at both the MS1 and MS2 levels [32] using unpaired t-tests with multiple testing correction after Storey [33]. A summary of the quality control for the LC–MS/MS runs is shown in Supplementary Materials Figure S1. The mass spectrometry data have been deposited in the ProteomeXchange Consortium via the PRIDE partner repository [34] with the dataset identifier PXD063243.

2.9. Constructing Protein–Protein Interaction (PPI) Networks

Functional grouping and pathway analysis were performed using PINE (Protein Interaction Network Extractor) software v 1.0.0 [35] with the STRING and GeneMANIA databases using a score confidence of 0.4 and a ClueGO p value cutoff < 0.05.

2.10. Statistical Analysis

Data collected from serum analysis and histopathological evaluation were checked for normality by the Shapiro–Wilk test. An ANOVA test was utilized to determine any differences between groups, with statistical significance set to p-value < 0.05. The results presented on graphs are expressed as means ± SD.

3. Results

3.1. Effect of the Opioid System Antagonism on the Lipid Profile in Mice with Advanced Atherosclerosis

Naloxone (NLX) administration did not alter total cholesterol (NaCl 620.90 mg/dL ± 73.36 mg/dL vs. NLX 703.70 mg/dL ± 142.12) [(1, 18) = 2.68; $p = 0.12$], LDL (NaCl 413.10 mg/dL ± 59.40 vs. NLX 434.10 mg/dL ± 97.60) (F[(1, 18) = 0.34; $p = 0.57$]), or triglyceride (NaCl 84.70 mg/dL ± 39.77 vs. NLX 106.60 mg/dL ± 36.30) (F[(1, 18) =1.65; $p = 0.21$]) levels in the ApoE$^{-/-}$ mice (Figure 1). However, the antagonism of the opioid system resulted in elevation of HDL concentration after the NLX treatment (NaCl 66.85 mg/dL ± 9.01 vs. NLX 97.30 mg/dL ± 13.55) (F[(1, 18) =33.00; $p < 0.001$]) (Figure 1).

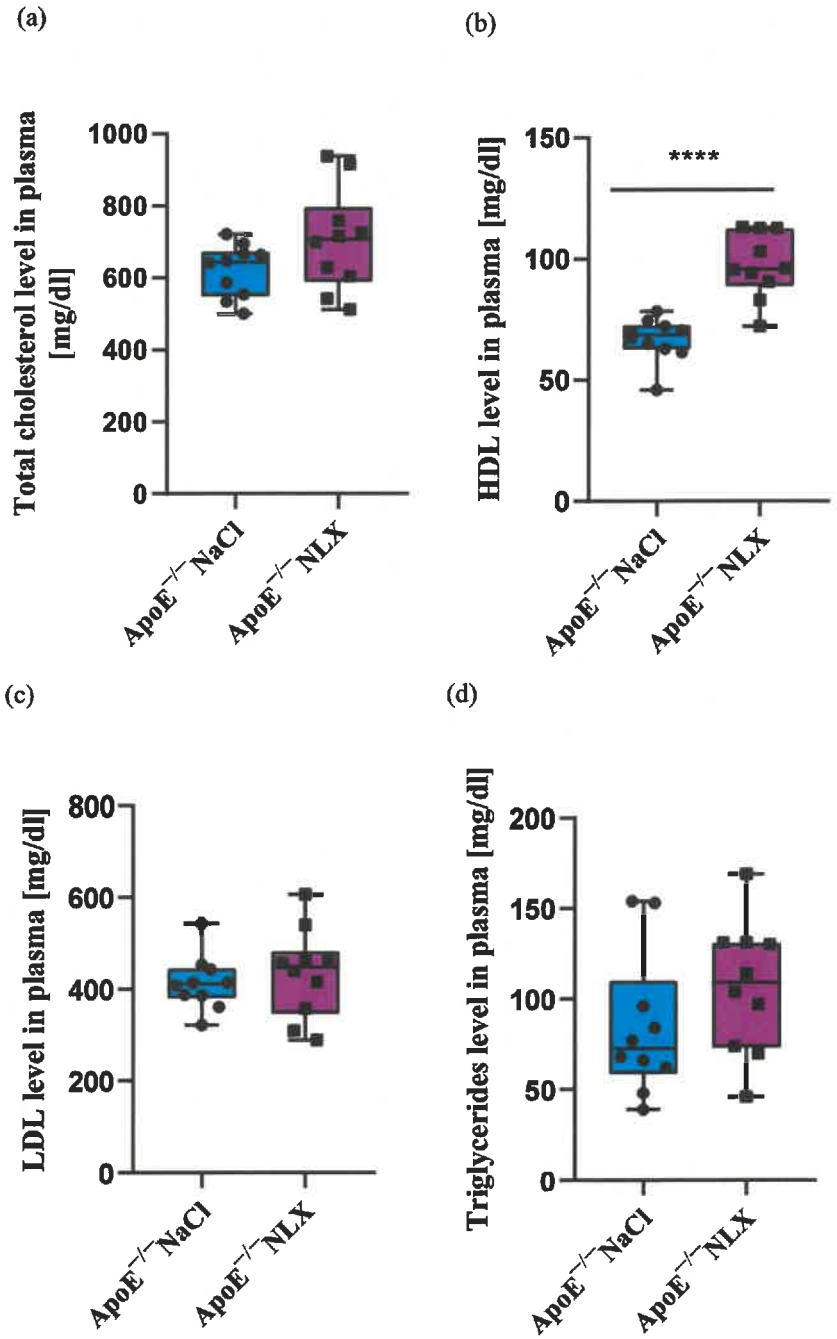

Figure 1. Lipid profile in plasma: (**a**) total cholesterol, (**b**) HDL, (**c**) LDL, (**d**) triglyceride levels in response to administration of NLX in ApoE$^{-/-}$ mice ($n = 10$ per group) **** $p < 0.0001$ (HDL: high-density lipoprotein; LDL: low-density lipoprotein).

3.2. Effect of the Administration of NLX on Atherosclerotic Plaque and Liver Steatosis in Mice with Advanced Atherosclerosis

After 7 days of NLX administration, we did not observe any significant changes in either atherosclerotic plaque localized in aortic arches (NaCl 21.30% ± 9.04 vs. NLX 26.21% ± 9.22) (F[(1, 12) = 1.01; $p = 0.33$]) (Figure 2a) or liver steatosis (NaCl 2.46% ± 3.51 vs. NLX 1.47% ± 1.95) (F[(1, 10) = 0.36; $p = 0.56$]) in the ApoE$^{-/-}$ mice (Figure 2b).

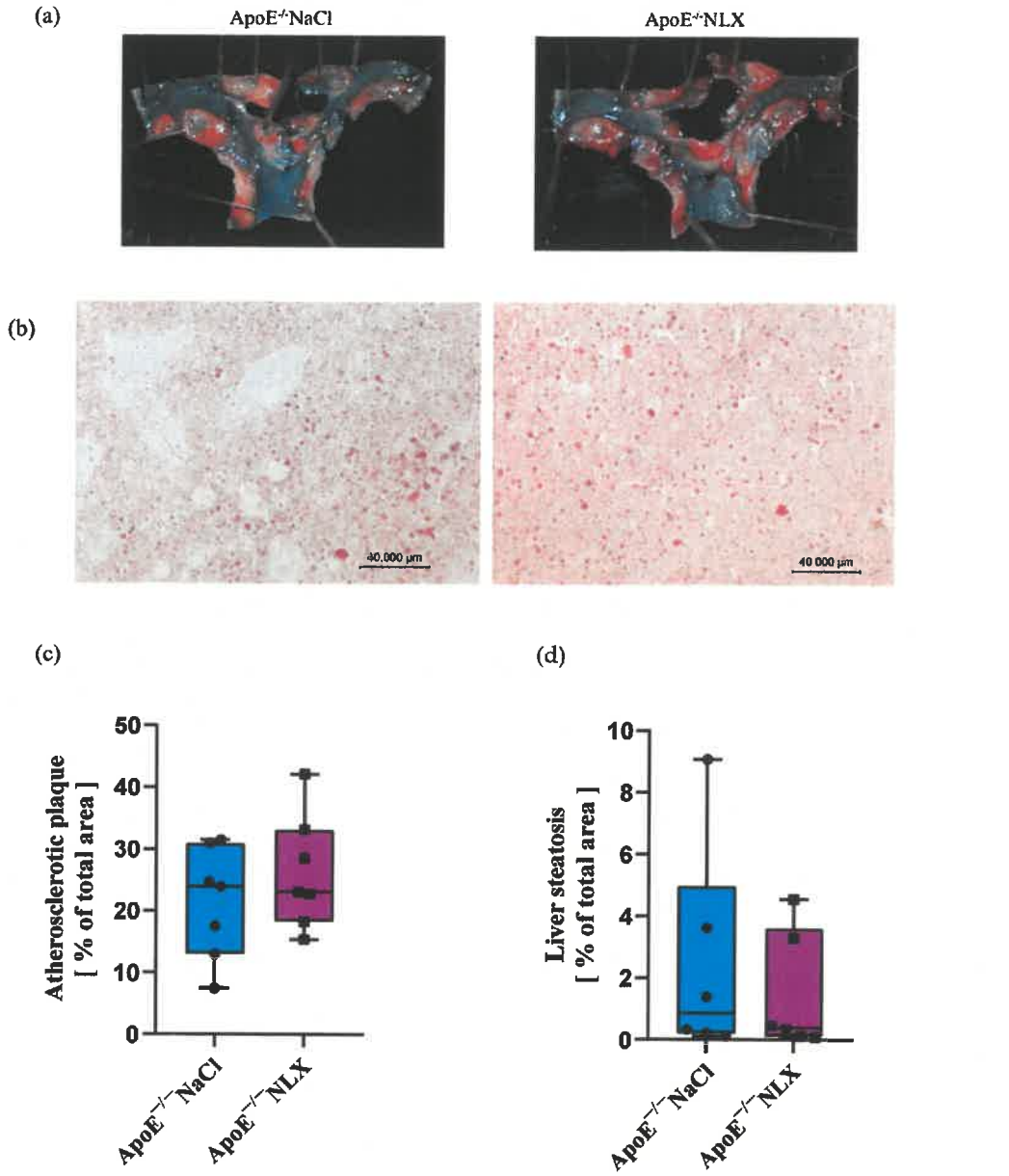

Figure 2. Representative photographs of ORO staining of (**a**) aortic arch ($n = 7$ per group) and (**b**) liver cross-section (microscopic photos performed at 20× magnification) ($n = 6$ per group). Quantified stained area in control and treated groups for (**c**) atherosclerotic plaque and (**d**) liver steatosis.

3.3. Effect of the NLX Administration on the Expression of Chosen Genes Involved in Lipid Metabolism

The NLX treatment in the ApoE$^{-/-}$ mice led to a statistically significant decrease in *Fabp4* gene expression (NaCl 1.36 ± 0.54 vs. NLX 0.80 ± 0.25) as shown by significant treatment factor, F[(1, 12) = 6.10; $p = 0.03$]. However, no changes were observed in the expression of the *Lpl* (NaCl 1.09 ± 0.68 vs. 0.98 ± 0.22) (F[(1, 12) = 0.74; $p = 0.41$]) and *Srebf1* (NaCl 1.02 ± 0.33 vs. 1.26 ± 0.43)) (F[(1, 12) = 1.30; $p = 0.28$]) genes (Figure 3).

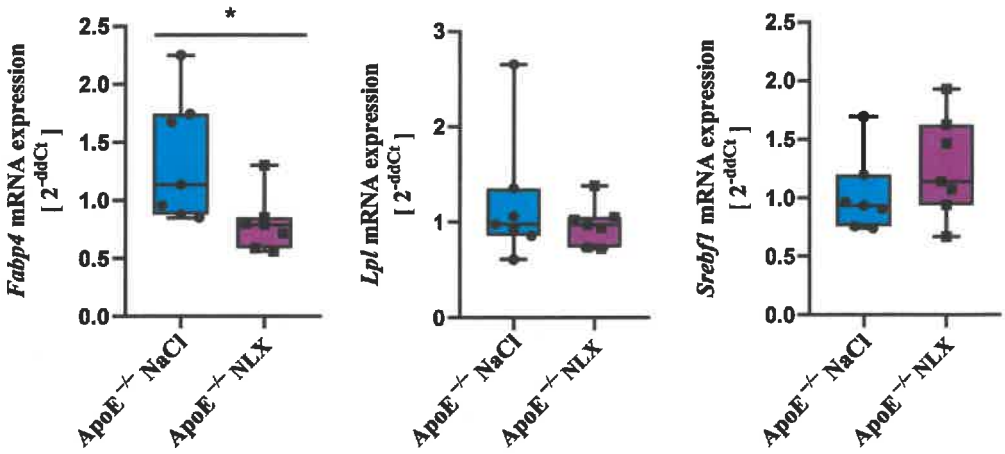

Figure 3. Expression of *Fabp4*, *Lpl*, and *Srebf1* mRNA in livers of ApoE$^{-/-}$ mice (n = 7 per group) * $p < 0.05$.

3.4. Influence of NLX Administration on Liver Fibrosis

The NLX administration did not cause statistically significant changes in liver fibrosis (NaCl 0.33% ± 0.20 vs. NLX 0.31% ± 0.12) (F[(1, 10) = 0.04; p = 0.84]) (Figure 4).

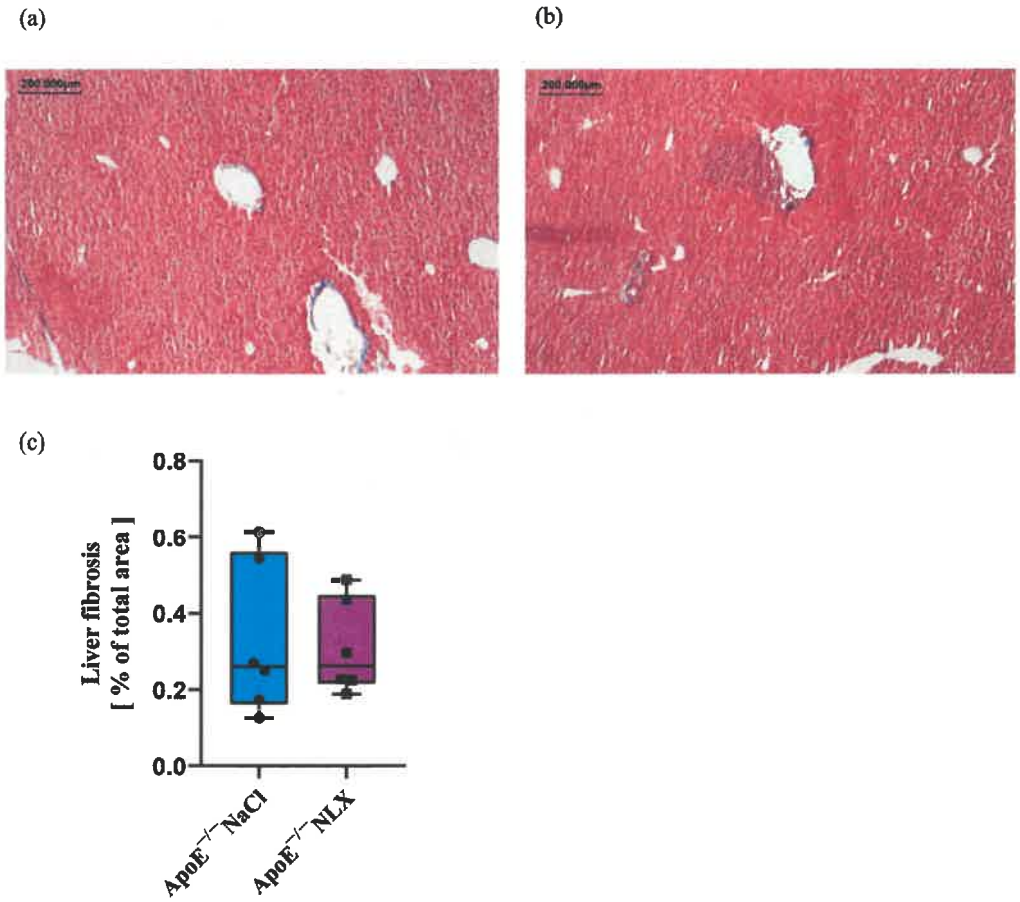

Figure 4. Representative photographs of Masson's trichrome staining of liver cross-sections in control (**a**) and treated (**b**) groups (microscopic photos performed at 4× magnification) (n = 6 per group). Quantified stained area in control and treated (**c**) groups for liver fibrosis.

3.5. Effect of the NLX Administration on Macrophage Expression in Mice Liver

The NLX treatment caused a statistically significant increase in macrophage expression in comparison to the non-treated group (NaCl 0.04% ± 0.03 vs. NLX 0.36% ± 0.16) ($F[(1, 9) = 25.96; p < 0.001]$) (Figure 5).

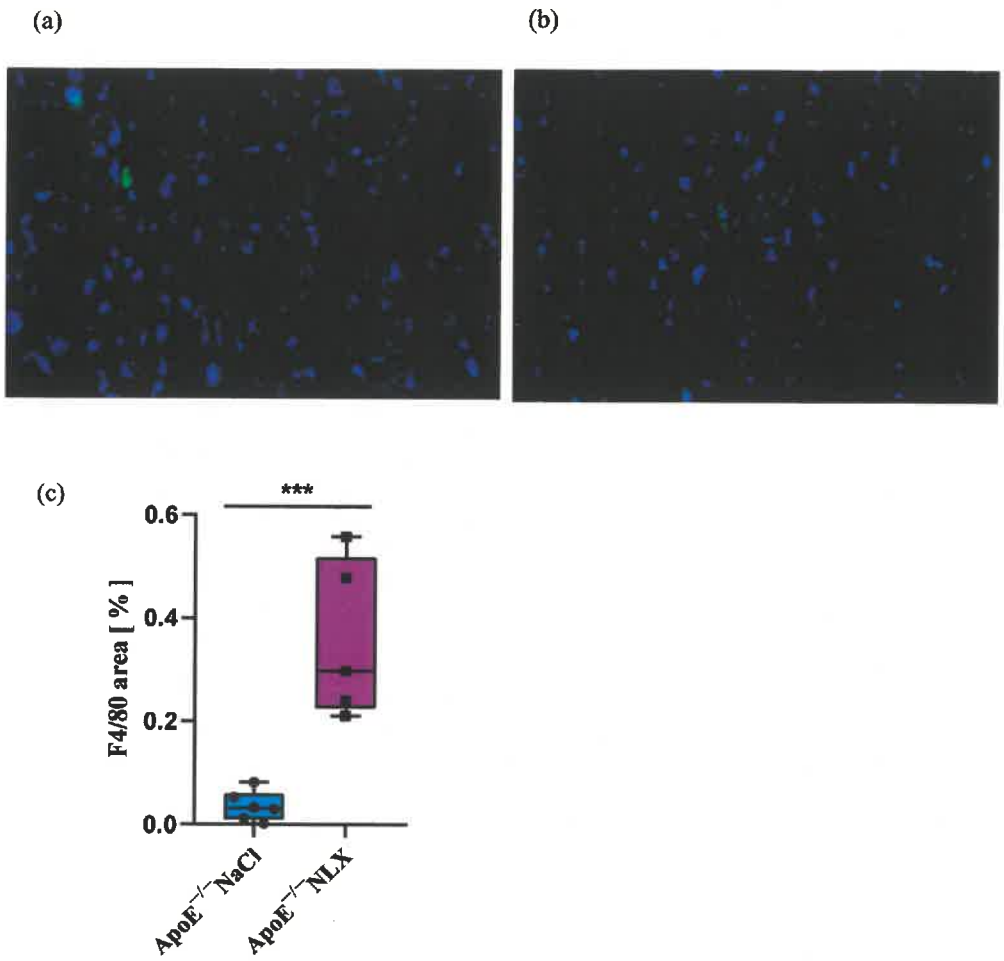

Figure 5. Representative photographs of immunofluorescence staining, with F4/80 antigen as a major macrophage marker, of liver cross-section in control (**a**) and treated (**b**) groups (microscopic photos performed at 20× magnification). Quantified stained area in control and treated groups (**c**) (NaCl $n = 6$, NLX $n = 5$) *** $p < 0.001$.

3.6. Influence of NLX Administration on Proteomic Analysis of Livers

To comprehensively investigate the changes in protein abundance upon NLX administration, a quantitative proteomics analysis was conducted. LC–MS/MS measurements operated in DIA mode and analyzed in Spectronaut 19 software with the direct-DIA approach resulted in the identification of 72,110 proteotypic peptides. In total, 6574 protein groups across all biological conditions were identified and quantified. The median protein group, CV, was approximately 11%, which reflects good reproducibility of data (Supplementary Materials Figure S1D). A summary of the quality control for the LC–MS/MS runs is shown in Supplementary Materials Figure S1. The detailed list of differentially abundant proteins and their fold changes across all the biological conditions is presented in Supplementary Materials Table S1. Using cutoffs of $q < 0.05$ and fold change ≥ 2 or ≤ -2, we found a total of 38 proteins altered in the liver of the NLX-treated mice compared to the control group (Figure 6a–c). This included proteins involved in muscle function and structure (e.g., RB1CC1, PDLIM3), proteins related to cell migration and proliferation (e.g., IFIT3), proteins associated with the inflammatory response and

immune system (e.g., GBP, STEAP4, FGL1), proteins involved in cell death (e.g., ZBP1), and proteins that bind heavy metals (e.g., MT1) (Supplementary Materials Table S1).

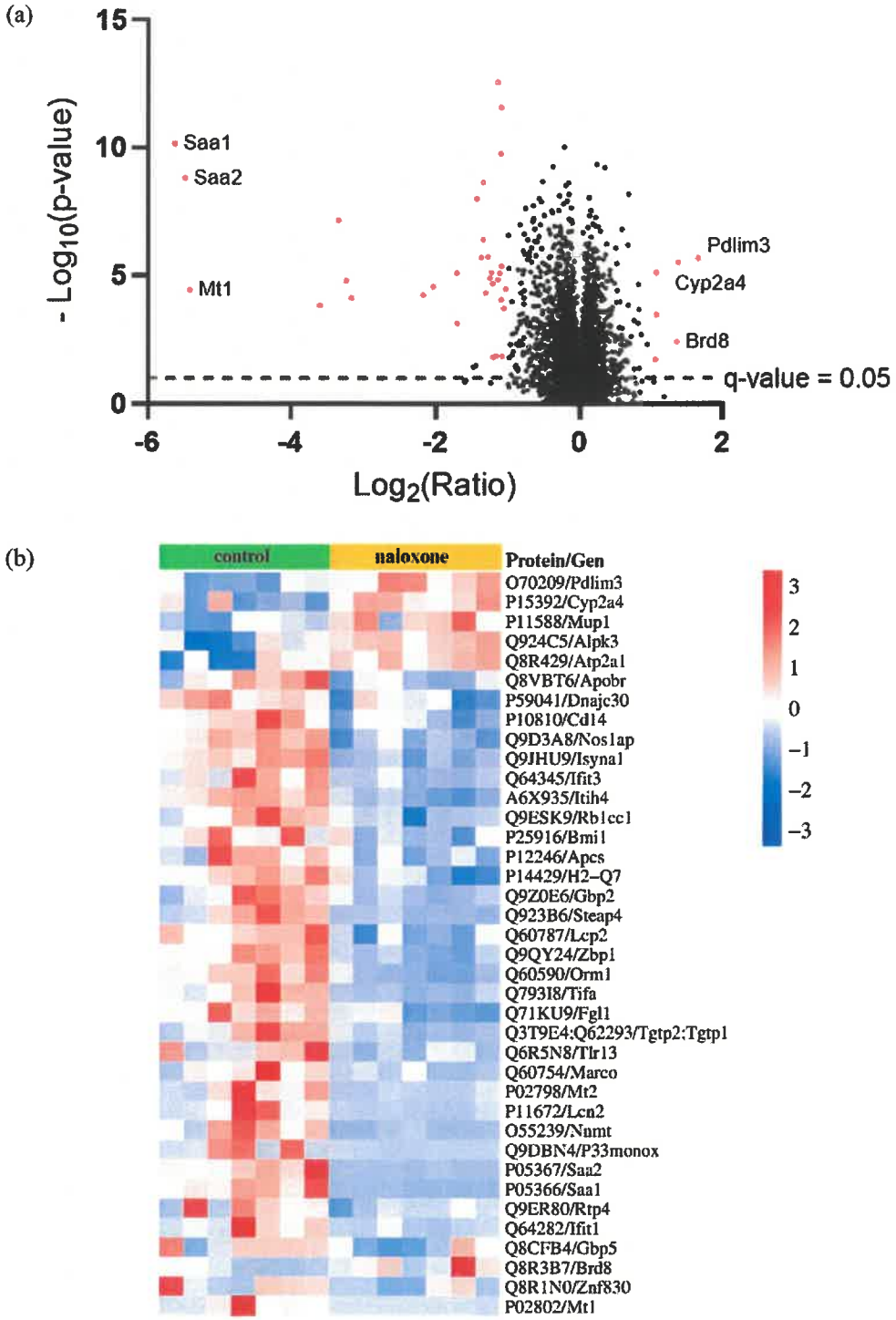

Figure 6. *Cont.*

(c)

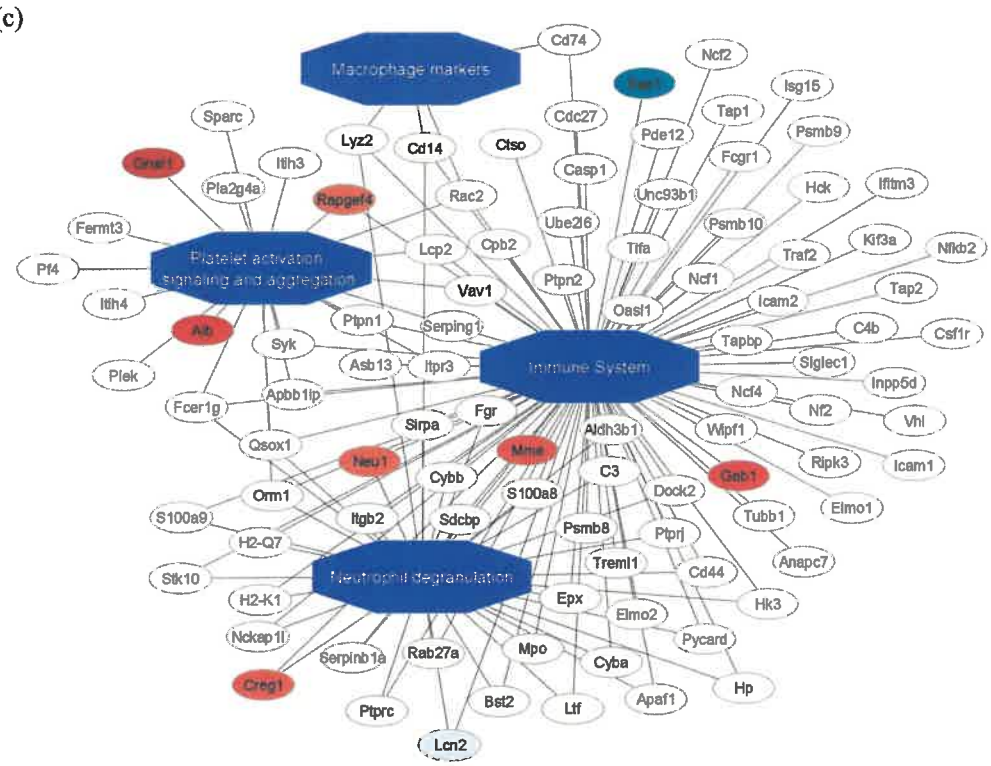

Figure 6. (**a**) Volcano plot for treated and non-treated mice with top six most up- and downregulated proteins shown; (**b**) proteomic data obtained from livers isolated from ApoE$^{-/-}$ mice after NLX administration compared to non-treated (z-score value; cut off; q value < 0.05, fold change ≥ 2.0 or ≤−2) (n = 7 per group); (**c**) enriched functional network in NTX-treated mice compared to control, as generated by PINE. Inhibited pathways are shown as blue central nodes along with red (upregulated) or blue (downregulated) protein nodes.

4. Discussion

The endogenous opioid system (EOS) is widely reported in the literature as playing a role in many diseases [24–27], but its direct involvement in the formation of atherosclerotic plaque and its effect on cholesterol levels are poorly described. Our study demonstrates the effect of blocking opioid receptors with naloxone (NLX) on cholesterol levels and atherosclerotic plaque formation in ApoE$^{-/-}$ mice with advanced atherosclerosis. After 7 days of NLX administration, we did not observe significant changes in the plasma levels of total cholesterol, low-density lipoprotein (LDL), or triglycerides. Our results are comparable to the results shown in other research, where the NLX treatment lasted for 10 weeks [21]. However, we observed a statistically significant increase in the level of high-density lipoprotein (HDL) in plasma after the NLX administration. Interestingly, a cross-sectional study of 2239 opioid users found that opioid use was associated with significantly lower levels of total cholesterol, LDL, and HDL [34,35].

Moreover, several reports indicate that an opioid receptor antagonist affects cholesterol levels. It has been shown that a 5-day pretreatment with naltrexone prevented stress-induced increases in cholesterol levels in female rats fed a cholesterol–cholic acid (CCA)-supplemented diet [24]. Moreover, in the same animal model, a 5-day release of 75 mg of morphine elevated total plasma cholesterol and LDL, reduced HDL, and increased cholesterol deposition in the aorta. However, the daily administration of 1 mg/kg naltrexone completely reversed these effects on both cholesterol levels and aortic cholesterol deposition [36].

Due to the role of the liver in regulating lipid metabolism, it may be a key factor in the processes related to the development of atherosclerosis. On the other hand, the progression of atherosclerosis contributes to pathological liver changes, such as steatosis [37,38]. This is supported by studies showing that patients with liver steatosis have significantly higher levels of LDL and lower levels of HDL, compared to those without liver steatosis [39]. Impaired HDL function has been postulated to be an independent risk factor for atherosclerosis in non-alcoholic fatty liver disease [40]. Furthermore, research indicates that liver steatosis is more prevalent in patients with carotid plaques and aortic calcification than in those with no vascular damage [41]. A study on children and adolescents revealed an association between increased intima–media thickness of the carotid artery, a high triglyceride/HDL-C ratio, elevated blood pressure, insulin resistance, and non-alcoholic fatty liver disease [42]. Although we observed a significant increase in plasma HDL levels following the NLX treatment, the functional relevance of this change remains to be determined. Recent studies emphasize that HDL cholesterol levels alone do not fully reflect their atheroprotective functions, such as cholesterol efflux capacity (CEC), antioxidant properties, or anti-inflammatory effects [43]. Therefore, it is possible that the HDL elevation observed in our model may not necessarily confer a cardioprotective benefit. In fact, increased levels of serum amyloid A (SAA)—which was downregulated in our study after naloxone treatment—have been shown to affect cholesterol efflux by displacing apoA-I from HDL particles, thereby impairing HDL function. This suggests that the observed decrease in SAA protein abundance may contribute to improved HDL functionality, although this hypothesis requires further experimental validation.

In our study, we also investigated the effects of opioid receptor blockade on atherosclerotic plaque development and liver steatosis in mice. We observed neither significant changes in the development of atherosclerotic plaques nor fat deposits in the liver after the NLX treatment. However, one study showed a significant reduction in atherosclerotic plaque after long-term, 10-week administration of NLX in 17-week-old mice. Moreover, the study demonstrated that naloxone inhibits macrophage activation induced by LPS (lipopolysaccharide) and oxidized LDL (oxLDL). Naloxone treatment reduced TNF-α production and superoxide production in stimulated macrophages [21]. This may indicate that prolonged administration of NLX at an early stage of atherosclerotic plaque development, rather than during the advanced stages observed in our studies, may significantly reduce plaque development and progression. Similarly, while we did not observe changes in liver steatosis, other studies have shown that long-term administration of NLX can reverse morphine-induced histopathological damage [44]. Interestingly, the administration of another opioid receptor antagonist, naltrexone, for 28 days, in BDL rats (rats with ligated bile ducts, used as a model of liver fibrosis) [45] significantly attenuates the development of liver fibrosis [27]. NLX, as an opioid system antagonist, by definition, has no intrinsic pharmacological activity apart from the ability to bind to opioid receptors and simply block them. It reveals a significant effect in the form of antagonizing opioid agonists; therefore, its effect, when applied in clinically therapeutic and safe doses, may not be visible without agonist-mediated opioid receptor activation [46].

Although histological analysis did not reveal changes in hepatic steatosis after NLX administration, we investigated the expression of genes associated with its development. The first gene we examined was *Srebf1*. This gene encodes Sterol Regulatory Element-Binding Transcription Factor 1 (SREBF1), which is a key factor in lipogenesis. Lipogenesis is a metabolic pathway that converts excess carbohydrates to fatty acids, which are ultimately esterified with glycerol-3-phosphate to triglycerides [47]. The important role of *Srebf1* in lipogenesis is confirmed by studies indicating that the expression of this gene in the livers of patients with non-alcoholic steatosis is significantly higher than in healthy

individuals [48]. Moreover, the reduced expression of the *Sreb-1c* gene in hepatocytes by activating 5′AMP-activated protein kinase (AMPK) protected against hepatic steatosis and hyperlipidemia in diet-induced insulin-resistant LDL receptor-deficient mice [49]. After the NLX administration, we did not observe changes in *Srebf1* expression in the livers of the ApoE$^{-/-}$ mice. The next gene we investigated was *Lpl*. It encodes an enzyme crucial for the hydrolysis of core triglycerides in chylomicrons and very low-density lipoproteins (VLDL), resulting in the formation of chylomicron remnants and intermediate-density lipoproteins (IDL), respectively. The reaction products catalyzed by LPL, fatty acids, and monoacylglycerol are partially absorbed by local tissues and processed. For instance, they are stored as neutral lipids in adipose tissue, oxidized or stored in skeletal and cardiac muscle, or deposited as cholesterol esters and triglycerides in macrophages [50,51]. Research indicates that patients with severe liver steatosis exhibit significantly higher serum LPL activity compared to those with mild or moderate steatosis [52]. Moreover, morbidly obese individuals show statistically increased hepatic LPL activity compared to controls, independent of liver fibrosis or fatty liver presence [53]. However, in our study, after treatment with NLX, we did not observe any changes in *Lpl* mRNA expression in the liver. We also investigated the expression of the *Fabp4* gene. It encodes a small, highly conserved cytosolic protein that binds long-chain fatty acids and other hydrophobic ligands, regulating lipid transport within the cell [54]. It is primarily found in adipose tissue but is also detected in macrophages, endothelial cells, and cardiac myocytes [54,55]. Studies have shown that the use of an Fabp4 inhibitor, at a dose of 50 mg/kg/day for 8 weeks, in combination with rosiglitazone (a drug used in type II diabetes, which acts as an insulin sensitizer), resulted in a reduction of rosiglitazone-induced hepatic steatosis in obese diabetic C57BL/KsJ *db/db* mice [56]. In our study, after the NLX treatment, we did not observe changes in hepatic steatosis in the histological examination; however, at the molecular level, we observed a significant decrease in *Fabp4* mRNA expression in the livers of the ApoE$^{-/-}$ mice (fold change 0.8). FABP4 plays a crucial role in the transport, metabolism, and storage of lipids. Elevated levels of FABP4 have been associated with liver steatosis, particularly in individuals with metabolic conditions like diabetes and obesity [57]. Therefore, we believe that the changes in *Fabp4* mRNA expression we observed are indicators of the initiation of fat accumulation in the liver, which was not yet visible at the histological level. Moreover, liver fibrosis, as one of the indicators of liver steatosis, was not altered after naloxone administration.

In rats with dimethylnitrosamine-induced liver fibrosis, naloxone reduced collagen deposition after five weeks of treatment [58]. Additionally, naltrexone significantly attenuated the progression of liver fibrosis in bile duct-ligated rats [27]. However, in the mentioned studies, naloxone was administered for a relatively longer period than in our study. Another marker indicating liver steatosis is an increased level of macrophages in the liver.

We evaluated the presence of macrophages in the livers of ApoE$^{-/-}$ mice following NLX administration. A 7-day NLX treatment increased the macrophage population compared to the control group. It is known that macrophages increase their number in the liver with steatosis. However, macrophages are highly heterogeneous cells with diverse physiological and pathophysiological functions, exhibiting both pro-atherogenic (M1) and protective (M2) effects [59,60]. We have not evaluated the subset of macrophages in the liver after naloxone treatment, which is a limitation of the study. Experiments performed by Liu et al. show that naloxone pretreatment significantly suppressed the production of tumor necrosis factor-alpha (TNF-alpha), interleukin-6, monocyte chemoattractant protein-1, and superoxide in macrophages after stimulation [23]. A similar effect was observed in murine RAW264.7 cells, showing an anti-inflammatory effect of naloxone on macrophages [61].

In our study, the most significant effect of the NLX was observed on HDL levels. Since the liver is an important site of cholesterol metabolism, we performed a proteomic analysis of the liver in ApoE$^{-/-}$ mice treated with naloxone. The analysis detected 6574 proteins, of which 38 were significantly up- or downregulated. Then, we selected four proteins, whose abundance levels were significantly altered after NLX administration and which influence the lipid profile and are involved in the development of atherosclerosis. The first of them is apolipoprotein B receptor (Q8VBT6) encoded by the *Apobr* gene, whose abundance decreased after the NLX treatment. It is a receptor for apolipoprotein B (ApoB), which plays a crucial role in the development of atherosclerosis [62]. Studies have also shown that the use of an ApoB inhibitor causes a decrease in the level of total cholesterol and LDL in mice [63] and the level of LDL in humans [64]. In our study, NLX treatment reduced the abundance of apolipoprotein B receptor. The next protein downregulated by NLX that is worth mentioning is serum amyloid A (SAA) (P05367), encoded by the *Saa2* gene. SAA is a small apolipoprotein that binds to HDLs. SAA is an acute-phase marker and inflammation factor, with its levels significantly elevated in human serum during chronic inflammation [65,66]. Additionally, studies have shown that in patients with endotoxin-induced inflammation, the ability of macrophages to efflux HDL correlates with increased levels of SAA1 and SAA2. In mice, acute inflammation similarly leads to a marked impairment in HDL efflux, accompanied by a substantial rise in SAA levels [67]. Another protein closely associated with cholesterol levels, whose abundance was altered in our study by NLX, is nicotinamide N-methyltransferase (O55239) encoded by the *Nnmt* gene. The abundance of this protein was significantly reduced after the NLX treatment [68,69]. Studies have also demonstrated that inhibition of NNMT in obese mice decreased total cholesterol levels in plasma [70], and knock-out of the *Nnmt* gene led to lower total cholesterol and LDL levels in mice with non-alcoholic steatohepatitis [71]. Another protein which plays a role in lipid metabolism and whose abundance was changed by NLX is major urinary protein 1 (P11588), encoded by the *Mup1* gene. Following NLX administration, we observed an increase in MUP1 protein abundance. MUP1 is a lipocalin family member abundantly secreted into the circulation by the liver [72]. Except for its basic role, which is binding to lipophilic pheromones to support chemical communication in rodents, MUP1 regulates glucose and lipid metabolism. What is worth noting is that MUP1 inhibits lipogenesis. Hepatic high-abundance of MUP1 suppressed the abundance of stearoyl-CoA desaturase-1 (SCD1), fatty acid synthase (FAS), carbohydrate response element-binding protein (ChREBP), and peroxisome proliferator-activated receptor-γ (PPARγ) in *db/db* mice [73].

5. Conclusions

In summary, the above results indicate a connection between the opioid system, cholesterol levels, and the development of atherosclerosis. However, our 7-day NLX administration model in mice with advanced atherosclerosis appears insufficient to demonstrate a direct effect of opioid receptor blockade on lipid profiles and atherosclerotic plaque development. It would be beneficial to conduct further studies with an extended treatment duration or in a model where atherosclerosis is just beginning to develop. It would also be worthwhile to conduct a proteomic study of blood vessel samples and examine the effect of local naloxone administration on the liver or the atherosclerotic vessel [74]. This would provide more information about the direct role of naloxone on the studied organs.

Supplementary Materials: The following supporting information can be downloaded at: https://www.mdpi.com/article/10.3390/biomedicines13081802/s1, Figure S1: Quality control of MS runs of the liver of control and naloxone-treated mice; Table S1: An overview of deregulated proteins, their encoding genes, and functions. References [75–109] are cited in Supplementary Materials.

Author Contributions: Conceptualization, K.J., D.S.S. and M.S.; methodology, D.S.S., M.S., K.J., P.P. and M.Ł.; software, D.S.S. and A.S.; validation, K.J., D.S.S. and P.P.; formal analysis, D.S.S., A.S., K.J., A.N. and P.P.; investigation, K.J., D.S.S. and M.S.; resources, M.S., K.J. and D.S.S.; data curation, K.J.; writing—original draft preparation, K.J. and D.S.S.; writing—review and editing, K.J., D.S.S., M.S., A.N., P.P., M.Ł. and Z.G.; visualization, K.J., D.S.S. and A.S.; supervision, D.S.S., M.S. and Z.G.; funding acquisition, D.S.S. and M.S. All authors have read and agreed to the published version of the manuscript.

Funding: This work was supported by the National Science Centre, Poland, project number 2019/35/D/NZ5/02820. This research was carried out with the use of research infrastructure co-financed by the Smart Growth Operational Program, POIR 4.2 project no. POIR.04.02.00-00-D023/20.

Institutional Review Board Statement: The animal study protocol was approved by the II Local Ethics Committee for Experiments on Animals in Warsaw (permission no. WAW2/093/2024, approval date 24 July 2024).

Informed Consent Statement: Not applicable.

Data Availability Statement: The original data presented in the study are openly available to the ProteomeXchange Consortium via the PRIDE partner repository with the dataset identifier PXD063243.

Conflicts of Interest: The authors declare no conflicts of interest.

References

1. Stein, C. Opioid Receptors. *Annu. Rev. Med.* **2016**, *67*, 433–451. [CrossRef] [PubMed]
2. Cooper, K.; Carmody, J. The characteristics of the opioid-related analgesia induced by the stress of swimming in the mouse. *Neurosci. Lett.* **1982**, *31*, 165–170. [CrossRef] [PubMed]
3. Juni, A.; Klein, G.; Pintar, J.E.; Kest, B. Nociception increases during opioid infusion in opioid receptor triple knock-out mice. *Neuroscience* **2007**, *147*, 439–444. [CrossRef] [PubMed]
4. Walters, A.S.; Li, Y.; Koo, B.B.; Ondo, W.G.; Weinstock, L.B.; Champion, D.; Afrin, L.B.; Karroum, E.G.; Bagai, K.; Spruyt, K. Review of the role of the endogenous opioid and melanocortin systems in the restless legs syndrome. *Brain* **2023**, *147*, 26–38. [CrossRef] [PubMed]
5. Cuitavi, J.; Torres-Pérez, J.V.; Lorente, J.D.; Campos-Jurado, Y.; Andrés-Herrera, P.; Polache, A.; Agustín-Pavón, C.; Hipólito, L. Crosstalk between Mu-Opioid receptors and neuroinflammation: Consequences for drug addiction and pain. *Neurosci. Biobehav. Rev.* **2023**, *145*, 105011. [CrossRef] [PubMed]
6. Drolet, G.; Dumont, E.C.; Gosselin, I.; Kinkead, R.; Laforest, S.; Trottier, J.F. Role of endogenous opioid system in the regulation of the stress response. *Prog. Neuropsychopharmacol. Biol. Psychiatry* **2001**, *25*, 729–741. [CrossRef] [PubMed]
7. Jelen, L.A.; Stone, J.M.; Young, A.H.; Mehta, M.A. The opioid system in depression. *Neurosci. Biobehav. Rev.* **2022**, *140*, 104800. [CrossRef] [PubMed]
8. Hsu, D.T.; Sanford, B.J.; Meyers, K.K.; Love, T.M.; Hazlett, K.E.; Walker, S.J.; Mickey, B.J.; Koeppe, R.A.; Langenecker, S.A.; Zubieta, J.-K. It still hurts: Altered endogenous opioid activity in the brain during social rejection and acceptance in major depressive disorder. *Mol. Psychiatry* **2015**, *20*, 193–200. [CrossRef] [PubMed]
9. Sternini, C.; Patierno, S.; Selmer, I.S.; Kirchgessner, A. The opioid system in the gastrointestinal tract. *Neurogastroenterol. Motil.* **2004**, *16*, 3–16. [CrossRef] [PubMed]
10. Martyniak, A.; Wędrychowicz, A.; Tomasik, P.J. Endogenous Opioids in Crohn's Disease. *Biomedicines* **2023**, *11*, 2037. [CrossRef] [PubMed]
11. Rabkin, S.W. Endogenous kappa opioids mediate the action of brain angiotensin II to increase blood pressure. *Neuropeptides* **2007**, *41*, 411–419. [CrossRef] [PubMed]
12. Treskatsch, S.; Feldheiser, A.; Shaqura, M.; Dehe, L.; Habazettl, H.; Röpke, T.K.; Shakibaei, M.; Schäfer, M.; Spies, C.D.; Mousa, S.A. Cellular localization and adaptive changes of the cardiac delta opioid receptor system in an experimental model of heart failure in rats. *Heart Vessel.* **2016**, *31*, 241–250. [CrossRef] [PubMed]
13. Treskatsch, S.; Shaqura, M.; Dehe, L.; Feldheiser, A.; Roepke, T.K.; Shakibaei, M.; Spies, C.D.; Schäfer, M.; Mousa, S.A. Upregulation of the kappa opioidergic system in left ventricular rat myocardium in response to volume overload: Adaptive changes of the cardiac kappa opioid system in heart failure. *Pharmacol. Res.* **2015**, *102*, 33–41. [CrossRef] [PubMed]
14. Okano, T.; Sato, K.; Shirai, R.; Seki, T.; Shibata, K.; Yamashita, T.; Koide, A.; Tezuka, H.; Mori, Y.; Hirano, T.; et al. β-Endorphin Mediates the Development and Instability of Atherosclerotic Plaques. *Int. J. Endocrinol.* **2020**, *2020*, 4139093. [CrossRef] [PubMed]

15. Koga, M.; Inada, K.; Yamada, A.; Maruoka, K.; Yamauchi, A. Nalmefene, an opioid receptor modulator, aggravates atherosclerotic plaque formation in apolipoprotein E knockout mice by enhancing oxidized low-density lipoprotein uptake in macrophages. *Biochem. Biophys. Rep.* **2024**, *38*, 101688. [CrossRef] [PubMed]
16. Herrington, W.; Lacey, B.; Sherliker, P.; Armitage, J.; Lewington, S. Epidemiology of Atherosclerosis and the Potential to Reduce the Global Burden of Atherothrombotic Disease. *Circ. Res.* **2016**, *118*, 535–546. [CrossRef] [PubMed]
17. Ananthaseshan, S.; Bojakowski, K.; Sacharczuk, M.; Poznanski, P.; Skiba, D.S.; Wittberg, L.P.; McKenzie, J.; Szkulmowska, A.; Berg, N.; Andziak, P.; et al. Red blood cell distribution width is associated with increased interactions of blood cells with vascular wall. *Sci. Rep.* **2022**, *12*, 13676. [CrossRef] [PubMed]
18. Fatkhullina, A.R.; Peshkova, I.O.; Koltsova, E.K. The role of cytokines in the development of atherosclerosis. *Biochemistry* **2016**, *81*, 1358–1370. [CrossRef] [PubMed]
19. De Koning, A.B.L.; Werstuck, G.H.; Zhou, J.; Austin, R.C. Hyperhomocysteinemia and its role in the development of atherosclerosis. *Clin. Biochem.* **2003**, *36*, 431–441. [CrossRef] [PubMed]
20. Kádár, A.; Glasz, T. Development of atherosclerosis and plaque biology. *Cardiovasc. Surg.* **2001**, *9*, 109–121. [CrossRef] [PubMed]
21. Katari, V.; Dalal, K.K.; Kondapalli, N.; Paruchuri, S.; Thodeti, C.K. Opioid receptors in cardiovascular function. *Br. J. Pharmacol.* **2025**, *182*, 3710–3725. [CrossRef] [PubMed]
22. Ondrovics, M.; Hoelbl-Kovacic, A.; Fux, D.A. Opioids: Modulators of angiogenesis in wound healing and cancer. *Oncotarget* **2017**, *8*, 25783–25796. [CrossRef] [PubMed]
23. Liu, S.L.; Li, Y.H.; Shi, G.Y.; Chen, Y.H.; Huang, C.W.; Hong, J.S.; Wu, H.L. A novel inhibitory effect of naloxone on macrophage activation and atherosclerosis formation in mice. *J. Am. Coll. Cardiol.* **2006**, *48*, 1871–1879. [CrossRef] [PubMed]
24. Bryant, H.; Story, J.; Yim, G.K. Assessment of endogenous opioid mediation in stress-induced hypercholesterolemia in the rat. *Biopsychosoc. Sci. Med.* **1998**, *50*, 576–585. [CrossRef] [PubMed]
25. Maslov, L.N.; Sokolov, A.A.; Fedorova, N.A.; Lishmanov, I.; Karpov, R.S. Clinical response to agonists of mu and beta opiate receptors in patients with ischemic heart disease: Effects of D-Ala2-Leu5-Arg6-enkephalin on hemodynamics, oxygen balance and lipid spectrum of blood. *Klin. Med.* **2002**, *80*, 53–57.
26. Jia, K.; Sun, D.; Ling, S.; Tian, Y.; Yang, X.; Sui, J.; Tang, B.; Wang, L. Activated δ-opioid receptors inhibit hydrogen peroxide-induced apoptosis in liver cancer cells through the PKC/ERK signaling pathway. *Mol. Med. Rep.* **2014**, *10*, 839–847. [CrossRef] [PubMed]
27. Ebrahimkhani, M.R.; Kiani, S.; Oakley, F.; Kendall, T.; Shariftabrizi, A.; Tavangar, S.M.; Moezi, L.; Payabvash, S.; Karoon, A.; Hoseininik, H.; et al. Naltrexone, an opioid receptor antagonist, attenuates liver fibrosis in bile duct ligated rats. *Gut* **2006**, *55*, 1606–1616. [CrossRef] [PubMed]
28. Chakass, D.; Philippe, D.; Erdual, E.; Dharancy, S.; Malapel, M.; Dubuquoy, C.; Thuru, X.; Gay, J.; Gaveriaux-Ruff, C.; Dubus, P.; et al. μ-Opioid receptor activation prevents acute hepatic inflammation and cell death. *Gut* **2007**, *56*, 974. [CrossRef] [PubMed]
29. Wiśniewski, J.R.; Gaugaz, F.Z. Fast and sensitive total protein and peptide assays for proteomic analysis. *Anal. Chem.* **2015**, *87*, 4110–4116. [CrossRef] [PubMed]
30. Wiśniewski, J.R. Quantitative evaluation of filter aided sample preparation (FASP) and multienzyme digestion FASP protocols. *Anal. Chem.* **2016**, *88*, 5438–5443. [CrossRef] [PubMed]
31. Bruderer, R.; Bernhardt, O.M.; Gandhi, T.; Miladinović, S.M.; Cheng, L.-Y.; Messner, S.; Ehrenberger, T.; Zanotelli, V.; Butscheid, Y.; Escher, C.; et al. Extending the limits of quantitative proteome profiling with data-independent acquisition and application to acetaminophen-treated three-dimensional liver microtissues. *Mol. Cell. Proteom.* **2015**, *14*, 1400–1410. [CrossRef] [PubMed]
32. Huang, T.; Bruderer, R.; Muntel, J.; Xuan, Y.; Vitek, O.; Reiter, L. Combining precursor and fragment information for improved detection of differential abundance in data independent acquisition. *Mol. Cell. Proteom.* **2020**, *19*, 421–430. [CrossRef] [PubMed]
33. Storey, J.D. A direct approach to false discovery rates. *J. R. Stat. Soc. Ser. B Stat. Methodol.* **2002**, *64*, 479–498. [CrossRef]
34. Vizcaíno, J.A.; Deutsch, E.W.; Wang, R.; Csordas, A.; Reisinger, F.; Ríos, D.; Dianes, J.A.; Sun, Z.; Farrah, T.; Bandeira, N.; et al. ProteomeXchange provides globally co-ordinated proteomics data submission and dissemination HHS Public Access Author manuscript. *Nat. Biotechnol.* **2014**, *32*, 223–226. [CrossRef] [PubMed]
35. Sundararaman, N.; Go, J.; Robinson, A.E.; Mato, J.M.; Lu, S.C.; Van Eyk, J.E.; Venkatraman, V. PINE: An Automation Tool to Extract and Visualize Protein-Centric Functional Networks. *J. Am. Soc. Mass. Spectrom.* **2020**, *31*, 1410–1421. [CrossRef] [PubMed]
36. Bryant, H.U.; Story, J.A.; Yim, G.K. Morphine-induced alterations in plasma and tissue cholesterol levels. *Life Sci.* **1987**, *41*, 545–554. [CrossRef] [PubMed]
37. Pais, R.; Giral, P.; Khan, J.F.; Rosenbaum, D.; Housset, C.; Poynard, T.; Ratziu, V.; LIDO Study Group. Fatty liver is an independent predictor of early carotid atherosclerosis. *J. Hepatol.* **2016**, *65*, 95–102. [CrossRef] [PubMed]
38. Libby, P. The changing landscape of atherosclerosis. *Nature* **2021**, *592*, 524–533. [CrossRef] [PubMed]
39. Völzke, H.; Robinson, D.M.; Kleine, V.; Deutscher, R.; Hoffmann, W.; Lüdemann, J.; Schminke, U.; Kessler, C.; John, U. Hepatic steatosis is associated with an increased risk of carotid atherosclerosis of Health in Pomerania. *World J. Gastroenterol.* **2005**, *11*, 1848–1853. [CrossRef] [PubMed]

40. Fadaei, R.; Poustchi, H.; Meshkani, R.; Moradi, N.; Golmohammadi, T.; Merat, S. Impaired HDL cholesterol efflux capacity in patients with non-alcoholic fatty liver disease is associated with subclinical atherosclerosis. *Sci. Rep.* **2018**, *8*, 11691. [CrossRef] [PubMed]
41. Baragetti, A.; Pisano, G.; Bertelli, C.; Garlaschelli, K.; Grigore, L.; Fracanzani, A.L.; Fargion, S.; Norata, G.D.; Catapano, A.L. Subclinical atherosclerosis is associated with Epicardial Fat Thickness and hepatic steatosis in the general population. *Nutr. Metab. Cardiovasc. Dis.* **2016**, *26*, 141–153. [CrossRef] [PubMed]
42. Pacifico, L.; Bonci, E.; Andreoli, G.; Romaggioli, S.; Di Miscio, R.; Lombardo, C.V.; Chiesa, C. Association of serum triglyceride-to-HDL cholesterol ratio with carotid artery intima-media thickness, insulin resistance and nonalcoholic fatty liver disease in children and adolescents. *Nutr. Metab. Cardiovasc. Dis.* **2014**, *24*, 737–743. [CrossRef] [PubMed]
43. Rohatgi, A.; Khera, A.; Berry, J.D.; Givens, E.G.; Ayers, C.R.; Wedin, K.E.; Neeland, I.J.; Yuhanna, I.S.; Rader, D.R.; de Lemos, J.A.; et al. HDL Cholesterol Efflux Capacity and Incident Cardiovascular Events. *N. Engl. J. Med.* **2014**, *371*, 2383–2393. [CrossRef] [PubMed]
44. Peirouvi, T.; Mirbaha, Y.; Fathi-Azarbayjani, A.; Jalali, A.S. Co-Administration of Morphine and Naloxone: Histopathological and Biochemical Changes in the Rat Liver. *Int. J. High. Risk Behav. Addict.* **2020**, *9*, e100594. [CrossRef]
45. Wu, S.; Wang, X.; Xing, W.; Li, F.; Liang, M.; Li, K.; He, Y.; Wang, J. An update on animal models of liver fibrosis. *Front. Med.* **2023**, *10*, 1160053. [CrossRef] [PubMed]
46. Saari, T.I.; Strang, J.; Dale, O. Clinical Pharmacokinetics and Pharmacodynamics of Naloxone. *Clin. Pharmacokinet.* **2024**, *63*, 397. [CrossRef] [PubMed]
47. Ferré, P.; Foufelle, F. Hepatic steatosis: A role for de novo lipogenesis and the transcription factor SREBP-1c. *Diabetes Obes. Metab.* **2010**, *12*, 83–92. [CrossRef] [PubMed]
48. Kohjima, M.; Higuchi, N.; Kato, M.; Kotoh, K.; Yoshimoto, T.; Fujino, T.; Yada, M.; Yada, R.; Harada, N.; Enjoji, M.; et al. SREBP-1c, regulated by the insulin and AMPK signaling pathways, plays a role in nonalcoholic fatty liver disease. *Int. J. Mol. Med.* **2008**, *21*, 507–511. [CrossRef] [PubMed]
49. Li, Y.; Xu, S.; Mihaylova, M.M.; Zheng, B.; Hou, X.; Jiang, B.; Park, O.; Luo, Z.; Lefai, E.; Shyy, J.Y.J.; et al. Cell Metabolism Article AMPK Phosphorylates and Inhibits SREBP Activity to Attenuate Hepatic Steatosis and Atherosclerosis in Diet-Induced Insulin-Resistant Mice. *Cell Metab.* **2011**, *13*, 376–388. [CrossRef] [PubMed]
50. Fisher, R.M.; Humphries, S.E.; Talmud, P.J. Common variation in the lipoprotein lipase gene: Effects on plasma lipids and risk of atherosclerosis. *Atherosclerosis* **1997**, *135*, 145–159. [CrossRef] [PubMed]
51. Spence, J.D.; Ban, M.R.; Hegele, R.A. Lipoprotein Lipase (LPL) Gene Variation and Progression of Carotid Artery Plaque. *Stroke* **2003**, *34*, 1176–1180. [CrossRef] [PubMed]
52. Notarnicola, M.; Misciagna, G.; Tutino, V.; Chiloiro, M.; Osella, A.R.; Guerra, V.; Bonfiglio, C.; Caruso, M.G. Increased serum levels of lipogenic enzymes in patients with severe liver steatosis. *Lipids Health Dis.* **2012**, *11*, 145. [CrossRef] [PubMed]
53. Pardina, E.; Baena-Fustegueras, J.A.; Llamas, R.; Catalán, R.; Galard, R.; Lecube, A.; Fort, J.M.; Llobera, M.; Allende, H.; Vargas, V.; et al. Lipoprotein lipase expression in livers of morbidly obese patients could be responsible for liver steatosis. *Obes. Surg.* **2009**, *19*, 608–616. [CrossRef] [PubMed]
54. Furuhashi, M.; Hotamisligil, G.S. Fatty acid-binding proteins: Role in metabolic diseases and potential as drug targets. *Nat. Rev. Drug Discov.* **2008**, *7*, 489–503. [CrossRef] [PubMed]
55. Furuhashi, M.; Saitoh, S.; Shimamoto, K.; Miura, T. Fatty acid-binding protein 4 (FABP4): Pathophysiological insights and potent clinical biomarker of metabolic and cardiovascular diseases. *Clin. Med. Insights Cardiol.* **2014**, *2014*, 23–33. [CrossRef] [PubMed]
56. Chen, M.T.; Huang, J.S.; Gao, D.D.; Li, Y.X.; Wang, H.Y. Combined treatment with FABP4 inhibitor ameliorates rosiglitazone-induced liver steatosis in obese diabetic db/db mice. *Basic. Clin. Pharmacol. Toxicol.* **2021**, *129*, 173–182. [CrossRef] [PubMed]
57. Rodríguez-Calvo, R.; Moreno-Vedia, J.; Girona, J.; Ibarretxe, D.; Martínez-Micaelo, N.; Merino, J.; Plana, N.; Masana, L. Relationship Between Fatty Acid Binding Protein 4 and Liver Fat in Individuals at Increased Cardiometabolic Risk. *Front. Physiol.* **2021**, *12*, 781789. [CrossRef] [PubMed]
58. De Minicis, S.; Candelaresi, C.; Marzioni, M.; Saccomano, S.; Roskams, T.; Casini, A.; Risaliti, A.; Salzano, R.; Cautero, N.; di Francesco, F.; et al. Role of endogenous opioids in modulating HSC activity in vitro and liver fibrosis in vivo. *Gut* **2008**, *57*, 352–364. [CrossRef] [PubMed]
59. Stöger, J.L.; Gijbels, M.J.J.; van der Velden, S.; Manca, M.; van der Loos, C.M.; Biessen, E.A.L.; Daemen, M.J.A.P.; Lutgens, E.; de Winther, M.P.J. Distribution of macrophage polarization markers in human atherosclerosis. *Atherosclerosis* **2012**, *225*, 461–468. [CrossRef] [PubMed]
60. Waldo, S.W.; Li, Y.; Buono, C.; Zhao, B.; Billings, E.M.; Chang, J.; Kruth, H.S. Heterogeneity of Human Macrophages in Culture and in Atherosclerotic Plaques. *Am. J. Pathol.* **2008**, *172*, 1112–1126. [CrossRef] [PubMed]
61. Wang, T.Y.; Su, N.Y.; Shih, P.C.; Tsai, P.S.; Huang, C.J. Anti-inflammation effects of naloxone involve phosphoinositide 3-kinase delta and gamma. *J. Surg. Res.* **2014**, *192*, 599–606. [CrossRef] [PubMed]

62. Olofsson, S.; Borèn, J. Apolipoprotein B: A clinically important apolipoprotein which assembles atherogenic lipoproteins and promotes the development of atherosclerosis. *J. Intern. Med.* **2005**, *258*, 395–410. [CrossRef] [PubMed]
63. Crooke, R.M.; Graham, M.J.; Lemonidis, K.M.; Whipple, C.P.; Koo, S.; Perera, R.J. An apolipoprotein B antisense oligonucleotide lowers LDL cholesterol in hyperlipidemic mice without causing hepatic steatosis. *J. Lipid Res.* **2005**, *46*, 872–884. [CrossRef] [PubMed]
64. Kastelein, J.J.P.; Wedel, M.K.; Baker, B.F.; Su, J.; Bradley, J.D.; Yu, R.Z.; Chuang, E.; Graham, M.J.; Crooke, R.M. Potent Reduction of Apolipoprotein B and Low-Density Lipoprotein Cholesterol by Short-Term Administration of an Antisense Inhibitor of Apolipoprotein B. *Circulation* **2006**, *114*, 1729–1735. [CrossRef] [PubMed]
65. van der Westhuyzen, D.R.; de Beer, F.C.; Webb, N.R. HDL cholesterol transport during inflammation. *Curr. Opin. Lipidol.* **2007**, *18*, 147–151. [CrossRef] [PubMed]
66. Clifton, P.M.; Mackinnon, A.M.; Barter, P.J. Effects of serum amyloid A protein (SAA) on composition, size, and density of high density lipoproteins in subjects with myocardial infarction. *J. Lipid Res.* **1985**, *26*, 1389–1398. [CrossRef] [PubMed]
67. Tang, C.; Babenko, I.; Hutchins, P.; Wimberger, J.; Suffredini, A.F.; Heinecke, J.W. Inflammatory remodeling of the HDL proteome impairs cholesterol efflux capacity. *J. Lipid Res.* **2015**, *56*, 1519–1530. [CrossRef] [PubMed]
68. Yang, D.; Zhang, X.; Yue, L.; Hu, H.; Wei, X.; Guo, Q.; Zhang, B.; Fan, X.; Xin, Y.; Oh, Y.; et al. Thiamethoxam induces nonalcoholic fatty liver disease in mice via methionine metabolism disturb via nicotinamide N-methyltransferase overexpression. *Chemosphere* **2021**, *273*, 129727. [CrossRef] [PubMed]
69. Komatsu, M.; Kanda, T.; Urai, H.; Kurokochi, A.; Kitahama, R.; Shigaki, S.; Ono, T.; Yukioka, H.; Hasegawa, K.; Tokuyama, H.; et al. NNMT activation can contribute to the development of fatty liver disease by modulating the NAD+metabolism. *Sci. Rep.* **2018**, *8*, 8637. [CrossRef] [PubMed]
70. Neelakantan, H.; Vance, V.; Wetzel, M.D.; Wang, H.-Y.L.; McHardy, S.F.; Finnerty, C.C.; Hommel, J.D.; Watowich, S.J. Selective and membrane-permeable small molecule inhibitors of nicotinamide N-methyltransferase reverse high fat diet-induced obesity in mice. *Biochem. Pharmacol.* **2018**, *147*, 141–152. [CrossRef] [PubMed]
71. Li, D.; Yi, C.; Huang, H.; Li, J.; Hong, S. Hepatocyte-specific depletion of *Nnmt* protects mice from non-alcoholic steatohepatitis. *J. Hepatol.* **2022**, *77*, 882–884. [CrossRef] [PubMed]
72. Chen, C.C.; Lee, T.Y.; Kwok, C.F.; Hsu, Y.P.; Shih, K.C.; Lin, Y.J.; Ho, L.T. Major urinary protein 1 interacts with cannabinoid receptor type 1 in fatty acid-induced hepatic insulin resistance in a mouse hepatocyte model. *Biochem. Biophys. Res. Commun.* **2015**, *460*, 1063–1068. [CrossRef] [PubMed]
73. Zhou, Y.; Jiang, L.; Rui, L. Identification of MUP1 as a Regulator for Glucose and Lipid Metabolism in Mice. *J. Biol. Chem.* **2009**, *284*, 11152–11159. [CrossRef] [PubMed]
74. Klusman, C.; Martin, B.; Perez, J.V.D.; Barcena, A.J.J.R.; Bernardino, M.R.; Valentin, E.M.D.S.; Damasco, J.A.; Del Mundo, H.C.; Court, K.; Godin, B.; et al. Rosuvastatin-Eluting Gold-Nanoparticle-Loaded Perivascular Wrap for Enhanced Arteriovenous Fistula Maturation in a Murine Model. *Adv. Fiber Mater.* **2023**, *5*, 1986–2001. [CrossRef]
75. The UniProt Consortium. UniProt: The Universal Protein Knowledgebase in 2023. *Nucleic Acids Res.* **2023**, *51*, D523–D531. [CrossRef] [PubMed]
76. Prasongsukarn, K.; Dechkhajorn, W.; Benjathummarak, S.; Maneerat, Y. TRPM2, PDLIM5, BCL3, CD14, GBA Genes as Feasible Markers for Premature Coronary Heart Disease Risk. *Front. Genet.* **2021**, *12*, 598296. [CrossRef] [PubMed]
77. Wei, M.; Li, P.; Guo, K. The impact of PSRC1 overexpression on gene and transcript expression profiling in the livers of ApoE-/- mice fed a high-fat diet. *Mol. Cell. Biochem.* **2020**, *465*, 125–139. [CrossRef] [PubMed]
78. Couture, J.P.; Nolet, G.; Beaulieu, E.; Blouin, R.; Gévry, N. The p400/Brd8 chromatin remodeling complex promotes adipogenesis by incorporating histone variant H2A.Z at PPARγ target genes. *Endocrinology* **2012**, *153*, 5796–5808. [CrossRef] [PubMed]
79. Greve, S.; Kuhn, G.A.; Saenz-de-Juano, M.D.; Ghosh, A.; von Meyenn, F.; Giller, K. The major urinary protein gene cluster knockout mouse as a novel model for translational metabolism research. *Sci. Rep.* **2022**, *12*, 13161. [CrossRef] [PubMed]
80. Van Sligtenhorst, I.; Ding, Z.-M.; Shi, Z.-Z.; Read, R.W.; Hansen, G.; Vogel, P. Cardiomyopathy in α-kinase 3 (ALPK3)-deficient mice. *Vet. Pathol.* **2012**, *49*, 131–141. [CrossRef] [PubMed]
81. Shrestha, N.; Sleep, S.; Helman, T.; Holland, O.; Cuffe, J.S.M.; Perkins, A.V.; Mcainch, A.J.; Headrick, J.P.; Hryciw, D.H. Maternal diet high in linoleic acid alters offspring fatty acids and cardiovascular function in a rat model. *Br. J. Nutr.* **2022**, *127*, 540–553. [CrossRef] [PubMed]
82. Shenoy, A.R.; Wellington, D.A.; Kumar, P.; Kassa, H.; Booth, C.J.; Cresswell, P.; MacMicking, J.D. GBP5 promotes NLRP3 inflammasome assembly and immunity in mammals. *Science* **2012**, *336*, 481–485. [CrossRef] [PubMed]
83. Chmielewski, S.; Olejnik, A.; Sikorski, K.; Pelisek, J.; Błaszczyk, K.; Aoqui, C.; Nowicka, H.; Zernecke, A.; Heemann, U.; Wesoly, J.; et al. STAT1-dependent signal integration between IFNγ and TLR4 in vascular cells reflect pro-atherogenic responses in human atherosclerosis. *PLoS ONE* **2014**, *9*, e113318. [CrossRef] [PubMed]
84. An, D.; Hao, F.; Zhang, F.; Kong, W.; Chun, J.; Xu, X.; Cui, M.Z. CD14 is a key mediator of both lysophosphatidic acid and lipopolysaccharide induction of foam cell formation. *J. Biological Chem.* **2017**, *292*, 14391–14400. [CrossRef] [PubMed]

85. Mu, K.; Sun, Y.; Zhao, Y.; Zhao, T.; Li, Q.; Zhang, M.; Li, H.; Zhang, R.; Hu, C.; Wang, C.; et al. Hepatic nitric oxide synthase 1 adaptor protein regulates glucose homeostasis and hepatic insulin sensitivity in obese mice depending on its PDZ binding domain. *EBioMedicine* **2019**, *47*, 352–364. [CrossRef] [PubMed]
86. Fujita, W.; Yokote, M.; Gomes, I.; Gupta, A.; Ueda, H.; Devi, L.A. Regulation of an Opioid Receptor Chaperone Protein, RTP4, by Morphine s. *Mol Pharmacol.* **2019**, *95*, 9–11. [CrossRef] [PubMed]
87. Décaillot, F.M.; Rozenfeld, R.; Gupta, A.; Devi, L.A. Cell surface targeting of mu-delta opioid receptor heterodimers by RTP4. *Proc. Natl. Acad. Sci. USA* **2008**, *105*, 16045–16050. [CrossRef] [PubMed]
88. Dong, R.; Jiang, G.; Tian, Y.; Shi, X. Identification of immune-related biomarkers and construction of regulatory network in patients with atherosclerosis. *BMC Med. Genom.* **2022**, *15*, 245. [CrossRef] [PubMed]
89. Ravindran, A.; Holappa, L.; Niskanen, H.; Skovorodkin, I.; Kaisto, S.; Beter, M.; Kiema, M.; Selvarajan, I.; Nurminen, V.; Aavik, E.; et al. Translatome profiling reveals Itih4 as a novel smooth muscle cell-specific gene in atherosclerosis. *Cardiovasc. Res.* **2024**, *120*, 869–882. [CrossRef] [PubMed]
90. Fujita, Y.; Ezura, Y.; Emi, M.; Sato, K.; Takada, D.; Iino, Y.; Katayama, Y.; Takahashi, K.; Kamimura, K.; Bujo, H.; et al. Hypercholesterolemia associated with splice-junction variation of inter-alpha-trypsin inhibitor heavy chain 4 (ITIH4) gene. *J. Hum. Genet.* **2004**, *49*, 24–28. [CrossRef] [PubMed]
91. Yao, J.; Jia, L.; Khan, N.; Lin, C.; Mitter, S.K.; Boulton, M.E.; Dunaief, J.L.; Klionsky, D.J.; Guan, J.L.; Thompson, D.A.; et al. Deletion of autophagy inducer RB1CC1 results in degeneration of the retinal pigment epithelium. *Autophagy* **2015**, *11*, 939–953. [CrossRef] [PubMed]
92. Goo, Y.H.; Son, S.H.; Yechoor, V.K.; Paul, A. Transcriptional Profiling of Foam Cells Reveals Induction of Guanylate-Binding Proteins Following Western Diet Acceleration of Atherosclerosis in the Absence of Global Changes in Inflammation. *J. Am. Heart Assoc. Cardiovasc. Cerebrovasc. Dis.* **2016**, *5*, 4. [CrossRef] [PubMed]
93. Shayo, S.C.; Ogiso, K.; Kawade, S.; Hashiguchi, H.; Deguchi, T.; Nishio, Y. Dietary obesity and glycemic excursions cause a parallel increase in STEAP4 and pro-inflammatory gene expression in murine PBMCs. *Diabetol Int.* **2022**, *13*, 358–371. [CrossRef] [PubMed]
94. Li, Z.; Liu, J.; Liu, Z.; Zhu, X.; Geng, R.; Ding, R.; Xu, H.; Huang, S. Comprehensive analysis identifies crucial genes associated with immune cells mediating progression of carotid atherosclerotic plaque. *Aging* **2024**, *16*, 3880–3895. [CrossRef] [PubMed]
95. Zheng, Y.; Qi, B.; Gao, W.; Qi, Z.; Liu, Y.; Wang, Y.; Feng, J.; Cheng, X.; Luo, Z.; Li, T. Macrophages-Related Genes Biomarkers in the Deterioration of Atherosclerosis. *Front. Cardiovasc. Med.* **2022**, *9*, 890321. [CrossRef] [PubMed]
96. Liu, R.; Cao, H.; Zhang, S.; Cai, M.; Zou, T.; Wang, G.; Zhang, D.; Wang, X.; Xu, J.; Deng, S.; et al. ZBP1-mediated apoptosis and inflammation exacerbate steatotic liver ischemia/reperfusion injury. *J. Clin. Investig.* **2024**, *134*. [CrossRef] [PubMed]
97. Han, J.; Opoku, E.; Smith, J.D. Abstract 252: Is Zbp1 An Atherosclerosis Modifier Gene? *Arterioscler. Thromb. Vasc. Biol.* **2023**, *43*, A252. [CrossRef]
98. Lin, T.-Y.; Wei, T.-Y.W.; Li, S.; Wang, S.-C.; He, M.; Martin, M.; Zhang, J.; Shentu, T.-P.; Xiao, H.; Kang, J.; et al. TIFA as a crucial mediator for NLRP3 inflammasome. *Proc. Natl. Acad. Sci. USA* **2016**, *113*, 15078–15083. [CrossRef] [PubMed]
99. Demchev, V.; Malana, G.; Vangala, D.; Stoll, J.; Desai, A.; Kang, H.W.; Li, Y.; Nayeb-Hashemi, H.; Niepel, M.; Cohen, D.E.; et al. Targeted Deletion of Fibrinogen Like Protein 1 Reveals a Novel Role in Energy Substrate Utilization. *PLoS ONE* **2013**, *8*, e58084. [CrossRef] [PubMed]
100. Bazan, H.A.; Brooks, A.J.; Vongbunyong, K.; Tee, C.; Douglas, H.F.; Klingenberg, N.C.; Woods, T.C. A pro-inflammatory and fibrous cap thinning transcriptome profile accompanies carotid plaque rupture leading to stroke. *Sci. Rep.* **2022**, *12*, 13499. [CrossRef] [PubMed]
101. Ito, S.; Naito, M.; Kobayashi, Y.; Takatsuka, H.; Jiang, S.; Usuda, H.; Umezu, H.; Hasegawa, G.; Arakawa, M.; Shultz, L.D.; et al. Roles of a macrophage receptor with collagenous structure (MARCO) in host defense and heterogeneity of splenic marginal zone macrophages. *Arch. Histol. Cytol.* **1999**, *62*, 83–95. [CrossRef] [PubMed]
102. Amersfoort, J.; Schaftenaar, F.H.; Douna, H.; van Santbrink, P.J.; Kröner, M.J.; van Puijvelde, G.H.M.; Quax, P.H.A.; Kuiper, J.; Bot, I. Lipocalin-2 contributes to experimental atherosclerosis in a stage-dependent manner. *Atherosclerosis* **2018**, *275*, 214–224. [CrossRef] [PubMed]
103. Shibata, K.; Sato, K.; Shirai, R.; Seki, T.; Okano, T.; Yamashita, T.; Koide, A.; Mitsuboshi, M.; Mori, Y.; Hirano, T.; et al. Lipocalin-2 exerts pro-atherosclerotic effects as evidenced by in vitro and in vivo experiments. *Heart Vessel.* **2020**, *35*, 1012–1024. [CrossRef] [PubMed]
104. Hu, S.; Zhu, Y.; Zhao, X.; Li, R.; Shao, G.; Gong, D.; Hu, C.; Liu, H.; Xu, K.; Liu, C.; et al. Hepatocytic lipocalin-2 controls HDL metabolism and atherosclerosis via Nedd4-1-SR-BI axis in mice. *Dev. Cell* **2023**, *58*, 2326–2337.e5. [CrossRef] [PubMed]
105. Riederer, M.; Erwa, W.; Zimmermann, R.; Frank, S.; Zechner, R. Adipose tissue as a source of nicotinamide N-methyltransferase and homocysteine. *Atherosclerosis* **2009**, *204*, 412–417. [CrossRef] [PubMed]

106. Hong, S.; Moreno-Navarrete, J.M.; Wei, X.; Kikukawa, Y.; Tzameli, I.; Prasad, D.; Lee, Y.; Asara, J.M.; Fernandez-Real, J.M.; Maratos-Flier, E.; et al. Nicotinamide N-methyltransferase regulates hepatic nutrient metabolism through Sirt1 protein stabilization. *Nat. Med.* **2015**, *21*, 887. [CrossRef] [PubMed]
107. Webb, N.R.; De Beer, M.C.; Wroblewski, J.M.; Ji, A.; Bailey, W.; Shridas, P.; Charnigo, R.J.; Noffsinger, V.P.; Witta, J.; Howatt, D.A.; et al. Deficiency of Endogenous Acute-Phase Serum Amyloid A Protects apoE−/− Mice from Angiotensin II-Induced Abdominal Aortic Aneurysm Formation. *Arterioscler. Thromb. Vasc. Biol.* **2015**, *35*, 1156–1165. [CrossRef] [PubMed]
108. Dong, Z.; Wu, T.; Qin, W.; An, C.; Wang, Z.; Zhang, M.; Zhang, Y.; Zhang, C.; An, F. Serum amyloid A directly accelerates the progression of atherosclerosis in apolipoprotein E-deficient mice. *Mol. Med.* **2011**, *17*, 1357–1364. [CrossRef] [PubMed]
109. Thompson, J.C.; Jayne, C.; Thompson, J.; Wilson, P.G.; Yoder, M.H.; Webb, N.; Tannock, L.R. A brief elevation of serum amyloid A is sufficient to increase atherosclerosis. *J. Lipid Res.* **2015**, *56*, 286–293. [CrossRef] [PubMed]

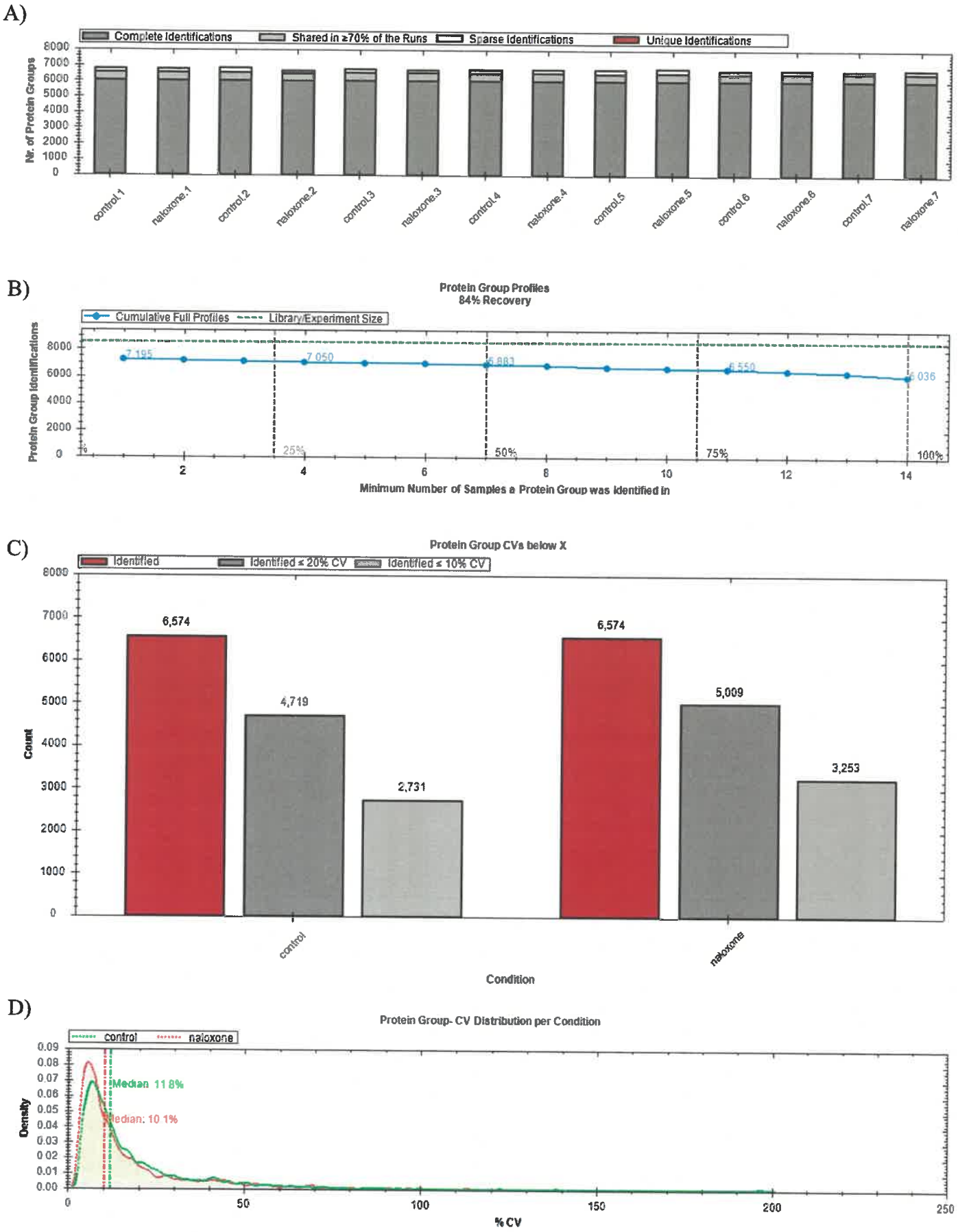

Figure 1. Quality control of MS runs of the liver of control and naloxone-treated mice. Protein group identification details across all LC-MS runs **(A)**. Spectral library recovery **(B)**. Coefficient of variations (CVs) for protein groups across all biological conditions **(C)**. Distribution of protein group CV in biological conditions **(D)**(n = 7 biological replicates).

Table 1. An overview of deregulated proteins, their encoding genes, and functions (functions obtained from UniProt database [1]).

Protein	Gene	Fold change	Main function	Function connected to lipid metabolism and atherosclerosis
O70209	*Pdlim3* (PDZ and LIM domain 3)	3.16	May play a role in the organization of actin filament arrays within muscle cells.	Upregulated in patients with familiar hypercholesterolemia (FH) or with FH-related coronary heart disease [2].
P15392	*Cyp2a4* (liver cytochrome 2a4)	2.60	Highly active in the 15-alpha-hydroxylation of testosterone.	Upregulated in ApoE$^{-/-}$ mice overexpressing proline/serine-rich coiled-coil 1 (PSRC1) that regulates blood lipid levels and inhibit atherosclerosis [3].
Q8R3B7	*Brd8* (bromo-conatining protein 8)	2.56	May act as a coactivator during transcriptional activation by hormone-activated nuclear receptors.	Brd8/p400 (p400) chromatin remodeling complex promotes adipogenesis [4].
P11588	*Mup1* (major urinary protein 1)	2.10	Binds pheromones that are released from drying urine of males.	Belong to lipocalins family that transport hydrophobic molecules as steroids, retinoids, lipids [5]. Significantly reduced in genetic and dietary fat-induced obesity and diabetes in bd/bd mice, while administration of recombinant MUP1 attenuated hyperglycemia and glucose intolerance in these mice [6].
Q924C5	*Alpk3* (alpha kinase 3)	2.10	Involved in cardiomyocyte differentiation.	ALPK3-deficient mice develop cardiac hypertrophy [7].
Q8R429	*Atp2a1* (ATPase sarcoplasmic/endoplasmic reticulum Ca^{2+} transporting 1)	2.09	Contributes to calcium sequestration involved in muscular excitation/contraction.	Atp2a1 is significantly increased in male offspring of murine mothers fed high linoleic acid diet but unchanged in female offspring [8].
Q8CFB4	*Gbp5* (Guanylate binding protein 5)	-2.04	Plays important roles in innate immunity against a diverse range of bacterial, viral and protozoan pathogens.	suggested as a potential atherosclerosis marker involving in inflammation [9,10].
Q8VBT6	*Apobr* (apolipoprotein B receptor)	-2.07	May provide essential lipids to reticuloendothelial cells. Could also be involved in foam cell formation with elevated triglyceride-rich lipoproteins and remnant lipoprotein.	-
P59041	*Dnajc30* (DnaJ heat shock protein family (Hsp40) member C30)	-2.11	Mitochondrial protein enriched in neurons that acts as a regulator of mitochondrial respiration	-

P10810	*Cd14* (cluster of differentiation 14)	-2.12	Expressed by macrophages, mediating the innate immune response to bacterial lipopolysaccharide.	Cd14 is involved in pathways contributing to worsening of atherosclerosis. *Cd14* knockdown blocks oxidized LDL uptake in macrophages and foam cell formation in fatty deposits in blood vessels [11].
Q9D3A8	*Nos1ap* (nitric oxide synthase 1 adaptor protein)	-2.13	Adapter protein involved in neuronal nitric-oxide (NO) synthesis.	Liver specific NOS1AP conditional knockout mice demonstrated increased lipid deposits in the liver [12].
Q9ER80	*Rtp4* (receptor transporter protein 4)	-2.13	Promotes functional expression of the opioid receptor heterodimer OPRD1-OPRM1. Probable chaperone protein which facilitates trafficking and functional cell surface expression of some G-protein coupled receptors.	Morphine administration to C57BL/6 mice increased Rtp4 mRNA expression in the hypothalamus as well as caused a significant increase in μ-δ opioid receptor heterodimers and μ-opioid receptors. RTP4 is necessary and sufficient for the regulation of opioid receptor presence on the cell surface [13] RTP4 protects mu-delta receptors from ubiquitination and degradation [14].
Q9JHU9	*Isyna1* (inositol-3-phosphate synthase 1)	-2.14	Key enzyme in myo-inositol biosynthesis pathway that catalyzes the conversion of glucose 6-phosphate to 1-myo-inositol 1-phosphate in a NAD-dependent manner.	-
Q64345	*Ifit3* (interferon induced protein with tetratricopeptide repeats 3)	-2.15	Acts as an inhibitor of cellular as well as viral processes, cell migration, proliferation, signaling, and viral replication.	Analysis on the mRNA expression profile of human atherosclerotic samples obtained from GEO database identified IFIH1, IFIT1, IFIT2, IFIT3, ISG15 and OAS3 as immune-related hub genes of atherosclerosis [15].
A6X935	*Itih4* (inter-alpha-trypsin inhibitor heavy chain 4)	-2.20	Type II acute-phase protein (APP) involved in inflammatory responses to trauma.	Itih4 has been identified as a smooth muscle cell-expressed gene in atherosclerotic plaques [16]. Genetic variation (SNP) in human *Itih4* gene determines cholesterol metabolism and its level in blood plasma [17].
Q9ESK9	*Rb1cc1* (RB1-inducible coiled-coil protein 1)	-2.20	Involved in autophagy. Plays a crucial role in muscular differentiation.	In Rb1cc1-CKO mice increased accumulation of lipid-filled vacuoles in the retinal pigment epithelium was observed [18].
Q8R1N0	*Znf830* (zinc finger protein 830)	-2.22	May play a role in pre-mRNA splicing as component of the spliceosome	-
P25916	*Bmi1*	-2.29	Component of a Polycomb group (PcG) multiprotein PRC1-like complex, a complex class required to	-

	(polycomb complex protein BMI-1)		maintain the transcriptionally repressive state of many genes.	
P12246	*Apcs* (serum amyloid P-component)	-2.31	Can interact with DNA and histones and may scavenge nuclear material released from damaged circulating cells.	-
P14429	*H2-Q7* (H-2 class I histocompatibility antigen, Q7 alpha chain)	-2.33	Involved in the presentation of foreign antigens to the immune system.	-
Q9Z0E6	*Gbp2* (Guanylate-binding protein 2)	-2.36	Interferon (IFN)-inducible GTPase that plays important roles in innate immunity against a diverse range of bacterial, viral and protozoan pathogens.	*Gbp2* expression was upregulated in mouse peritoneal macrophage culture treated with oxLDL [19].
Q923B6	*Steap4* (metalloreductase STEAP4)	-2.41	Plays a role in systemic metabolic homeostasis, integrating inflammatory and metabolic responses. Involved in inflammatory arthritis, through the regulation of inflammatory cytokines.	Diet-induced obesity caused a significant increase in STEAP4 mRNA expression in rats PBMCs [20].
Q60787	*Lcp2* (lymphocyte cytosolic protein 2)	-2.46	Involved in T-cell antigen receptor mediated signaling	LCP2 was found, among others, to be connected with carotid atherosclerotic plaques [21]. Analysis of aortas of ApoE$^{-/-}$ mice fed a Western diet for 6 months demonstrated high expression of LCP2 as compared to the control group [22].
Q9QY24	*Zbp1* (Z-DNA-binding protein 1)	-2.52	Key innate sensor that recognizes and binds Z-RNA structures, which are produced by a number of viruses, and triggers different forms of cell death.)	Deletion of ZBP1 substantially decreases the steatotic liver ischemia/reperfusion injury [23]. *Zbp1* knockout mice treated with LDLr antisense oligos and fed a western-type diet demonstrated tendency to a decrease in median aortic lesion area compared to WT group. Also, median necrotic lesion area and % necrotic lesion area were decreased [24].
Q60590	*Orm1* (alpha-1-acid glycoprotein 1)	-2.52	Functions as a transport protein in the blood stream.	-
Q793I8	*Tifa* (TNF-α receptor-associated factor-interacting protein with a forkhead-associated domain)	-2.57	Adapter molecule that plays a key role in the activation of pro-inflammatory NF-kappa-B signaling following detection of bacterial pathogen-associated molecular pattern metabolites (PAMPs).	TIFA protein levels were significantly increased in the aortas of ApoE$^{-/-}$ mice receiving a Western diet compared to the chow diet; furthermore, oxidized LDL treatment increased *Tifa* mRNA and protein levels in cultured human umbilical vein endothelial cells [25].

Q71KU9	*Fgl1* (fibrinogen-like protein 1)	-2.68	Immune suppressive molecule that inhibits antigen-specific T-cell activation by acting as a major ligand of LAG3. Secreted by, and promotes growth of, hepatocytes	Liver injury enhance the expression of *Fgl1* in brown adipose tissue. Fgl1 null mice have greater body mass and abnormal plasma lipid profiles than wild type mice [26].
Q64282	*Ifit1* (Interferon-induced protein with tetratricopeptide repeats 1)	-3.24	Interferon-induced antiviral RNA-binding protein, acting as a sensor of viral single-stranded RNAs and inhibiting expression of viral messenger RNAs.	Based on Gene Expression Omnibus database IFIT1 has been identified as associated with atherosclerosis [15]. IFIT1 together with IFIT3 have been evidenced to be involved in pro-inflammatory polarization of macrophages and decreased collagen deposition leading to atherosclerotic plaque vulnerability [27].
Q3T9E4; Q62293	*Tgtp2; Tgtp1* (T-cell-specific guanine nucleotide triphosphate-binding protein 2;-1)	-3.25	Involved in innate cell-autonomous resistance to intracellular pathogens such as Toxoplasma gondii; Involved in innate cell-autonomous resistance to intracellular pathogens, such as Toxoplasma gondii.	-
Q6R5N8	*Tlr13* (Toll-like receptor 13)	-4.10	Component of innate and adaptive immunity that recognizes and binds 23S rRNA from bacteria. TLRs (Toll-like receptors) control host immune response against pathogens.	-
Q60754	*Marco* (macrophage receptor with collagenous structure)	-4.50	Pattern recognition receptor (PRR) which binds Gram-positive and Gram-negative bacteria.	Macrophage receptor with collagenous structure (MARCO) are membrane glycoproteins mediating the uptake of chemically modified low density lipoproteins [28].
P02798	*Mt2* (metallothionein-2)	-8.92	Metallothioneins have a high content of cysteine residues that bind various heavy metals.	-
P11672	*Lcn2* (lipocalin 2)	-9.37	Iron-trafficking protein involved in multiple processes such as apoptosis, innate immunity and renal development.	*Lcn2* knockout mice developed larger atherosclerotic lesions during earlier stages of atherosclerosis compared to control [29]. Chronic administration of LCN2 in $ApoE^{-/-}$ mice markedly accelerated the development of aortic atherosclerotic lesions and increased lesion infiltration with monocyte/macrophage [30]. Overexpression of human Lcn2 in hepatocytes attenuates the development of atherosclerosis in western diet-fed $Ldlr^{-/-}$ mice [31].

O55239	*Nnmt* (nicotinamide N-methyltransferase)	-10.15	Acts as a metabolic regulator primarily on white adipose tissue energy expenditure as well as hepatic gluconeogenesis and cholesterol biosynthesis.	NNMT plays an important role in hepatic detoxification. Product of the NNMT catalysis is homocysteine which is considered a marker of cardiovascular disease, probably acting via atherogenesis [32]. Inhibition of hepatic *Nnmt* expression in vivo affects cholesterol metabolism [33].
Q9DBN4	*P33-monox* (putative monooxygenase p33MONOX)	-12.16	Potential NADPH-dependent oxidoreductase. May be involved in the regulation of neuronal survival, differentiation and axonal outgrowth.	-
P02802	*Mt1* (metallothionein 1)	-42.61	Metallothioneins have a high content of cysteine residues that bind various heavy metals; these proteins are transcriptionally regulated by both heavy metals and glucocorticoids.	-
P05367	*Saa2* (serum amyloid A2)	-44.70	Major acute phase reactant. Apolipoprotein of the HDL complex	Absence of SAA1 and SAA2 attenuated angiotensin-induced abdominal aneurysm formation in $ApoE^{-/-}$ mice [34].
P05366	*Saa1* (serum amyloid A1)	-49.41	Major acute phase reactant	$ApoE^{-/-}$ mice overexpressed murine SAA1 exhibited modest but persistent increase in SAA that contributed to increased atherosclerosis via increased inflammatory cell infiltration [35]. $Rag1^{-/-}ApoE^{-/-}$ and $ApoE^{-/-}$ mice injected with adenoviral vector encoding human SAA1 had increased atherosclerosis compared with controls. It was also established that SAA treatment contribute to increased LDL retention in vascular smooth muscle cell culture [36].

[1] UniProt: the Universal Protein Knowledgebase in 2023. Nucleic Acids Res 2023;51:D523–31. https://doi.org/10.1093/nar/gkac1052.

[2] Prasongsukarn K, Dechkhajorn W, Benjathummarak S, Maneerat Y. TRPM2, PDLIM5, BCL3, CD14, GBA Genes as Feasible Markers for Premature Coronary Heart Disease Risk. Front Genet 2021;12. https://doi.org/10.3389/FGENE.2021.598296.

[3] Wei M, Li P, Guo K. The impact of PSRC1 overexpression on gene and transcript expression profiling in the livers of ApoE-/- mice fed a high-fat diet. Mol Cell Biochem 2020;465:125–39. https://doi.org/10.1007/S11010-019-03673-X.

[4] Couture JP, Nolet G, Beaulieu E, Blouin R, Gévry N. The p400/Brd8 chromatin remodeling complex promotes adipogenesis by incorporating histone variant H2A.Z at PPARγ target genes. Endocrinology 2012;153:5796–808. https://doi.org/10.1210/EN.2012-1380.

[5] Greve S, Kuhn GA, Saenz-de-Juano MD, Ghosh A, von Meyenn F, Giller K. The major urinary protein gene cluster knockout mouse as a novel model for translational metabolism research. Sci Rep 2022;12:13161. https://doi.org/10.1038/S41598-022-17195-Y.

[6] Zhou Y, Jiang L, Rui L. Identification of MUP1 as a Regulator for Glucose and Lipid Metabolism in Mice. Journal of Biological Chemistry 2009;284:11152–9. https://doi.org/10.1074/JBC.M900754200.

[7] Van Sligtenhorst I, Ding Z-M, Shi Z-Z, Read RW, Hansen G, Vogel P. Cardiomyopathy in α-kinase 3 (ALPK3)-deficient mice. Vet Pathol 2012;49:131–41. https://doi.org/10.1177/0300985811402841.

[8] Shrestha N, Sleep S, Helman T, Holland O, Cuffe JSM, Perkins A V., Mcainch AJ, Headrick JP, Hryciw DH. Maternal diet high in linoleic acid alters offspring fatty acids and cardiovascular function in a rat model. Br J Nutr 2022;127:540–53. https://doi.org/10.1017/S0007114521001276.

[9] Shenoy AR, Wellington DA, Kumar P, Kassa H, Booth CJ, Cresswell P, MacMicking JD. GBP5 promotes NLRP3 inflammasome assembly and immunity in mammals. Science 2012;336:481–5. https://doi.org/10.1126/SCIENCE.1217141.

[10] Chmielewski S, Olejnik A, Sikorski K, Pelisek J, Błaszczyk K, Aoqui C, Nowicka H, Zernecke A, Heemann U, Wesoly J, et al. STAT1-dependent signal integration between IFNγ and TLR4 in vascular cells reflect pro-atherogenic responses in human atherosclerosis. PLoS One 2014;9. https://doi.org/10.1371/JOURNAL.PONE.0113318.

[11] An D, Hao F, Zhang F, Kong W, Chun J, Xu X, Cui MZ. CD14 is a key mediator of both lysophosphatidic acid and lipopolysaccharide induction of foam cell formation. Journal of Biological Chemistry 2017;292:14391–400. https://doi.org/10.1074/JBC.M117.781807.

[12] Mu K, Sun Y, Zhao Y, Zhao T, Li Q, Zhang M, Li H, Zhang R, Hu C, Wang C, et al. Hepatic nitric oxide synthase 1 adaptor protein regulates glucose homeostasis and hepatic insulin sensitivity in obese mice depending on its PDZ binding domain. EBioMedicine 2019;47:352–64. https://doi.org/10.1016/J.EBIOM.2019.08.033.

[13] Fujita W, Yokote M, Gomes I, Gupta A, Ueda H, Devi LA. Regulation of an Opioid Receptor Chaperone Protein, RTP4, by Morphine s. MOLECULAR PHARMACOLOGY Mol Pharmacol 2019;95:11–9. https://doi.org/10.1124/mol.118.112987.

[14] Décaillot FM, Rozenfeld R, Gupta A, Devi LA. Cell surface targeting of mu-delta opioid receptor heterodimers by RTP4. Proc Natl Acad Sci U S A 2008;105:16045–50. https://doi.org/10.1073/PNAS.0804106105.

[15] Dong R, Jiang G, Tian Y, Shi X. Identification of immune-related biomarkers and construction of regulatory network in patients with atherosclerosis. BMC Med Genomics 2022;15. https://doi.org/10.1186/S12920-022-01397-4.

[16] Ravindran A, Holappa L, Niskanen H, Skovorodkin I, Kaisto S, Beter M, Kiema M, Selvarajan I, Nurminen V, Aavik E, et al. Translatome profiling reveals Itih4 as a novel smooth muscle cell-specific gene in atherosclerosis. Cardiovasc Res 2024;120:869–82. https://doi.org/10.1093/cvr/cvae028.

[17] Fujita Y, Ezura Y, Emi M, Sato K, Takada D, Iino Y, Katayama Y, Takahashi K, Kamimura K, Bujo H, et al. Hypercholesterolemia associated with splice-junction variation of inter-alpha-trypsin inhibitor heavy chain 4 (ITIH4) gene. J Hum Genet 2004;49:24–8. https://doi.org/10.1007/s10038-003-0101-8.

[18] Yao J, Jia L, Khan N, Lin C, Mitter SK, Boulton ME, Dunaief JL, Klionsky DJ, Guan JL, Thompson DA, et al. Deletion of autophagy inducer RB1CC1 results in degeneration of the retinal pigment epithelium. Autophagy 2015;11:939–53. https://doi.org/10.1080/15548627.2015.1041699.

[19] Goo YH, Son SH, Yechoor VK, Paul A. Transcriptional Profiling of Foam Cells Reveals Induction of Guanylate-Binding Proteins Following Western Diet Acceleration of Atherosclerosis in the Absence of Global Changes in Inflammation. Journal of the American Heart Association: Cardiovascular and Cerebrovascular Disease 2016;5. https://doi.org/10.1161/JAHA.115.002663.

[20] Shayo SC, Ogiso K, Kawade S, Hashiguchi H, Deguchi T, Nishio Y. Dietary obesity and glycemic excursions cause a parallel increase in STEAP4 and pro-inflammatory gene expression in murine PBMCs. Diabetol Int 2022;13:358–71. https://doi.org/10.1007/s13340-021-00542-1.

[21] Li Z, Liu J, Liu Z, Zhu X, Geng R, Ding R, Xu H, Huang S. Comprehensive analysis identifies crucial genes associated with immune cells mediating progression of carotid atherosclerotic plaque. Aging 2024;16:3880–95. https://doi.org/10.18632/AGING.205566.

[22] Zheng Y, Qi B, Gao W, Qi Z, Liu Y, Wang Y, Feng J, Cheng X, Luo Z, Li T. Macrophages-Related Genes Biomarkers in the Deterioration of Atherosclerosis. Front Cardiovasc Med 2022;9. https://doi.org/10.3389/FCVM.2022.890321.

[23] Liu R, Cao H, Zhang S, Cai M, Zou T, Wang G, Zhang D, Wang X, Xu J, Deng S, et al. ZBP1-mediated apoptosis and inflammation exacerbate steatotic liver ischemia/reperfusion injury. J Clin Invest 2024;134. https://doi.org/10.1172/JCI180451.

[24] Han J, Opoku E, Smith JD. Abstract 252: Is Zbp1 An Atherosclerosis Modifier Gene? Arterioscler Thromb Vasc Biol 2023;43. https://doi.org/10.1161/ATVB.43.SUPPL_1.252.

[25] Lin T-Y, Wei T-YW, Li S, Wang S-C, He M, Martin M, Zhang J, Shentu T-P, Xiao H, Kang J, et al. TIFA as a crucial mediator for NLRP3 inflammasome. Proc Natl Acad Sci U S A 2016;113:15078–83. https://doi.org/10.1073/pnas.1618773114.

[26] Demchev V, Malana G, Vangala D, Stoll J, Desai A, Kang HW, Li Y, Nayeb-Hashemi H, Niepel M, Cohen DE, et al. Targeted Deletion of Fibrinogen Like Protein 1 Reveals a Novel Role in Energy Substrate Utilization. PLoS One 2013;8:e58084. https://doi.org/10.1371/JOURNAL.PONE.0058084.

[27] Bazan HA, Brooks AJ, Vongbunyong K, Tee C, Douglas HF, Klingenberg NC, Woods TC. A pro-inflammatory and fibrous cap thinning transcriptome profile accompanies carotid plaque rupture leading to stroke. Sci Rep 2022;12:13499. https://doi.org/10.1038/S41598-022-17546-9.

[28] Ito S, Naito M, Kobayashi Y, Takatsuka H, Jiang S, Usuda H, Umezu H, Hasegawa G, Arakawa M, Shultz LD, et al. Roles of a macrophage receptor with collagenous structure (MARCO) in host defense and heterogeneity of splenic marginal zone macrophages. Arch Histol Cytol 1999;62:83–95. https://doi.org/10.1679/aohc.62.83.

[29] Amersfoort J, Schaftenaar FH, Douna H, van Santbrink PJ, Kröner MJ, van Puijvelde GHM, Quax PHA, Kuiper J, Bot I. Lipocalin-2 contributes to experimental atherosclerosis in a stage-dependent manner. Atherosclerosis 2018;275:214–24. https://doi.org/10.1016/J.ATHEROSCLEROSIS.2018.06.015.

[30] Shibata K, Sato K, Shirai R, Seki T, Okano T, Yamashita T, Koide A, Mitsuboshi M, Mori Y, Hirano T, et al. Lipocalin-2 exerts pro-atherosclerotic effects as evidenced by in vitro and in vivo experiments. Heart Vessels 2020;35:1012–24. https://doi.org/10.1007/S00380-020-01556-6/FIGURES/7.

[31] Hu S, Zhu Y, Zhao X, Li R, Shao G, Gong D, Hu C, Liu H, Xu K, Liu C, et al. Hepatocytic lipocalin-2 controls HDL metabolism and atherosclerosis via Nedd4-1-SR-BI axis in mice. Dev Cell 2023;58:2326-2337.e5. https://doi.org/10.1016/J.DEVCEL.2023.09.007.

[32] Riederer M, Erwa W, Zimmermann R, Frank S, Zechner R. Adipose tissue as a source of nicotinamide N-methyltransferase and homocysteine. Atherosclerosis 2009;204:412–7. https://doi.org/10.1016/J.ATHEROSCLEROSIS.2008.09.015.

[33] Hong S, Moreno-Navarrete JM, Wei X, Kikukawa Y, Tzameli I, Prasad D, Lee Y, Asara JM, Fernandez-Real JM, Maratos-Flier E, et al. Nicotinamide N-methyltransferase regulates hepatic nutrient metabolism through Sirt1 protein stabilization. Nat Med 2015;21:887. https://doi.org/10.1038/NM.3882.

[34] Webb NR, De Beer MC, Wroblewski JM, Ji A, Bailey W, Shridas P, Charnigo RJ, Noffsinger VP, Witta J, Howatt DA, et al. Deficiency of Endogenous Acute-Phase Serum Amyloid A Protects apoE-/- Mice From Angiotensin II-Induced Abdominal Aortic Aneurysm Formation. Arterioscler Thromb Vasc Biol 2015;35:1156–65. https://doi.org/10.1161/ATVBAHA.114.304776.

[35] Dong Z, Wu T, Qin W, An C, Wang Z, Zhang M, Zhang Y, Zhang C, An F. Serum amyloid A directly accelerates the progression of atherosclerosis in apolipoprotein E-deficient mice. Mol Med 2011;17:1357–64. https://doi.org/10.2119/MOLMED.2011.00186.

[36] Thompson JC, Jayne C, Thompson J, Wilson PG, Yoder MH, Webb N, Tannock LR. A brief elevation of serum amyloid A is sufficient to increase atherosclerosis. J Lipid Res 2015;56:286–93. https://doi.org/10.1194/JLR.M054015.

Hindawi
Mediators of Inflammation
Volume 2021, Article ID 4977209, 9 pages
https://doi.org/10.1155/2021/4977209

Review Article

Cardiovascular Effects Mediated by HMMR and CD44

Kinga Jaskuła,[1] **Mariusz Sacharczuk**,[1,2] **Zbigniew Gaciong**,[3] **and Dominik S. Skiba**[1]

[1]*Department of Experimental Genomics, Institute of Genetics and Animal Biotechnology, Polish Academy of Sciences, Postępu 36A, Jastrzebiec, Poland*
[2]*Faculty of Pharmacy with the Laboratory Medicine Division, Department of Pharmacodynamics, Medical University of Warsaw, Centre for Preclinical Research and Technology, Banacha 1B, Warsaw, Poland*
[3]*Department of Internal Medicine, Hypertension and Vascular Diseases, Medical University of Warsaw, Banacha 1A, Warsaw, Poland*

Correspondence should be addressed to Dominik S. Skiba; d.skiba@igbzpan.pl

Received 27 May 2021; Accepted 7 June 2021; Published 10 July 2021

Academic Editor: Elena Dozio

Cardiovascular disease (CVD) is the leading cause of death worldwide. The most dangerous life-threatening symptoms of CVD are myocardial infarction and stroke. The causes of CVD are not entirely clear, and new therapeutic targets are still being sought. One of the factors involved in CVD development among vascular damage and oxidative stress is chronic inflammation. It is known that hyaluronic acid plays an important role in inflammation and is regulated by numerous stimuli, including proinflammatory cytokines. The main receptors for hyaluronic acid are CD44 and RHAMM. These receptors are membrane proteins that differ in structure, but it seems that they can perform similar or synergistic functions in many diseases. Both RHAMM and CD44 are involved in cell migration and wound healing. However, their close association with CVD is not fully understood. In this review, we describe the role of both receptors in CVD.

1. Introduction

Cardiovascular disease (CVD) is a main cause of death globally, causing an estimated 17.9 million deaths annually. CVD is a general term for a group of heart and blood vessel diseases including coronary heart disease, cerebrovascular disease, and peripheral arterial disease. Late manifestations of CVD are heart attack and stroke mainly caused by previous vascular damage. Chronic inflammation is one of the causes of vascular damage or narrowing [1]. CD44 plays an important role in both inflammation and vascular injury [2]. Inflammation is associated with increased vascular permeability, recruitment of inflammatory cells, and release of inflammatory mediators. The cascade of inflammatory reactions can alter blood flow in the altered tissues by inflammatory cells infiltrating vascular tissues and releasing proteases, cytokines, and reactive oxygen species, which trigger vasoconstriction or relaxation [3], neointimal growth [4], and angiogenesis and tissue remodeling [5, 6]. The main ligand for the CD44 receptor is hyaluronic acid (HA) which binds also to RHAMM (hyaluronan-mediated motility receptor) [7]. HA is regulated by numerous stimuli, including proinflammatory cytokines [8]. Thus, the local production of cytokines within inflammatory lesions in the vessels increases the expression of HA on endothelial cells facilitating CD44-HA interactions and hence causing extravasation of inflammatory cells [9]. The role of CD44 in cardiovascular disease is well described; however, the role of another RHAMM receptor in CVDs is little known. This review discusses the role of both receptors in CVDs and their connections.

2. CD44 and RHAMM: Structure and Expression

CD44 is a widely expressed cellular adhesion molecule that serves as the major receptor for components of the extracellular matrix (ECM) [10]. Apart from HA, CD44 binds other carbohydrate ligands, such as heparan sulfate [11], as well as noncarbohydrate ligands: collagen and osteopontin [12]. CD44 occurs as a series of isoforms with molecular weights ranging from 85 to over 200 kDa [13]. The most commonly

expressed CD44 receptor is the 85-90 kDa glycoprotein which represents the standard CD44 molecule which does not contain products with spliced exon variants [14]. CD44 is structurally and functionally polymorphic. Its gene consists of at least 20 exons, of which 12 can be alternatively spliced. The heterogeneity of the protein is mainly due to the variable splicing of 10 exons encoding the extracellular region located between the invariant HA-binding domain at the NH2 terminus and the membrane proximal extracellular domain [15]. The most common isoform of CD44, called standard form (CD44s), does not contain any exon variants. It consists of a large extracellular domain of 248 amino acids, a 21-amino acid segment encompassing the membrane, and a relatively short cytoplasmic part of 72 amino acids [16]. The *CD44* gene contains 20 exons, of which exons 1-5, 15-17, and 19 encode the CD44 isoform, while exons 6.6a and 7-14 (also designated as vl-v10) are alternatively spliced to generate variant isoforms with insertion into the membrane proximal region of the extracellular domain between amino acids 202 and 203. The amino terminal region is relatively conserved in mammalian species (about 85% homology) and contains a hyaluronan-binding domain, while the membrane proximal region is relatively unconservative (about 35-45% sequence similarity between species) and has several sites for glycosylation and chondroitin sulfate attachment [17, 18]. The transmembrane domain ensures a way to interact with cofactors and adapter proteins and to direct the influx of lymphocytes [19]. The intracellular domain of CD44 has short- and long-tail configurations and performs nuclear localization functions for the regulation of transcription [20].CD44 is expressed in a variety of cell types (Figures 1(a) and 1(b)), including lymphocytes, macrophages, erythrocytes, fibroblasts, neurons, epithelial cells, and endothelial cells [18]. CD44 supports the adhesion of leukocytes to endothelial cells [10], induces the secretion of chemokines from macrophages, and regulates the proliferation and migration of vascular smooth muscle cells [21].

In contrast to CD44, the main hyaluronan receptor, RHAMM, is less well studied and mainly is involved in cell locomotion. It was firstly described by Turley et al. [22, 23] and soon was linked to *ras* transformation and tumor progression [24]. The *HMMR* gene encodes an 85 kDa protein—RHAMM—with an extensive helix structure and a basic globular domain at the amino terminus [25]. It has approximately 35% protein sequence homology to KIF15, a member of the kinesin family [26]. RHAMM does not contain a signal peptide for export via the Golgi apparatus and the endoplasmic reticulum [7]. RHAMM is a member of the hyaladherin protein family, has two hyaluronan-binding domains, and interacts with it through 9–11-amino acid basic motifs [27]. The extracellular part of RHAMM activates signaling cascades that control the expression of cell cycle genes and genes related to cell motility [28, 29]. The intracellular domain of RHAMM is required for the formation of the mitotic spindle and may play a role in the direction of cell motility [30]. The *HMMR* gene is located on the human chromosome 5q33.2 and contains 18 exons [31]. RHAMM, also described as CD168, does not have a transmembrane domain but is anchored by the glycosylphosphatidylinositol (GPI) group in the plasma membrane where it can interact with CD44 and participate in many cell functions, including cell motility, wound healing, and modification of the Ras signaling cascade. Interestingly, RHAMM does not contain a signal peptide and is believed to be transported to the cell surface by unconventional transport mechanisms where it binds to the cell surface by docking to HA synthase [32] and, like CD44, transmits signals affecting cell mobility [27]. It has been shown that RMAMM interacts with hyaluronan in an ionic manner via a 35-amino acid basic C-terminal region, which can be further subdivided into two motifs of 10 and 11 amino acids, respectively [33]. RHAMM is present on the cell surface, in the cytoplasm, and in the nucleus of different types of cells [25] and regulates cell movement and proliferation [24, 25]. RHAMM under physiological conditions is poorly expressed on various cell types (Figures 1(a) and 1(b)) such as lymphocytes, smooth muscle cells, macrophages, and fibroblasts; however, its expression rises in pathological conditions [34, 35].

Although CD44 and RHAMM have different primary amino acid sequences and although CD44 is conservatively expressed in cells and RHAMM is tightly regulated, both receptors possess transforming properties that may be related to their ability to promote motility [34, 36]. Research indicates that during inflammation, wound healing, and tumor formation, cell migration is mediated by CD44 and may require RHAMM surface expression [36]. This means that these receptors may act synergistically in some diseases.

3. Atherosclerosis and Vascular Inflammation

Atherosclerosis is an inflammatory disease of the walls of large and medium arteries. Its etiology is not fully understood, but there are several factors influencing its development. Chronic inflammation and increased levels of low-density lipoprotein (LDL) in the blood play a major role in the development of atherosclerosis. Abnormal blood flow in the vessels can cause increased wall tension and promote the production of proteoglycans by arterial smooth muscle cells (SMCs), which can bind and retain lipoprotein molecules, facilitating their oxidative modification, thereby promoting an inflammatory response at lesion sites [38]. Vascular endothelial cells become activated by proinflammatory stimuli and begin to express selective adhesion molecules on the surface, which recruit monocytes and T lymphocytes and which are likely to be involved in the recruitment of blood-borne cells for atherosclerotic lesions [39, 40].

Atherosclerosis at the developed stage is characterized by the formation of atherosclerotic plaque containing macrophages, dendritic cells (DC), foam cells, lymphocytes, and other inflammatory cells. In advanced age, atherosclerotic plaque calcifications appear [41]. Not only the vascular wall is affected but also the adventitia and adipose tissue attached to the vessel express some degree of inflammation which may precede vascular dysfunction [42, 43]. Dendritic cells and lymphocytes are found in the adventitia and perivascular adipose tissue of normal arteries, but their number is significantly increased in the atherosclerotic arteries [43]. Under

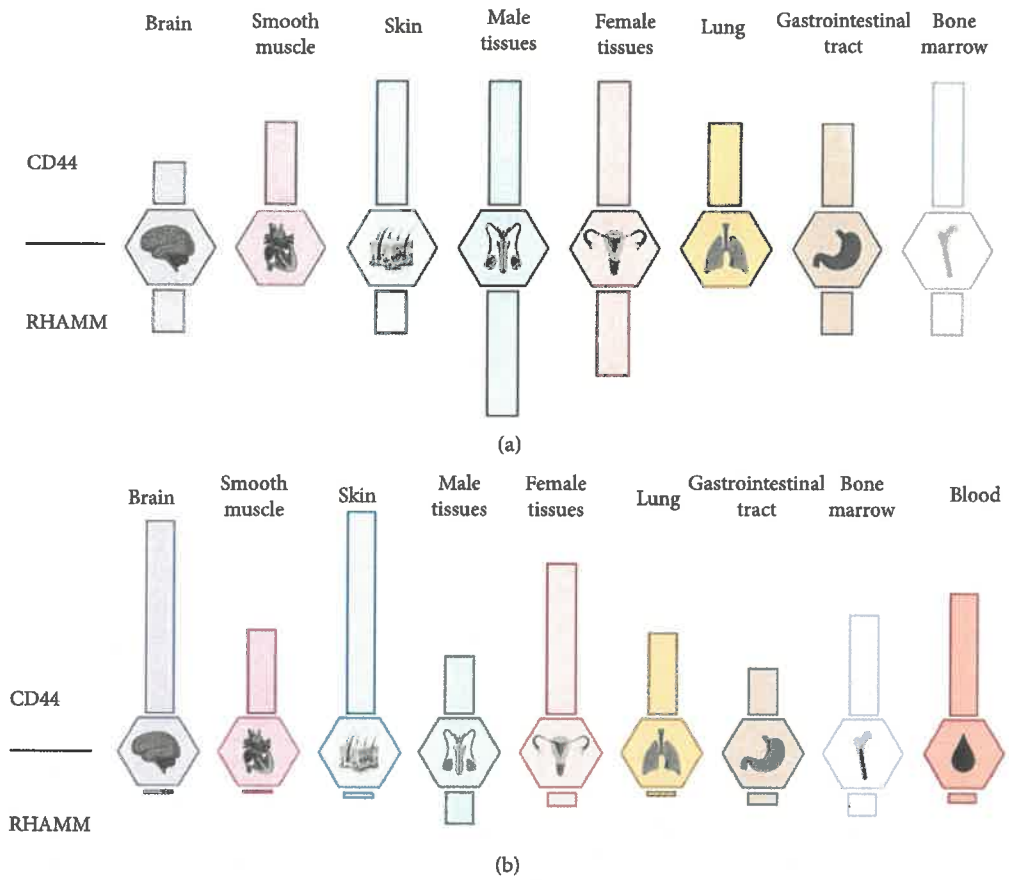

FIGURE 1: Protein (a) and mRNA (b) expression of CD44. Prepared on the basis of data from the Human Protein Atlas [37]. Protein expression reported with the units: not detected, low, medium, and high. mRNA expression reported as normalized expression (NX) combined from three transcriptomics datasets (HPA, GTEx, and FANTOM5). Created with BioRender.com.

internal atherosclerotic lesions, leukocytes organize themselves into clusters resembling tertiary lymphoid tissue [44]. These features of atherosclerotic plaques illustrate that atherosclerosis is a complex disease in which many elements of the vascular, metabolic, and immune systems take part. Atherosclerotic changes result from inflammatory triggers, subsequent release of various cytokines, proliferation of smooth muscle cells, synthesis of the connective tissue matrix, and accumulation of macrophages and lipids [39, 45, 46]. In those processes, CD44 and RHAMM may play an important role (Figure 2).

Numerous studies suggest that the CD44 cell adhesion molecule may promote atherosclerosis by mediating the recruitment of inflammatory cells into platelets and activation of vascular cells [47, 48]. In the atherosclerosis model of apoE$^{-/-}$ mice, vascular expression of CD44 was highest in areas prone to damage [48, 49]. This was confirmed in human studies where CD44 was present in areas of human atherosclerotic plaques, rich in macrophages, and susceptible to rupture, compared to healthy vascular tissues [50, 51]. Elevated expression of CD44 correlated with a 10-fold increase in the secretion of proinflammatory cytokines such as interleukin-1β (IL-1β) and IL-6 by endothelial cells and macrophages. These cytokines in turn increased CD44 expression [50, 51]. Such a positive feedback loop may exacerbate arteriosclerosis, leading to plaque instability. The elimination of CD44 in mice with the apoE knockout led to a significant reduction in aortic lesions and a reduction in the number of macrophages present in the lesions by 90% [48]. Moreover, gene expression profiling in the aorta of CD44 knockout mice compared to a wild type led to the discovery that CD44 regulates focal adhesion formation, extracellular matrix deposition, and angiogenesis, critical processes for atherosclerosis [49]. To investigate the mechanism by which CD44 controls atherosclerosis, bone marrow chimeras were generated using bone marrow transplant from a wild type (WT) and CD44-null donor to apoE$^{-/-}$ and apoE$^{-/-}$ CD44$^{-/-}$. The expression of CD44 in both the vascular and bone marrow cells contributed to the development of changes in the apoE$^{-/-}$ model. It means that CD44, on both the resident and recruited cells, is essential for its full proatherogenic effect *in vivo* [47]. Moreover, the CD44 deletion also favored an increase in fibrotic lesions in apoE$^{-/-}$ CD44$^{-/-}$ mice compared to apoE$^{-/-}$ mice, which indicates that CD44 also regulates the lesion composition and influences the stability of atherosclerotic plaques [47].

So far, RHAMM has not been directly associated with atherosclerosis, but it is known that it plays a vital role in inflammation, an important factor in the pathogenesis of atherosclerosis [36]. It has been shown that RHAMM interacts with growth factor receptors such as PDGFR [52], TGF-β receptor I [53], or bFGFR [54]. Growth factors regulate the function of ERK signaling and are responsible for the regulation of cell proliferation and differentiation [52]. In

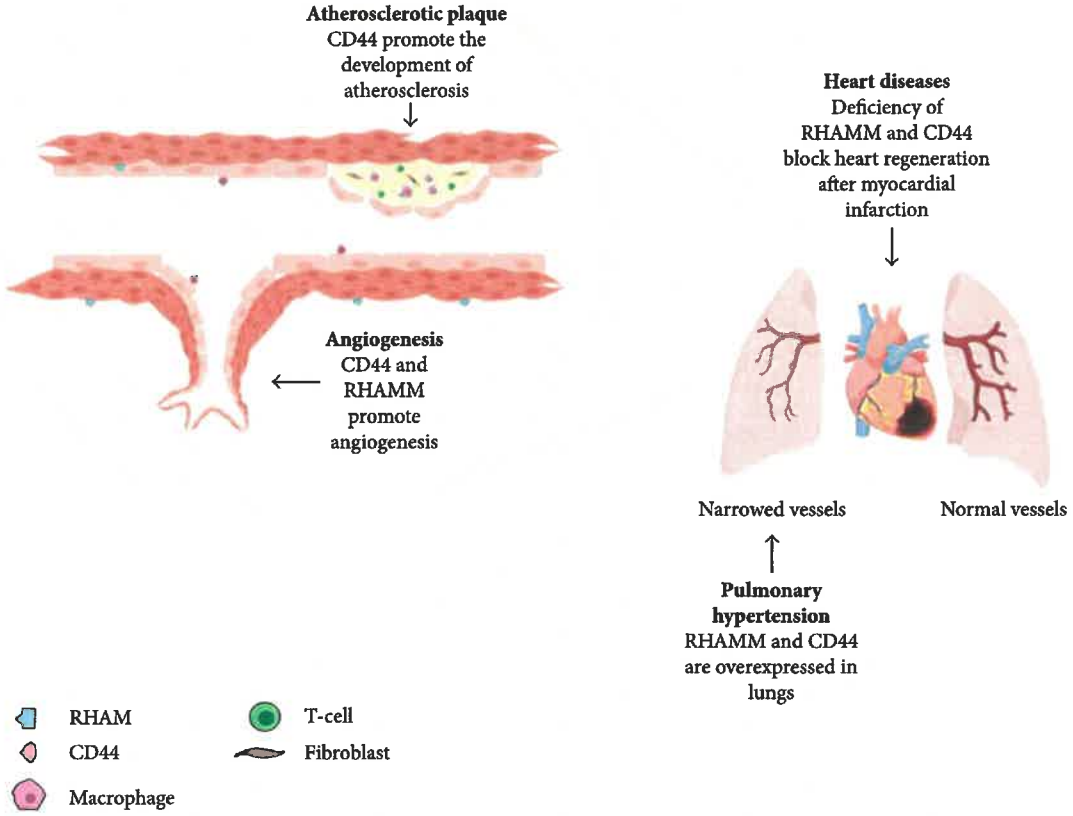

FIGURE 2: Diagram describing the role of RHAMM and CD44 receptors in the cardiovascular system. Created with BioRender.com.

addition, ERK signaling has been shown to play a role in altering cholesterol homeostasis in human macrophages [55]. By interacting, RHAMM takes part in the mobility necessary for the inflammation by activating ERK1/2/MAPK. Nuclear RHAMM is also associated with the ERK1/2/MAP kinase, which mediates the activation of PAI-1 and MMP-9, which are involved in cell mobility and inflammation [56]. RHAMM also participates in HA-dependent regulation. HA is produced during tissue damage, causing activation of inflammatory cells to induce innate immune response and regulation of the behavior of epithelial cells and fibroblasts [57–59]. Additional confirmation of the importance of RHAMM is the fact that the use of a 15-mer peptide with homology to RHAMM-binding sequences has been shown to block HA signaling and reduce inflammation and fibrogenesis [60].

Macrophages in atherosclerotic plaque formation play a fundamental role [61]. Macrophages colonizing the atherosclerotic plaque have a reduced migration capacity, which leads to the maintenance of inflammation and further progression into the atherosclerotic plaque [62]. Moreover, they participate in the intake and accumulation of lipoproteins. Cholesterol uptake by macrophages leads to their transformation to foam cells in the vascular wall. At this stage of atherosclerosis, fatty streaks are observed in the vasculature. The RHAMM receptor is expressed on macrophages. In a rat model of acute lung damage, the expression of RHAMM and HA is increased in macrophages responding to intratracheal injury [63, 64]. Moreover, *Hmmr*$^{-/-}$ transgenic mice have been shown to exhibit reduced macrophage chemotaxis [65]. Another element essential in the development of atherosclerotic lesions includes vascular smooth muscle cells (VSMCs). VSMCs, under the influence of vascular damage, are able to change the quiescent "contractile" phenotype into a "proinflammatory" phenotype. Activated VSMCs can effectively multiply and migrate, helping to repair vascular walls. However, in the chronic inflammation that occurs in atherosclerosis, VSMCs are misregulated, leading to extracellular matrix formation in the plaque areas [66]. Research has shown that RHAMM can be an important element in these processes. *In vitro* studies have shown that HA mediates VSMC migration through CD44 and RHAMM receptors as well as VSMC proliferation but only through the CD44 receptor [2, 67, 68]. On the basis of the culture of bovine vascular smooth muscle cells, an increase in RHAMM expression was observed after scratch wound assay. It was concluded that vascular damage leads to an increase in RHAMM expression and is localized in the VSMC at the edge of the lesion [68].

4. Ischemic Heart Disease

Ischemic heart disease is one of the most common causes of death in developed countries. After myocardial infarction

(MI), billions of cardiomyocytes undergo apoptosis, pyroptosis, and necrosis, resulting in a noncontractile collagen scar that reduces heart function [69]. The mammalian heart's ability to replace lost cardiomyocytes is limited, while adult zebrafish (*Danio rerio*) can successfully regenerate the heart following apical ventricular amputation throughout its lifetime [70, 71]. A key factor in the regeneration process in zebrafish is the ability of preexisting cardiomyocytes to proliferate after organ damage [72–74].

After analyzing the proteomic changes following ventricular apex resection in adult zebrafish, increased expression of the RHAMM was identified. It was also investigated that after zebrafish ventricular resection, the area of scar tissue was significantly larger in the RHAMM knockdown fish, suggesting that the RHAMM knockdown blocked heart regeneration. The importance of hyaluronic acid in the regeneration of the heart was also determined. It was found that after inhibition of HA synthesis, after ventricular resection in zebrafish, significant scar tissue was still present compared to minimal or no scar tissue in controls [75].

Studies on the role of CD44 in regeneration after MI have shown a correlation between inflammatory mediators and CD44 in regulating the inflammatory response, repairing the heart, and differentiating the heart fibroblasts after MI [76]. Studies in CD44-deficient mice that underwent myocardial infarction showed prolonged inflammation, reduced collagen deposition in scars, decreased myofibroblast infiltration, and decreased TGF-β signaling [77]. Following acute MI, IL-6 has been shown to enhance CD44 and HA synthase (HAS-1 and HAS-2) expression in cardiac fibroblasts, resulted in a matrix rich in HA. As a result, proinflammatory cytokines and the expression of smooth muscle α-actin were induced through CD44-HA interactions. This interaction, together with circulating IL-6, changed the nature of the ECM, modulated the differentiation of cardiac fibroblasts, and promoted the immune responses [78].

5. Vascular Remodeling

Restrictive remodeling assumes that SMCs reorganize the ECM, while the factors causing constrained remodeling compared to external remodeling remain poorly defined [79]. The contraction of the vessel wall is similar to that of a cutaneous wound. SMCs repopulate the sites of vascular damage and cause the production and remodeling of the ECM, which changes the geometry of the vessel wall. It is known that matrix remodeling depends in part on direct adhesion interactions of ECM cells. In *in vitro* studies on SMCs, HA consistently increased the adhesion of SMCs to collagen-precoated plates and blocking or removing RHAMM weakened SMC adhesion to collagen with or without exogenous HA [80]. That suggests that the endogenous production of HA is sufficient to activate RHAMM. RHAMM activation by HA significantly influences the adhesive interactions between SMC and ECM and contributes to remodeling of the wall and narrowing of the lumen after carotid artery ligation [80]. RHAMM-blocking strategies at sites of vascular injury may be potentially useful in the prevention of clinical restenosis.

The role that CD44 plays in remodeling, for example, after angioplasty, is unclear. Available data published on that topic does not clearly indicate whether CD44 may be a remodeling factor or may play a protective role by inhibiting neointimal formation [81, 82]. However, studies have shown that the deficiency of the *CD44* gene significantly enhanced neointimal hyperplasia, which suggests that the *CD44* gene is involved in the process of pathological remodeling and may play a protective role. The remodeling response to injury involves circulating cells that arise from the bone marrow as well as cells from the local artery wall. Compared with damaged femoral arteries in $CD44^{+/+}$ mice, $CD44^{-/-}$ mice showed significantly greater femoral vascular remodeling. In remodeled femoral arteries from $CD44^{-/-}$ mice, no significant changes were observed in CD44 expression when compared to intact arteries. After the use of low-mass weight (LMW) heparin, the damaged arteries showed a significant reduction in neointimal thickness and a significant increase in CD44 expression. This suggests that CD44 may be the route by which LMW heparin diminishes the remodeling process [83].

6. Angiogenesis

Angiogenesis is the formation of new blood vessels from existing vessels (Figure 2). It can occur in a pathological form in the context of circulatory diseases or cancer and in a physiological form in the case of tissue ischemia, wound healing, etc. [84]. To investigate the involvement of CD44 in blood vessel formation, *in vivo* angiogenesis was studied in CD44-deficient mice [85]. Initial studies were performed in a model in which vessels develop around and within subcutaneously implanted Matrigel plugs containing B16 murine melanoma tumor cells as a source of angiogenic growth factors. Vascularization of the plugs was observed in wild-type animals, but not in CD44 knockout mice, confirming the involvement of CD44 in the pathological formation of blood vessels [86]. In addition, in a mouse oral carcinogenesis model, after implantation of Matrigel plugs with suspended cancer cells into the dorsal chamber of the skin fold, $CD44^{+/+}$ mice showed a higher microvascular density than $CD44^{-/-}$ [87]. It has also been shown that inhibition of CD44 reduces the adhesion of endothelial cells (EC) to HA immobilized on the plastic surface [54]. This means that an increase in CD44 expression may allow the adhesion of the EC to the components of the ECM, which is one of the processes enabling the formation of new blood vessels [1]. Whether CD44 plays a role in physiological angiogenesis has also been investigated. Wound closure in animals with the CD44 knockout was shown to be delayed within 1 to 3 days after wounding, relative to wild-type animals. Vascular density at the edge of the wounds on day 3 was reduced by around 20% in $CD44^{-/-}$ animals compared to wild-type mice. This means that the lack of CD44 results in an early delay in skin wound closure, which is associated with reduced neovascularization of the injured tissue. The above results thus confirmed that CD44 may be involved in physiological angiogenesis [86]. The differentiation and organization of EC in blood vessels is a critical step in angiogenesis [88]. To

investigate the role of RHAMM receptors in blood vessel formation, the effect of anti-RHAMM antibodies on EC function and *in vivo* angiogenesis was determined. Using the endothelial tube formation model on Matrigel, anti-RHAMM antibodies were found to inhibit tube formation by human endothelial cells. It was also investigated that the use of an anti-RHAMM antibody in a mouse model of angiogenesis significantly reduced the vascularization of the plugs [54].

7. Idiopathic Pulmonary Arterial Hypertension

Idiopathic pulmonary arterial hypertension (IPAH) is a disorder characterized by persistent elevated pulmonary arterial pressure with unknown causes [89]. The primary mechanism of IPAH is pulmonary vascular remodeling involving pre- and intra-acinar arteries, such as stenotic lesions and complex lesions characterized by plexiform lesions (Figure 2) [90]. The plexiform injury has been studied in relation to idiopathic pulmonary arterial hypertension as a marker of the severity or rapid progression of pulmonary hypertension [91], but it also contributed to the pathogenesis of the disease. Studies have shown that CD44 was frequently expressed in plexiform lung lesions in IPAH patients and was mainly located in endothelial cells that make up the microvasculature of the lesions and surrounding T lymphocytes. However, CD44 was not found in any of the vascular cells of normal pulmonary arteries. This suggests that CD44 is involved in the pathogenesis of idiopathic pulmonary arterial hypertension [92]. The role of RHAMM in pulmonary hypertension is not fully understood. However, studies have shown that loss of PPARγ (peroxisome proliferator-activated receptor γ) is associated with pulmonary hypertension [93]. It has been shown that PPARγ expression is significantly reduced in plexiform lesions in humans with PH. Reduced PPARγ expression was also demonstrated in vascular lesions in a rat model of severe pulmonary hypertension [94]. It has also been investigated that by pharmacological inhibition of PPARγ, RHAMM was upregulated in pulmonary arterial endothelial cells in a sheep model of pulmonary hypertension. The increased expression of RHAMM was also confirmed in human pulmonary microvascular endothelial cells (HMVEC) with PPARγ depletion. These results suggest that HMMR plays a large role in hypertension but it would be worthwhile to conduct more research in this area [95].

8. Conclusions

CD44 and RHAMM mediate different cardiovascular effects in normal and pathological conditions. Herein, we discussed the role of these receptors not only in cardiovascular diseases such as atherosclerosis, pulmonary hypertension, and ischemic heart disease but also in cardiovascular processes such as vascular inflammation, vascular remodeling, and angiogenesis. Expression of RHAMM in contrast to CD44 is relatively low in vascular cells and blood. However, RHAMM expression rises in pathological conditions. Expression of CD44 was found to be upregulated in areas prone to atherosclerosis. The important role of RHAMM in atherosclerosis development is its role in the motility of the immune cells. The gained ability of migration mediated by RHAMM allows cells to the inflammatory response. This process is important also in other conditions where vascular remodeling is present. In conditions after myocardial infarction, CD44 and RHAMM help in wound healing by reorganization of the extracellular matrix and collagen deposition. Inhibition or lack of RHAMM or CD44 blocks angiogenesis in both the physiological and pathological conditions. Summarizing the role of both described receptors is similar apart from its different role in vascular remodeling. However, the RHAMM receptor is significantly less studied in cardiovascular diseases.

Conflicts of Interest

The authors declare that there are no conflicts of interest.

Acknowledgments

This work was supported by the National Science Centre, Poland (project numbers 2019/35/D/NZ5/02820 and 2014/15/B/NZ5/03566).

References

[1] G. W. Sullivan, I. J. Sarembock, and J. Linden, "The role of inflammation in vascular diseases," *Journal of Leukocyte Biology*, vol. 67, no. 5, pp. 591–602, 2000.

[2] M. Jain, Q. He, W. S. Lee et al., "Role of CD44 in the reaction of vascular smooth muscle cells to arterial wall injury," *The Journal of Clinical Investigation*, vol. 97, no. 3, pp. 596–603, 1996.

[3] A. B. Peitzman, B. G. Harbrecht, A. O. Udekwu, T. R. Billiar, E. Kelly, and R. L. Simmons, "Hemorrhagic shock," *Current Problems in Surgery*, vol. 32, no. 11, pp. 925–1002, 1995.

[4] G. K. Hansson, "Immunological control mechanisms in plaque formation," in *Arteriosclerosis*, vol. 89, Dr. Dietrich Steinkopff Verlag GmbH and Co. KG, 1994.

[5] R. L. Wilensky, K. L. March, I. Gradus-Pizlo, G. Sandusky, N. Fineberg, and D. R. Hathaway, "Vascular injury, repair, and restenosis after percutaneous transluminal angioplasty in the atherosclerotic rabbit," *Circulation*, vol. 92, no. 10, pp. 2995–3005, 1995.

[6] F. Mach, U. Schönbeck, R. P. Fabunmi et al., "T lymphocytes induce endothelial cell matrix metalloproteinase expression by a CD40L-dependent mechanism: implications for tubule formation," *The American Journal of Pathology*, vol. 154, no. 1, pp. 229–238, 1999.

[7] J. Jiang, R. Casalegno-Garduno, H. Chen, A. Schmitt, M. Schmitt, and C. A. Maxwell, "Multifunctional proteins bridge mitosis with motility and cancer with inflammation and arthritis," *ScientificWorldJournal*, vol. 10, pp. 1244–1257, 2010.

[8] H. J. Cao, H. S. Wang, Y. Zhang, H. Y. Lin, R. P. Phipps, and T. J. Smith, "Activation of human orbital fibroblasts through CD40 engagement results in a dramatic induction of hyaluronan synthesis and prostaglandin endoperoxide H synthase-2 expression," *The Journal of Biological Chemistry*, vol. 273, no. 45, pp. 29615–29625, 1998.

[9] E. Puré and C. A. Cuff, "A crucial role for CD44 in inflammation," *Trends in Molecular Medicine*, vol. 7, no. 5, pp. 213–221, 2001.

[10] A. I. Khan, S. M. Kerfoot, B. Heit et al., "Role of CD44 and hyaluronan in neutrophil recruitment," *Journal of Immunology*, vol. 173, no. 12, pp. 7594–7601, 2004.

[11] S. Jalkanen and M. Jalkanen, "Lymphocyte CD44 binds the COOH-terminal heparin-binding domain of fibronectin," *The Journal of Cell Biology*, vol. 116, no. 3, pp. 817–825, 1992.

[12] G. F. Weber, S. Ashkar, M. J. Glimcher, and H. Cantor, "Receptor-ligand interaction between CD44 and osteopontin (Eta-1)," *Science*, vol. 271, no. 5248, pp. 509–512, 1996.

[13] S. Goodison, V. Urquidi, and D. Tarin, "CD44 cell adhesion molecules," *Molecular Pathology*, vol. 52, no. 4, pp. 189–196, 1999.

[14] A. Aruffo, I. Stamenkovic, M. Melnick, C. B. Underhill, and B. Seed, "CD44 is the principal cell surface receptor for hyaluronate," *Cell*, vol. 61, no. 7, pp. 1303–1313, 1990.

[15] M. P. Martegani, F. Del Prete, A. Gasbarri, P. G. Natali, and A. Bartolazzi, "Structural variability of CD44v molecules and reliability of immunodetection of CD44 isoforms using mAbs specific for CD44 variant exon products," *The American Journal of Pathology*, vol. 154, no. 1, pp. 291–300, 1999.

[16] G. Borland, J. A. Ross, and K. Guy, "Forms and functions of CD44," *Immunology*, vol. 93, no. 2, pp. 139–148, 1998.

[17] C. M. Isacke and H. Yarwood, "The hyaluronan receptor, CD44," *The International Journal of Biochemistry & Cell Biology*, vol. 34, no. 7, pp. 718–721, 2002.

[18] S. Ilangumaran, B. Borisch, and D. C. Hoessli, "Signal transduction via CD44: role of plasma membrane microdomains," *Leukemia & Lymphoma*, vol. 35, no. 5-6, pp. 455–469, 1999.

[19] K. Williams, K. Motiani, P. V. Giridhar, and S. Kasper, "CD44 integrates signaling in normal stem cell, cancer stem cell and (pre)metastatic niches," *Experimental Biology and Medicine*, vol. 238, no. 3, pp. 324–338, 2013.

[20] I. Okamoto, Y. Kawano, H. Tsuiki et al., "CD44 cleavage induced by a membrane-associated metalloprotease plays a critical role in tumor cell migration," *Oncogene*, vol. 18, no. 7, pp. 1435–1446, 1999.

[21] C. M. McKee, M. B. Penno, M. Cowman et al., "Hyaluronan (HA) fragments induce chemokine gene expression in alveolar macrophages: the role of HA size and CD44," *The Journal of Clinical Investigation*, vol. 98, no. 10, pp. 2403–2413, 1996.

[22] E. A. Turley and J. Torrance, "Localization of hyaluronate and hyaluronate-binding protein on motile and non- motile fibroblasts," *Experimental Cell Research*, vol. 161, no. 1, pp. 17–28, 1985.

[23] E. A. Turley, D. Moore, and L. J. Hayden, "Characterization of hyaluronate binding proteins isolated from 3T3 and murine sarcoma virus transformed 3T3 cells," *Biochemistry*, vol. 26, no. 11, pp. 2997–3005, 1987.

[24] C. L. Hall, B. Yang, X. Yang et al., "Overexpression of the hyaluronan receptor RHAMM is transforming and is also required for *H-ras* transformation," *Cell*, vol. 82, no. 1, pp. 19–28, 1995.

[25] C. Hardwick, K. Hoare, R. Owens et al., "Molecular cloning of a novel hyaluronan receptor that mediates tumor cell motility," *The Journal of Cell Biology*, vol. 117, no. 6, pp. 1343–1350, 1992.

[26] C. A. Maxwell, J. J. Keats, M. Crainie et al., "RHAMM is a centrosomal protein that interacts with dynein and maintains spindle pole stability," *Molecular Biology of the Cell*, vol. 14, no. 6, pp. 2262–2276, 2003.

[27] B. Yang, B. L. Yang, R. C. Savani, and E. A. Turley, "Identification of a common hyaluronan binding motif in the hyaluronan binding proteins RHAMM, CD44 and link protein," *The EMBO Journal*, vol. 13, no. 2, pp. 286–296, 1994.

[28] Slevin, "Oligosaccharides of hyaluronan induce angiogenesis through distinct CD44 and RHAMM-mediated signalling pathways involving Cdc2 and γ-adducin," *International Journal of Oncology*, vol. 35, no. 4, p. 35, 2009.

[29] S. Mohapatra, X. Yang, J. A. Wright, E. A. Turley, and A. H. Greenberg, "Soluble hyaluronan receptor RHAMM induces mitotic arrest by suppressing Cdc2 and cyclin B1 expression," *The Journal of Experimental Medicine*, vol. 183, no. 4, pp. 1663–1668, 1996.

[30] R. Silverman-Gavrila, L. Silverman-Gavrila, G. Hou, M. Zhang, M. Charlton, and M. P. Bendeck, "Rear polarization of the microtubule-organizing center in neointimal smooth muscle cells depends on PKCα, ARPC5, and RHAMM," *The American Journal of Pathology*, vol. 178, no. 2, pp. 895–910, 2011.

[31] C. Wang, J. Entwistle, G. Hou, Q. Li, and E. A. Turley, "The characterization of a human _RHAMM_ cDNA: conservation of the hyaluronan- binding domains," *Gene*, vol. 174, no. 2, pp. 299–306, 1996.

[32] L. Klewes, E. A. Turley, and P. Prehm, "The hyaluronate synthase from a eukaryotic cell line," *The Biochemical Journal*, vol. 290, no. 3, pp. 791–795, 1993.

[33] B. Yang, L. Zhang, and E. A. Turley, "Identification of two hyaluronan-binding domains in the hyaluronan receptor RHAMM," *The Journal of Biological Chemistry*, vol. 268, no. 12, pp. 8617–8623, 1993.

[34] L. M. Pilarski, A. Masellis-Smith, A. R. Belch, B. Yang, R. C. Savani, and E. A. Turley, "RHAMM, a receptor for hyaluronan-mediated motility, on normal human lymphocytes, thymocytes and malignant B cells: a mediator in B cell malignancy?," *Leukemia & Lymphoma*, vol. 14, no. 5-6, pp. 363–374, 1994.

[35] C. Tolg, S. R. Hamilton, K. A. Nakrieko et al., "Rhamm-/- fibroblasts are defective in CD44-mediated ERK1,2 motogenic signaling, leading to defective skin wound repair," *The Journal of Cell Biology*, vol. 175, no. 6, pp. 1017–1028, 2006.

[36] S. Misra, V. C. Hascall, R. R. Markwald, and S. Ghatak, "Interactions between hyaluronan and its receptors (CD44, RHAMM) regulate the activities of inflammation and cancer," *Frontiers in Immunology*, vol. 6, p. 201, 2015.

[37] M. Uhlen, L. Fagerberg, B. M. Hallstrom et al., "Tissue-based map of the human proteome," *Science*, vol. 347, no. 6220, article 1260419, 2015.

[38] D. E. Andreou and I. Andreadou, "Atherosclerosis: an inflammatory disease," *New England Journal of Medicine*, vol. 340, no. 2, pp. 115–126, 1999.

[39] M. A. Crowther, "Pathogenesis of atherosclerosis," *Hematology. American Society of Hematology. Education Program*, vol. 2005, no. 1, pp. 436–441, 2005.

[40] G. K. Hansson, "Inflammation, atherosclerosis, and coronary artery disease," *The New England Journal of Medicine*, vol. 352, no. 16, pp. 1685–1695, 2005.

[41] C. Weber and H. Noels, "Atherosclerosis: current pathogenesis and therapeutic options," *Nature Medicine*, vol. 17, no. 11, pp. 1410–1422, 2011.

[42] E. Galkina, A. Kadl, J. Sanders, D. Varughese, I. J. Sarembock, and K. Ley, "Lymphocyte recruitment into the aortic wall before and during development of atherosclerosis is partially L-selectin dependent," *The Journal of Experimental Medicine*, vol. 203, no. 5, pp. 1273–1282, 2006.

[43] D. S. Skiba, R. Nosalski, T. P. Mikolajczyk et al., "Anti-atherosclerotic effect of the angiotensin 1-7 mimetic AVE0991 is mediated by inhibition of perivascular and plaque inflammation in early atherosclerosis," *British Journal of Pharmacology*, vol. 174, no. 22, pp. 4055–4069, 2017.

[44] P. Srikakulapu, D. Hu, C. Yin et al., "Artery tertiary lymphoid organs control multilayered territorialized atherosclerosis B-cell responses in aged ApoE-/- mice," *Arteriosclerosis, Thrombosis, and Vascular Biology*, vol. 36, no. 6, pp. 1174–1185, 2016.

[45] C. Weber, A. Zernecke, and P. Libby, "The multifaceted contributions of leukocyte subsets to atherosclerosis: lessons from mouse models," *Nature Reviews. Immunology*, vol. 8, no. 10, pp. 802–815, 2008.

[46] G. K. Hansson and P. Libby, "The immune response in atherosclerosis: a double-edged sword," *Nature Reviews. Immunology*, vol. 6, no. 7, pp. 508–519, 2006.

[47] L. Zhao, E. Lee, A. M. Zukas et al., "CD44 expressed on both bone marrow-derived and non-bone marrow-derived cells promotes atherogenesis in ApoE-deficient mice," *Arteriosclerosis, Thrombosis, and Vascular Biology*, vol. 28, no. 7, pp. 1283–1289, 2008.

[48] C. A. Cuff, D. Kothapalli, I. Azonobi et al., "The adhesion receptor CD44 promotes atherosclerosis by mediating inflammatory cell recruitment and vascular cell activation," *The Journal of Clinical Investigation*, vol. 108, no. 7, pp. 1031–1040, 2001.

[49] L. Zhao, J. A. Hall, N. Levenkova et al., "CD44 regulates vascular gene expression in a proatherogenic environment," *Arteriosclerosis, Thrombosis, and Vascular Biology*, vol. 27, no. 4, pp. 886–892, 2007.

[50] D. Hägg, S. Sjöberg, L. M. Hultén et al., "Augmented levels of CD44 in macrophages from atherosclerotic subjects: a possible IL-6-CD44 feedback loop?," *Atherosclerosis*, vol. 190, no. 2, pp. 291–297, 2007.

[51] A. Krettek, G. K. Sukhova, U. Schönbeck, and P. Libby, "Enhanced expression of CD44 variants in human atheroma and abdominal aortic aneurysm: possible role for a feedback loop in endothelial cells," *The American Journal of Pathology*, vol. 165, no. 5, pp. 1571–1581, 2004.

[52] S. Zhang, M. C. Y. Chang, D. Zylka, S. Turley, R. Harrison, and E. A. Turley, "The hyaluronan receptor RHAMM regulates extracellular-regulated kinase∗," *The Journal of Biological Chemistry*, vol. 273, no. 18, pp. 11342–11348, 1998.

[53] D. Park, Y. Kim, H. Kim et al., "Hyaluronic acid promotes angiogenesis by inducing RHAMM-TGFβ receptor interaction via CD44-PKCδ," *Molecules and Cells*, vol. 33, no. 6, pp. 563–574, 2012.

[54] R. C. Savani, G. Cao, P. M. Pooler, A. Zaman, Z. Zhou, and H. M. DeLisser, "Differential involvement of the hyaluronan (HA) receptors CD44 and receptor for HA-mediated motility in endothelial cell function and angiogenesis," *The Journal of Biological Chemistry*, vol. 276, no. 39, pp. 36770–36778, 2001.

[55] N. Li, J. E. McLaren, D. R. Michael, M. Clement, C. A. Fielding, and D. P. Ramji, "ERK is integral to the IFN-γ–mediated activation of STAT1, the expression of key genes implicated in atherosclerosis, and the uptake of modified lipoproteins by human macrophages," *Journal of Immunology*, vol. 185, no. 5, pp. 3041–3048, 2010.

[56] C. Tolg, J. B. McCarthy, A. Yazdani, and E. A. Turley, "Hyaluronan and RHAMM in wound repair and the "cancerization" of stromal tissues," *BioMed Research International*, vol. 2014, Article ID 103923, 18 pages, 2014.

[57] M. Slevin, J. Krupinski, J. Gaffney et al., "Hyaluronan-mediated angiogenesis in vascular disease: uncovering RHAMM and CD44 receptor signaling pathways," *Matrix Biology*, vol. 26, no. 1, pp. 58–68, 2007.

[58] D. Jiang, J. Liang, J. Fan et al., "Regulation of lung injury and repair by toll-like receptors and hyaluronan," *Nature Medicine*, vol. 11, no. 11, pp. 1173–1179, 2005.

[59] N. Itano, F. Atsumi, T. Sawai et al., "Abnormal accumulation of hyaluronan matrix diminishes contact inhibition of cell growth and promotes cell migration," *Proceedings of the National Academy of Sciences of the United States of America*, vol. 99, no. 6, pp. 3609–3614, 2002.

[60] C. Tolg, S. R. Hamilton, E. Zalinska et al., "A RHAMM mimetic peptide blocks hyaluronan signaling and reduces inflammation and fibrogenesis in excisional skin wounds," *The American Journal of Pathology*, vol. 181, no. 4, pp. 1250–1270, 2012.

[61] K. J. Moore, F. J. Sheedy, and E. A. Fisher, "Macrophages in atherosclerosis: a dynamic balance," *Nature Reviews. Immunology*, vol. 13, no. 10, pp. 709–721, 2013.

[62] G. J. Randolph, "Mechanisms that regulate macrophage burden in atherosclerosis," *Circulation Research*, vol. 114, no. 11, pp. 1757–1771, 2014.

[63] A. Zaman, Z. Cui, J. P. Foley et al., "Expression and role of the hyaluronan receptor RHAMM in inflammation after bleomycin injury," *American Journal of Respiratory Cell and Molecular Biology*, vol. 33, no. 5, pp. 447–454, 2005.

[64] R. C. Savani, G. Hou, P. Liu et al., "A role for hyaluronan in macrophage accumulation and collagen deposition after bleomycin-induced lung injury," *American Journal of Respiratory Cell and Molecular Biology*, vol. 23, no. 4, pp. 475–484, 2000.

[65] J. P. Foley, D. Lam, H. Jiang et al., "Toll-like receptor 2 (TLR2), transforming growth factor-β, hyaluronan (HA), and receptor for HA-mediated motility (RHAMM) are required for surfactant protein A-stimulated macrophage chemotaxis∗„," *The Journal of Biological Chemistry*, vol. 287, no. 44, pp. 37406–37419, 2012.

[66] D. A. Chistiakov, A. N. Orekhov, and Y. V. Bobryshev, "Vascular smooth muscle cell in atherosclerosis," *Acta Physiologica*, vol. 214, no. 1, pp. 33–50, 2015.

[67] K. G. Maier, B. Sadowitz, S. Cullen, X. Han, and V. Gahtan, "Thrombospondin-1-induced vascular smooth muscle cell migration is dependent on the hyaluronic acid receptor CD44," *American Journal of Surgery*, vol. 198, no. 5, pp. 664–669, 2009.

[68] R. C. Savani, C. Wang, B. Yang et al., "Migration of bovine aortic smooth muscle cells after wounding injury: the role of hyaluronan and RHAMM," *The Journal of Clinical Investigation*, vol. 95, no. 3, pp. 1158–1168, 1995.

[69] J. Schaper, "Ultrastructural changes of the myocardium in regional ischaemia and infarction," *European Heart Journal*, vol. 7, suppl B, pp. 3–9, 1986.

[70] K. D. Poss, L. G. Wilson, and M. T. Keating, "Heart regeneration in zebrafish," *Science*, vol. 298, no. 5601, pp. 2188–2190, 2002.

[71] J. Itou, H. Kawakami, T. Burgoyne, and Y. Kawakami, "Life-long preservation of the regenerative capacity in the fin and heart in zebrafish," *Biol Open*, vol. 1, no. 8, pp. 739–746, 2012.

[72] C. Jopling, E. Sleep, M. Raya, M. Martí, A. Raya, and J. C. I. Belmonte, "Zebrafish heart regeneration occurs by cardiomyocyte dedifferentiation and proliferation," *Nature*, vol. 464, no. 7288, pp. 606–609, 2010.

[73] K. Kikuchi, J. E. Holdway, A. A. Werdich et al., "Primary contribution to zebrafish heart regeneration by *gata4*$^{+}$ cardiomyocytes," *Nature*, vol. 464, no. 7288, pp. 601–605, 2010.

[74] C. L. Lien, M. Schebesta, S. Makino, G. J. Weber, and M. T. Keating, "Gene expression analysis of zebrafish heart regeneration," *PLoS Biology*, vol. 4, no. 8, pp. e260–e296, 2006.

[75] M. A. Missinato, K. Tobita, N. Romano, J. A. Carroll, and M. Tsang, "Extracellular component hyaluronic acid and its receptor Hmmr are required for epicardial EMT during heart regeneration," *Cardiovascular Research*, vol. 107, no. 4, pp. 487–498, 2015.

[76] M. Suleiman, N. Abdulrahman, H. Yalcin, and F. Mraiche, "The role of CD44, hyaluronan and NHE1 in cardiac remodeling," *Life Sciences*, vol. 209, pp. 197–201, 2018.

[77] P. Huebener, T. Abou-Khamis, P. Zymek et al., "CD44 is critically involved in infarct healing by regulating the inflammatory and fibrotic response," *Journal of Immunology*, vol. 180, no. 4, pp. 2625–2633, 2008.

[78] J. Müller, S. Gorressen, M. Grandoch et al., "Interleukin-6-dependent phenotypic modulation of cardiac fibroblasts after acute myocardial infarction," *Basic Research in Cardiology*, vol. 109, no. 6, p. 440, 2014.

[79] R. L. Geary, S. T. Nikkari, W. D. Wagner, J. K. Williams, M. R. Adams, R. H. Dean et al., "Wound healing: a paradigm for lumen narrowing after arterial reconstruction," *Journal of Vascular Surgery*, vol. 27, no. 1, pp. 96–108, 1998.

[80] X. Ma, J. D. Pearce, D. B. Wilson, W. P. English, M. S. Edwards, and R. L. Geary, "Loss of the hyaluronan receptor RHAMM prevents constrictive artery wall remodeling," *Journal of Vascular Surgery*, vol. 59, no. 3, pp. 804–813, 2014.

[81] J. A. Travis, M. G. Hughes, J. M. Wong, W. D. Wagner, and R. L. Geary, "Hyaluronan enhances contraction of collagen by smooth muscle cells and adventitial fibroblasts," *Circulation Research*, vol. 88, no. 1, pp. 77–83, 2001.

[82] A. E. Vendrov, N. R. Madamanchi, Z. S. Hakim, M. Rojas, and M. S. Runge, "Thrombin and NAD(P)H oxidase-mediated regulation of CD44 and BMP4-Id pathway in VSMC, restenosis, and atherosclerosis," *Circulation Research*, vol. 98, no. 10, pp. 1254–1263, 2006.

[83] G. Zhao, R. S. Shaik, H. Zhao, J. Beagle, S. Kuo, and C. A. Hales, "Low molecular weight (LMW) heparin inhibits injury-induced femoral artery remodeling in mouse via upregulating CD44 expression," *Journal of Vascular Surgery*, vol. 53, no. 5, pp. 1359–1367.e3, 2011.

[84] L. Chen, C. Fu, Q. Zhang, C. He, F. Zhang, and Q. Wei, "The role of CD44 in pathological angiogenesis," *The FASEB Journal*, vol. 34, no. 10, pp. 13125–13139, 2020.

[85] P. Teder, R. W. Vandivier, D. Jiang et al., "Resolution of lung inflammation by CD44," *Science*, vol. 296, no. 5565, pp. 155–158, 2002.

[86] G. Cao, R. C. Savani, M. Fehrenbach et al., "Involvement of endothelial CD44 during _in vivo_ angiogenesis," *The American Journal of Pathology*, vol. 169, no. 1, pp. 325–336, 2006.

[87] N. Ludwig, M. J. Szczepanski, A. Gluszko et al., "CD44(+) tumor cells promote early angiogenesis in head and neck squamous cell carcinoma," *Cancer Letters*, vol. 467, pp. 85–95, 2019.

[88] E. L. Pardue, S. Ibrahim, and A. Ramamurthi, "Role of hyaluronan in angiogenesis and its utility to angiogenic tissue engineering," *Organogenesis*, vol. 4, no. 4, pp. 203–214, 2008.

[89] L. J. Rubin, "Primary pulmonary hypertension," *The New England Journal of Medicine*, vol. 336, no. 2, pp. 111–117, 1997.

[90] G. G. Pietra, F. Capron, S. Stewart et al., "Pathologic assessment of vasculopathies in pulmonary hypertension," *Journal of the American College of Cardiology*, vol. 43, no. 12, pp. S25–S32, 2004.

[91] G. G. Pietra, W. D. Edwards, J. M. Kay et al., "Histopathology of primary pulmonary hypertension. A qualitative and quantitative study of pulmonary blood vessels from 58 patients in the National Heart, Lung, and Blood Institute, Primary Pulmonary Hypertension Registry," *Circulation*, vol. 80, no. 5, pp. 1198–1206, 1989.

[92] K. Ohta-Ogo, H. Hao, H. Ishibashi-Ueda et al., "CD44 expression in plexiform lesions of idiopathic pulmonary arterial hypertension," *Pathology International*, vol. 62, no. 4, pp. 219–225, 2012.

[93] R. E. Nisbet, R. L. Sutliff, and C. M. Hart, "The role of peroxisome proliferator-activated receptors in pulmonary vascular disease," *PPAR Research*, vol. 2007, 10 pages, 2007.

[94] S. Ameshima, H. Golpon, C. D. Cool et al., "Peroxisome proliferator-activated receptor gamma (PPARγ) expression is decreased in pulmonary hypertension and affects endothelial cell growth," *Circulation Research*, vol. 92, no. 10, pp. 1162–1169, 2003.

[95] J. Tian, A. Smith, J. Nechtman et al., "Effect of PPARγ inhibition on pulmonary endothelial cell gene expression: gene profiling in pulmonary hypertension," *Physiological Genomics*, vol. 40, no. 1, pp. 48–60, 2009.